NTIS # PB2008-

SSC-455

FEASIBILITY, CONCEPTUAL DESIGN AND OPTIMIZATION OF A LARGE COMPOSITE HYBRID HULL

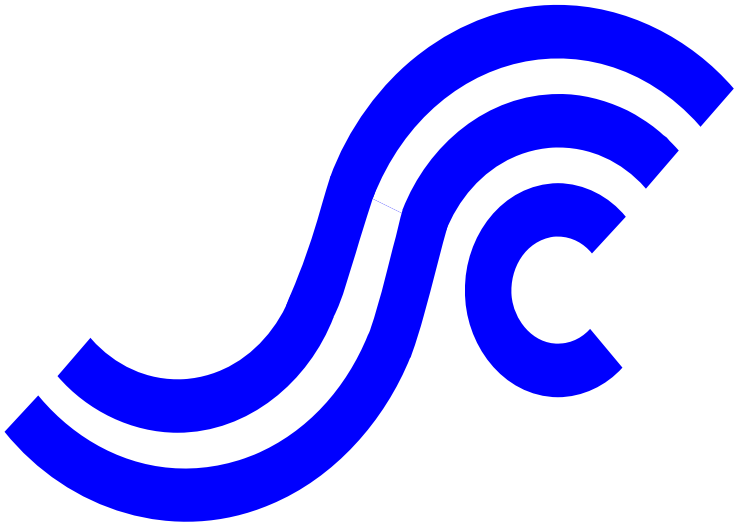

SHIP STRUCTURE COMMITTEE

2008

Ship Structure Committee

RADM Brian M. Salerno
U. S. Coast Guard Assistant Commandant,
Assistant Commandant for Marine Safety, Security and Stewardship
Chairman, Ship Structure Committee

{Name}
{Title}
Naval Sea Systems Command

Dr. Roger Basu
Senior Vice President
American Bureau of Shipping

Mr. Joseph Byrne
Director, Office of Ship Construction
Maritime Administration

Mr. William Nash
Director General, Marine Safety,
Safety & Security
Transport Canada

Mr. Kevin Baetsen
Director of Engineering
Military Sealift Command

Dr. Neil Pegg
Group Leader - Structural Mechanics
Defence Research & Development Canada - Atlantic

CONTRACTING OFFICER TECHNICAL REP.
Mr. Chao Lin / MARAD
Mr. Glenn Ashe / ABS
DRDC / USCG

EXECUTIVE DIRECTOR
Lieutenant Commander, Jason Smith
U. S. Coast Guard

SHIP STRUCTURE SUB-COMMITTEE

AMERICAN BUREAU OF SHIPPING

Mr. Glenn Ashe
Mr. Derek Novak
Mr. Phil Rynn
Mr. Balji Menon

DEFENCE RESEARCH & DEVELOPMENT CANADA ATLANTIC
Dr. David Stredulinsky
Mr. John Porter

MARITIME ADMINISTRATION
Mr. Chao Lin
Mr. Carl Setterstrom
Mr. Richard Sonnenschein

MILITARY SEALIFT COMMAND
Mr. Michael W. Touma
Mr. Paul Handler

ONR / NAVY/ NSWCCD
{Name}
{Name}
{Name}
{Name}

TRANSPORT CANADA
Paul Denis Vallee

US COAST GUARD

CDR Charles Rawson
Mr. James Person
Mr. Rubin Sheinberg

SOCIETY OF NAVAL ARCHITECTS AND MARINE ENGINEERS
Mr. Jaideep Sirkar
Mr. Al Rowen
Mr. Norman Hammer

Member Agencies:

American Bureau of Shipping
Defence Research Development Canada
Maritime Administration
Military Sealift Command
Naval Sea Systems Command
Society of Naval Architects & Marine Engineers
Transport Canada
United States Coast Guard

Ship
Structure
Committee

Address Correspondence to:

Executive Director
Ship Structure Committee
U.S. Coast Guard (CG-5212/SSC)
2100 2nd Street, SW
Washington, D.C. 20593-0001
Web site: http://www.shipstructure.org

SSC – 455
SR – 1452

OCTOBER 3, 2008

FEASIBILITY, CONCEPTUAL DESIGN AND OPTIMIZATION OF A LARGE COMPOSITE HYBRID HULL

The aim of this project was to investigate the feasibility of designing a large composite hybrid hull with increased structural performance. Feasibility was evaluated based upon the design's weight and cost in comparison to a conventional all-steel construction design.

The finite element analysis revealed that the addition of composite material to the creased panels improved its buckling capacity; but in order to get a noticeable improvement, high performance composite materials are required.

The conclusion of the report is that the proposed hybrid hull concept is technically feasible but, due to the need for advanced materials, may result in extremely high hull costs.

BRIAN M. SALERNO
Rear Admiral, U.S. Coast Guard
Chairman, Ship Structure Committee

Technical Report Documentation Form

1. Report No. SSC-455	2. Government Accession No.	3. Recipient's Catalogue No.
4. Title and Subtitle Feasibility, Conceptual Design and Optimization of a Large Composite Hybrid Hull		5. Report Date August 2008 6. Performing Organization Document No. 6092C.FR
7. Author(s) Dale Braun, Mladen Pejcic		8. Performing Organization Report No. SR 1452
9. Performing Agency Name and Address BMT Fleet Technology Limited 311 Legget Drive Kanata, ON (CANADA) K2K 1Z8		10. Work Unit No. (TRAIS) 11. Contract or Grant No.
12. Sponsoring Agency Name and Address Ship Structure Committee U.S. Coast Guard (G-MSE/SSC) 2100 Second Street, SW Washington, D.C. 20593-0001		13. Type of Publication and Period Covered Final Report 14. Sponsoring Agency Code CG-5

15. Supplementary Notes

Sponsored by the Ship Structure Committee. Jointly funded by its member agencies.

16. Abstract

A new ship hull structural concept is presented in the report, and feasibility of its application to large naval ship construction investigated. In this concept, the shell and decks are made up of hybrid steel-composite panels. The panels comprise of shallow-bent steel membrane with composite material filling the concave face of the membrane. FE analysis of a few variants of the panel reveals that the addition of composite material to the creased panels improves the buckling capacity; but in order to get a noticeable improvement, high performance composite materials are required.

Creasing the panel changes its behaviour in a significant way. The buckling strength is lower than with the flat plating, but it remains relatively constant if the thickness of the skin is reduced by significant amounts, unlike with conventional flat panels where the strength declines sharply with the reduction in plating thickness.

The conclusions of the report are that the proposed hybrid hull concept is technically feasible but, due to the need for advanced materials, may result in very high hull cost.

17. Key Words	18. Distribution Statement Distribution unlimited, available from: National Technical Information Service Springfield, VA 22161 (703) 487-4650		
19. Security Classif. (of this report) Unclassified	20. SECURITY CLASSIF. (of this page) Unclassified	21. No. of Pages	22. Price

CONVERSION FACTORS
(Approximate conversions to metric measures)

To convert from	to	Function	Value
LENGTH			
inches	meters	divide	39.3701
inches	millimeters	multiply by	25.4000
feet	meters	divide by	3.2808
VOLUME			
cubic feet	cubic meters	divide by	35.3149
cubic inches	cubic meters	divide by	61.024
SECTION MODULUS			
$inches^2$ $feet^2$	$centimeters^2$ $meters^2$	multiply by	1.9665
$inches^2$ $feet^2$	$centimeters^3$	multiply by	196.6448
$inches^4$	$centimeters^3$	multiply by	16.3871
MOMENT OF INERTIA			
$inches^2$ $feet^2$	$centimeters^2$ meters	divide by	1.6684
$inches^2$ $feet^2$	$centimeters^4$	multiply by	5993.73
$inches^4$	$centimeters^4$	multiply by	41.623
FORCE OR MASS			
long tons	tonne	multiply by	1.0160
long tons	kilograms	multiply by	1016.047
pounds	tonnes	divide by	2204.62
pounds	kilograms	divide by	2.2046
pounds	Newtons	multiply by	4.4482
PRESSURE OR STRESS			
$pounds/inch^2$	$Newtons/meter^2$ (Pascals)	multiply by	6894.757
kilo $pounds/inch^2$	mega $Newtons/meter^2$ (mega Pascals)	multiply by	6.8947
BENDING OR TORQUE			
foot tons	meter tons	divide by	3.2291
foot pounds	kilogram meters	divide by	7.23285
foot pounds	Newton meters	multiply by	1.35582
ENERGY			
foot pounds	Joules	multiply by	1.355826
STRESS INTENSITY			
kilo $pound/inch^2$ $inch^{1/2}$ ($ksi\sqrt{in}$)	mega Newton $MNm^{3/2}$	multiply by	1.0998
J-INTEGRAL			
kilo pound/inch	$Joules/mm^2$	multiply by	0.1753
kilo pound/inch	kilo $Joules/m^2$	multiply by	175.3

TABLE OF CONTENTS

LIST OF FIGURES

LIST OF TABLES

1. INTRODUCTION

1.1 Contract Background

BMT Fleet Technology Limited (BMT) was awarded contract W7707-063377/A by Public Works and Government Service Canada (PWGSC) on behalf of Defence Research and Development Canada – Atlantic (DRDC Atlantic). The work is to perform project number SR-1452 of the United State Coast Guard-managed Interagency Ship Structure Committee (SSC). DRDC Atlantic is managing this work on behalf of the SSC.

A project kick off meeting was held at BMT on 24 October 2006, attended by BMT personnel and Mr. James Kent, United States Military Sealift Command (Project Technical Committee Chair) and Mr. Dave Stredulinsky, Defence Research & Development Canada – Atlantic.

1.2 Project Objectives

The broad aims of the project are to examine a possible technology for making a significant improvement to ship structural design through the use of composite materials, used in a hybrid manner with steel. In this project, success will be achieved if a workable hybrid approach can be shown to achieve increased structural performance in comparison with conventional all-steel construction. The increase in performance may be in weight or cost efficiency (or both). The table below lists the key project objectives.

Objective: To study the feasibility of an advanced hybrid hull design for large ships. The main concept is to design a hull that makes efficient use of steel and composite material to jointly resist the global (primary) load, act as a watertight barrier and resist local pressure (secondary and tertiary loads). Scope 3.1.1: The Contractor shall conduct a feasibility study of the use of hybrid hull in large ships, at least as large as a steel destroyer ship (length 120 m, beam 15 m, and molded draft 4.5 m) but preferably as large as a steel cruiser ship (length 160 m, beam 15 m, and molded draft 7 m). Tasks 3.2.1: The Contractor shall establish a preliminary design of a large hybrid hull based on the general concept stated under 'Objective'. The Contractor's specific concept for a large hybrid hull shall be presented to and approved by the Scientific Authority prior to establishing the preliminary design. The hull characteristics should be at least as large as a steel destroyer ship (length 120 m, beam 15 m, and molded draft 4.5 m) but preferably as large as a steel cruiser ship (length 160 m, beam 15 m, and molded draft 7 m).

These objectives differ somewhat from the original version in the contract but were agreed by correspondence with the SSC (Project Technical Committee Chair – Mr Kent, e-mail 22 January 2007) and the contracting authority (Ms. Susan Thorpe, e-mail 5 March 2007).

1.3 Refined Objectives

The project will focus on the hybrid panel (semi-monocoque) concept as shown in Figure 1.1. The hybrid concept will be compared to a conventional all-steel design. There are a few local variants of the concept (see Figure 2.2).

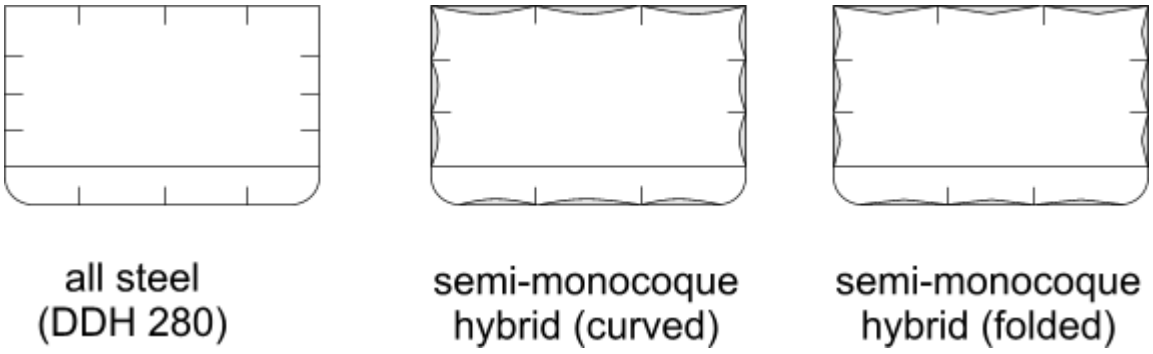

Figure 1.1: Hybrid Hull Concept Development

Monocoque or unibody is a construction technique that uses the external skin of an object to support some or most of the load on the structure. This stands in contrast with using an internal framework (or truss) that is then covered with a non-primary load-bearing skin. In semi-monocoque construction, the external hull plays a significant role in resisting the primary (hull girder) stresses, in addition to the shell and framing resisting the secondary and tertiary (local) loads and stresses.

The project considered designing a new cruiser-sized hull for the baseline, but it was considered that project funds would be better expended on the investigation of the hybrid version of a known hull rather than incurring cost for design of a steel hull. BMT, DRDC Atlantic and the Project Committee Chair investigated the availability of cruiser sized design information from US, Canadian and British navies. The most recent and largest warship for which usable information could be obtained was the Canadian Navy DDH-280 IROQUOIS Class destroyer.

2. HYBRID HULL STRUCTURAL CONCEPT

2.1 Use of Composites in Hull Construction

Composite construction in ships has many desirable features, particularly for military applications. Composites have a higher strength-to-weight ratio than steel, which can lead to reduced weight in the vessel's structure without compromising strength. This provides advantages such as increased payloads, greater speeds, larger ranges and reduced fuel usage. Composites can also have improved resistance to corrosion and a longer fatigue life when compared to steel, as well as having high durability. This has the potential to lead to lower maintenance requirements for a composite vessel, which, along with reduced weight and quantity of material required, can lead to reduced costs for the vessel. From a manufacturing perspective, it may be easier to construct complicated shapes from composites, such as the bow and stern sections required for good hydrodynamic performance. Composites also have reduced retained stresses from construction as compared to steel. For military applications, composites have very desirable stealth characteristics. Unlike steels, composites are non-magnetic, making them less susceptible to mines and torpedoes. They can also be made so they absorb radar energy rather than reflecting it, leading to lower radar cross-sections. Composites have significantly higher damping properties than steels and are, therefore, much quieter in the water. Their thermal properties also allow for considerably lower thermal signatures [1].

Composites have been used successfully in smaller craft construction for many years. However, entirely composite construction in larger vessels is not currently considered feasible. Composite materials do not have the necessary strength to be able to resist the global loads these larger vessels are subjected to, such as bending, shear and torsion. Steel, which has been used successfully in large ships for decades, provides sufficient strength and stiffness to resist these global loads. This has led to the concept of hybrid construction, where the ship structure is constructed of both steel and composites. The use of steel will ensure that the vessel has sufficient global strength, while still allowing the advantages of composite construction to be achieved. The good fatigue and durability properties of composites may also allow for the use of higher strength steels. Using higher strength steels leads to reduced structural weight, but their use in conventional steel ships is limited by fatigue, buckling and corrosion considerations.

Different composite materials were considered early in the project and the findings are presented in Appendix A.

2.2 Hybrid Concept Development

The hybrid concept faces many technical challenges. Composite materials are complex, so designers and manufacturers must have a good understanding of the various types available for use and how to construct these properly. The use of two different materials (steel and composite) will result in load discontinuities, which must be modelled with some accuracy in order to predict the structural response. Development of reliable, practical steel to composite joining techniques is another requirement for the hybrid concept.

The hybrid hull concept envisaged in the Request for Proposals (RFP) consisted of a 3-D steel space frame to resist the global loads, and a composite material to act as a watertight barrier and resist local pressure (secondary and tertiary loads). However, the extreme structural discontinuity between the two materials posed significant concerns in the development of a reliable joint. It was also recognized that the efficiency of present day steel construction comprising shell plate stiffened by frames and stringers could not be met with the original hybrid concept. This led to the development of the semi-monocoque structure shown in Figure 1.1.

In this concept, the shell and decks are made up of hybrid steel-composite panels. Each panel comprizes a dished or shallow-bent, high-strength steel membrane with composite material filling the concave face of the membrane (see Figure 1.1). This concept makes efficient use of the properties of the materials in the hybrid, and the shell structure resists both local (normal) and global (axial) loads. The hybrid steel-composite panels use the steel for strength and the composite to prevent buckling and corrosion. By forming the thin steel into a shallow curve, the steel's membrane capacity (which is much greater than its flexural strength) provides greatly enhanced local strength. The composite material both braces and protects the steel and provides a flat skin (allowing for hydrodynamic performance and aesthetics). From a global strength perspective, the thin steel skin, stiffened against buckling, is very efficient in resisting in-plane loads from hull girder bending. The monocoque approach is very stiff and strong in shear and torsion as well. A more detailed example of this concept applied to the DDH-280 form is shown in Figure 2.1.

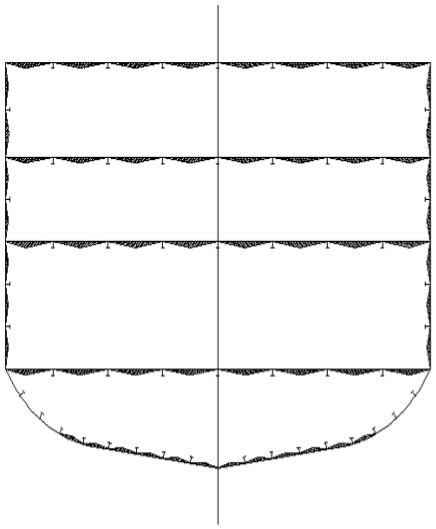

Figure 2.1: Detailed Panel Layout Example

The primary strength element of this hull concept is the plate panel. The hybrid panels shown in Figure 2.2 were initially considered for analysis to determine the influence of the various design parameters on the strength, and the strength/weight ratios.

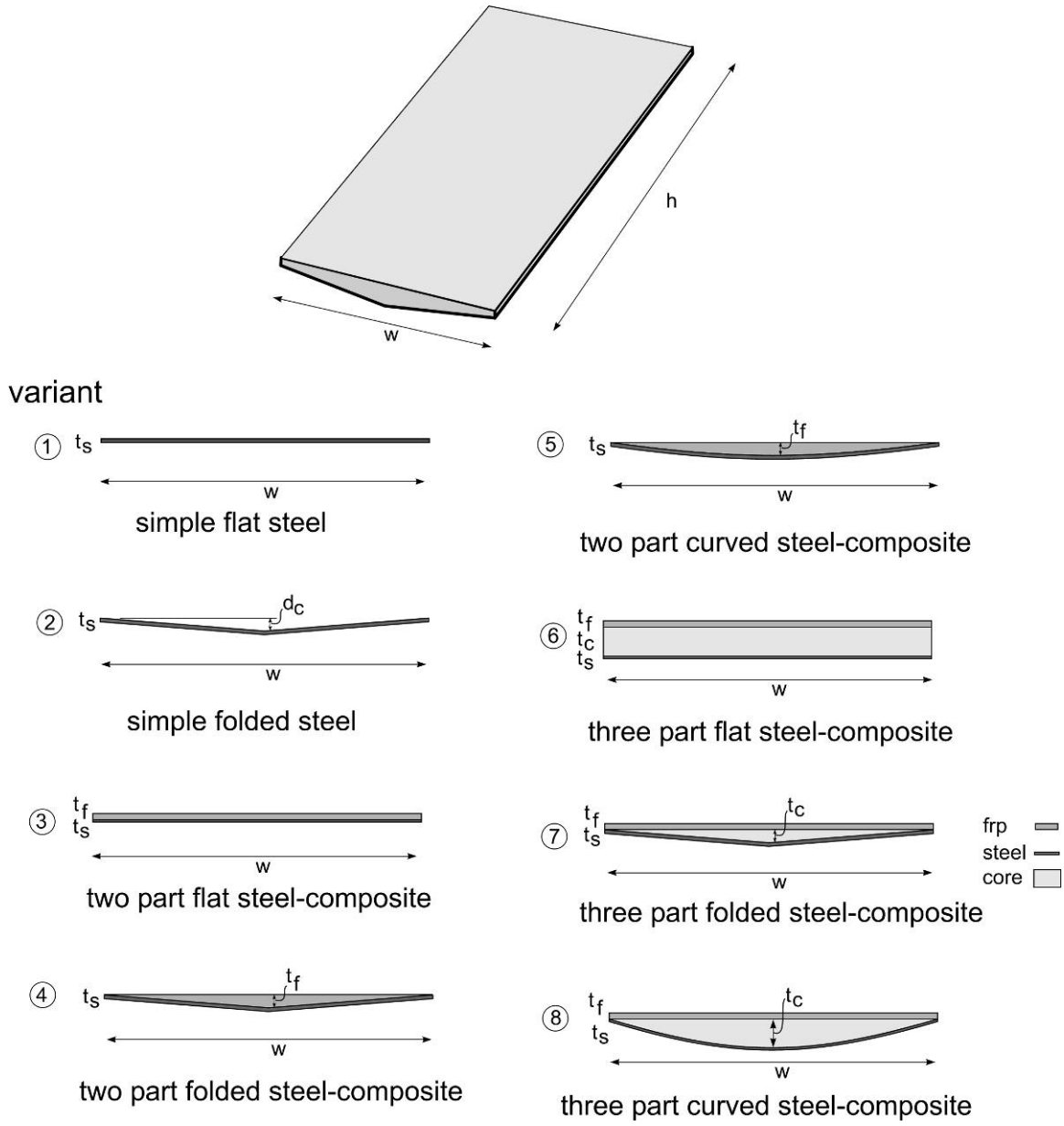

Figure 2.2: Hybrid Panel Types

The initial exploration of panel capacities was performed according to the evaluation matrix outlined in Table 2.1. After the initial analysis matrix is complete, an assessment of the potential solutions will be made and a refined matrix will be developed. Following this stage, viable panels should be available to continue to the next step. The panel capacity was to be examined using analytical and finite element methods, for both pure in-plane loads, pure lateral loads and the combination of the two. The full non-linear behaviour was to be established and compared to all-steel panels.

Table 2.1: Initial Analysis Matrix

	variant							
	1	2	3	4	5	6	7	8
description / parameter	Flat 1-layer	Folded 1-layer	Flat 2-layer	Folded 2-layer	Curved 2-layer	Flat 3-layer	Folded 3-layer	Curved 3-layer
Panel height, h	2000, 4000 mm							
Panel width, w	800, 1200, 2000 mm							
Steel thickness, t_s	5, 10, 20 mm							
Steel modulus, E_s	200 GPa							
Steel strength, σ_y	300, 500, 800 MPa							
frp thickness, t_f			10, 30, 90 mm					
frp modulus, E_f			4, 8 GPa					
frp strength (x), σ_{fx}			20, 40, 60 MPa					
frp strength (‖) σ_{fp}			50, 100, 150 MPa					
core thickness, t_c						50, 80, 120 mm		
core shear strength, τ_c						5, 10, 15 MPa		

After the preliminary analysis the focus of the study was narrowed to a subset of the initially proposed panel types. The simple flat steel panel (variant 1 in Figure 2.2) was taken as the baseline type and folded panels with and without composite fairing (variants 2 and 4) were selected for detailed analysis.

3. PARENT HULL

The steel baseline hull form used is the DDH-280 destroyer class of the Canadian Navy, also known as the Iroquois Class. Commissioned in 1972, the DDH 280 "Iroquois" was the first of the Tribal-Class Destroyers for the Canadian Navy. Given the time this class of vessels has been in service, it was regarded as a proven hull and an appropriate basis for the hybrid hull structural design, as it allowed the focus to be placed on determining potential for structural improvements through the use of hybrid construction. A picture of the DDH-280 is shown below in Figure 3.1.

Figure 3.1: DDH-280 Destroyer

Principal particulars of the vessel are presented in Table 3.1

Table 3.1: DDH-280: Principal Particulars

Length overall	129.8 m
Beam	15.24 m
Draught	4.42 m
Hull depth	9 m
Displacement	5100 t
Speed	29 kn

Apart from the publicly available information about the parent vessel (principal particulars, displacement, speed, etc.) BMT obtained a full set of structural drawings and the General Arrangement Plan (GA). This information was used as a basis for the structural, hydrostatic and seakeeping models developed in the course of the project.

Several attempts were made to obtain the weight distribution data for the parent hull without success. Since this information was needed for loads calculations, in particular for the still water and dynamic bending moments, an assumption had to be made in order to complete the analysis.

In the absence of better inputs, a linear longitudinal weight distribution was assumed. The assumption has certainly resulted in the calculated loads departing from the actual ones but since the study is of comparative nature, this was deemed acceptable.

4. FE ANALYSIS

4.1 FE Introduction

The Finite Element (FE) model corresponds to an isolated, stiffened panel from the bottom shell of the DDH-280. Still in operation, the vessel has had some minor modifications to the structure over its service life (typically, additional stiffening elements at specific locations). Figure 4.1illustrates the midships (Frame 34) structural arrangement at the bottom shell in way of the keel and at the location of the finite element model. At this location, the stiffened panels span between transverse frames that are spaced at about 6 ft (or 1830 mm). The distance between the centerline longitudinal girder and the first primary longitudinal girder is 9 ft (or 2743 mm).

For the parametric study, three configurations of the stiffened panel are considered:

i. the existing conventional, flat steel panel;
ii. a set of steel panels having bent shell plating and with varying shell thickness; and
iii. a set of hybrid panels having bent shell plating and with varying shell thickness.

The hybrid panel design includes the application of a layer of composite to the outer surface of the bent, bottom shell plating. The thickness of the composite layer is taken as a function of the height of the bend in the plate relative to the flat condition for (i), above. While not identified as a specific product or technology, the material properties (with regards to strength) of the composite are similar to that of a chopped-strand or premix fibre reinforced plastic. The effect of the composite on the buckling capacity of the stiffened panel is evaluated assuming linear-elastic properties and a range of values for the modulus of elasticity. The performance of the composite, whether acting independently or in conjunction with the steel structure, across the full range of operating conditions (and including fabrication, maintenance and repair) is not considered within the scope of this analysis.

An initial hydrostatic pressure is applied to the bottom face of the bottom shell (consistent with the still-water operating draft of the vessel). To determine the critical buckling load, an in-plane displacement is applied incrementally to the panel's transverse ends until the peak load is reached. Aside from the deflections associated with the application of the hydrostatic pressure, no initial imperfections or residual stresses are included in the analysis. Also, the behaviour of the stiffened panels in the post-buckling range is not investigated. As only the buckling capacity of the panel, and not the actual mechanism of failure (i.e. out of plane buckling of stiffeners, plating buckling, etc), is of interest for this analysis, these failure modes are not captured in this analysis.

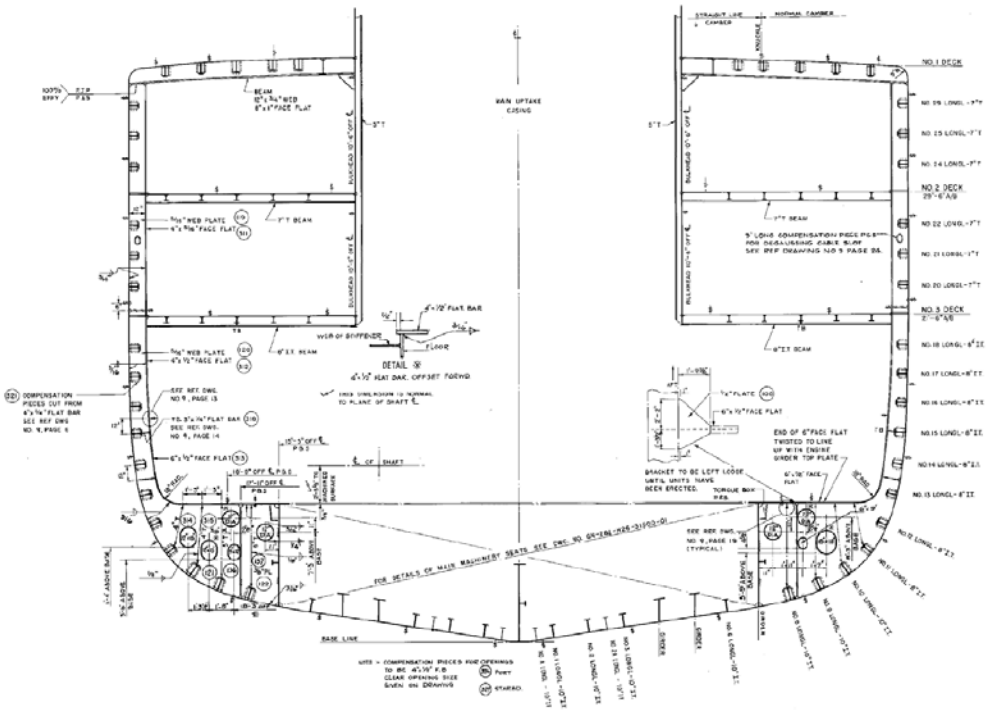

(a) Midship section at Frame 34 Looking Aft

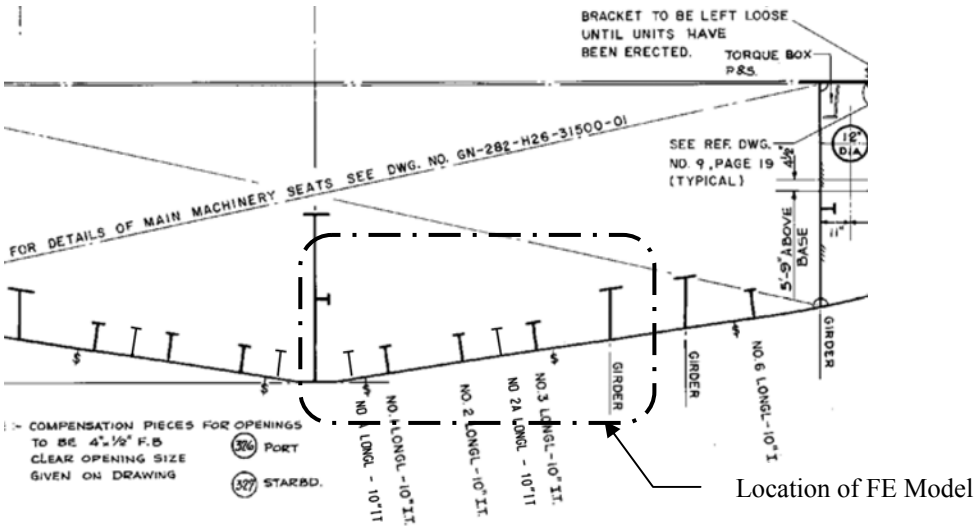

(b) Detail at Shell Bottom

Figure 4.1: DDH 280 Framing at Location of FE Model

4.2 Finite Element Model Description

4.2.1 Geometry

The geometry of the finite element model is based on the structural arrangement of the DDH 280 "Iroquois" taken at the bottom shell at midships, between Frame 33 and Frame 34. Between the ship centerline and the first primary longitudinal girder off centerline, the existing structure consists of bottom shell plating 7/16 inches thick (11.1 mm) with five inverted tee longitudinal stiffeners. The inverted tees are 10.1 inches deep (254 mm) having a 0.24 inches thick web (6.1 mm) and a face flat measuring 4 inches wide (101.6 mm) and 0.33 inches thick (8.4 mm). The bottom shell is inclined relative to the baseline. The existing frame spacing at midships is 6 feet (1830 mm).

As shown in Figure 4.1(b), the area of interest extends between Frame 33 and Frame 34 and from the centerline at keel to the first primary longitudinal girder off centerline, at a distance of 9 feet 0 inches. The secondary stiffening originally consisted of three longitudinals spaced (approximately) equally over the 9-foot-0-inch span. Since about 1996, the midships drawing of Figure 4.1(a) illustrates two additional longitudinal stiffeners, of the same size and type, inserted between the keel and longitudinal #1 and between longitudinals #2 and #3.

The geometry of the finite element is consistent with the structural arrangement in the area of Figure 4.1(b), with the following simplifications: the stiffened panel is taken as flat, rather than inclined and the longitudinal stiffeners are taken as equally spaced at 18 inches (457 mm) across the panel width. Figure 4.2(a) illustrates the geometry for the finite element model representing the conventional panel configuration. As shown, the flat shell plate is stiffened by five equally spaced, inverted tee longitudinals. A baseline condition for the parametric study is given using this model geometry and the existing scantlings.

Figure 4.2(b) illustrates the geometry corresponding to the bent shell plate configuration used for the evaluation of the conventional steel panel with bent shell plate and of the hybrid panel design. For the parametric study, only the thickness of the shell plating and the height of the plate bend have been varied for a panel. For the hybrid panels, the height of the plate bend is considered as a scalar function of the plate thickness:

$$h_{bend} = f_{bend}\, t_{shell}$$

where, h_{bend} is the distance between the flat baseline and the bottom face of the bent shell plating; f_{bend} is the bend factor and t_{shell} is the thickness of the shell plating.

The panels have also been evaluated using a frame spacing of either 6 feet (1830 mm), which is equal to the existing frame spacing at this location, or 9 feet (2743 mm). It is noted that a panel spanning 9 feet between transverse frames would have a different stiffener arrangement and/or scantlings. The 9-foot panel is analyzed using the same scantlings and arrangement solely for the purpose of making a direct comparison to the 6-foot panel and for illustration of the effects associated with the bent shell plate, with and without the application of a composite.

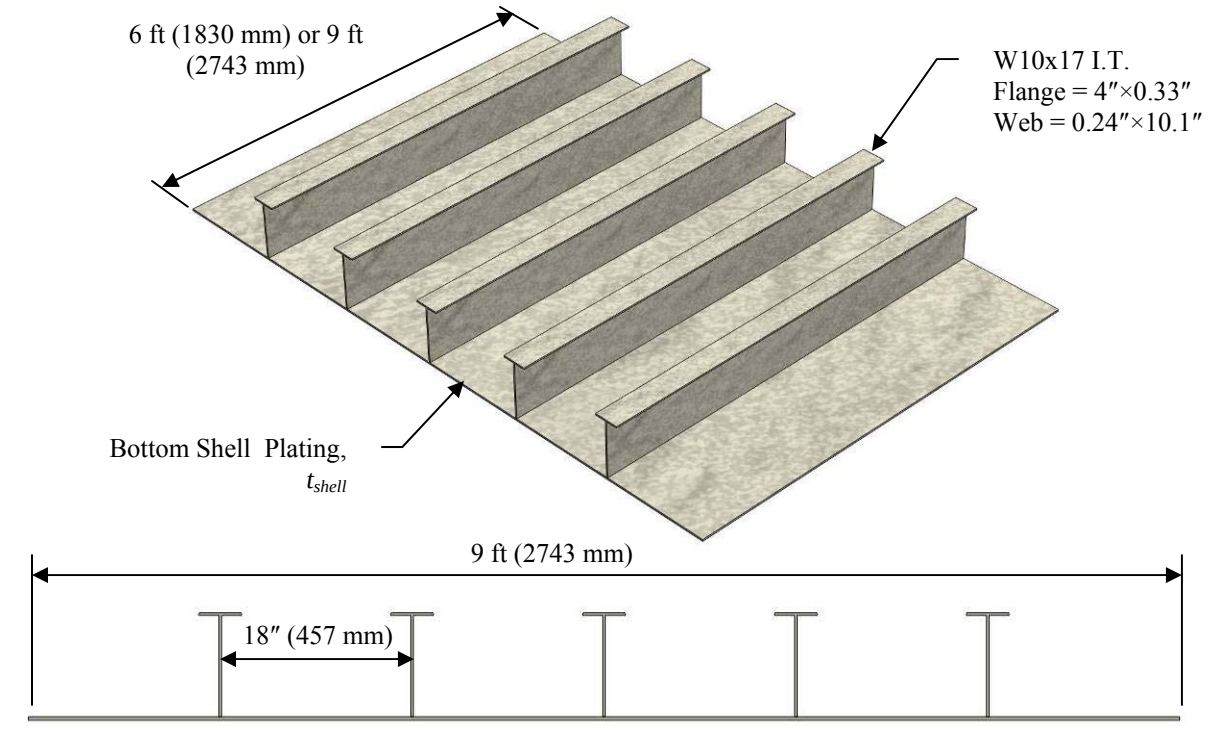

(a) Conventional Steel Panel

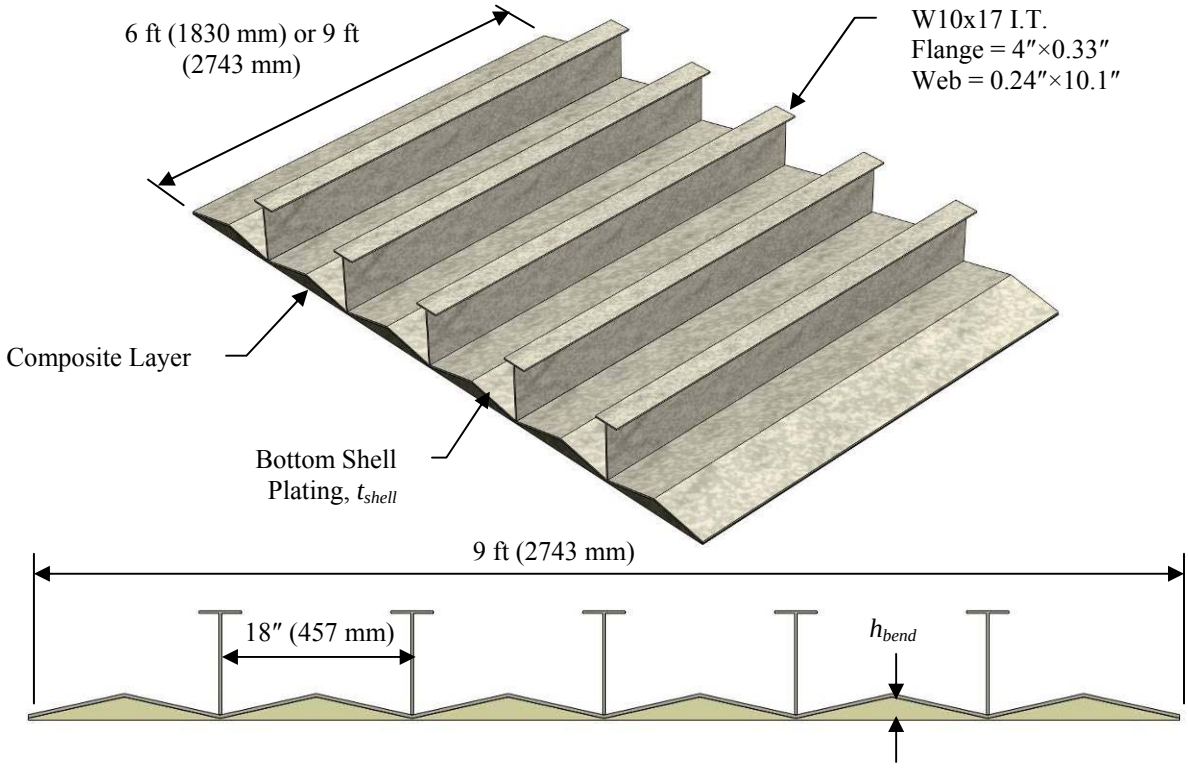

(b) Hybrid Panel

Figure 4.2: Conventional Steel and Hybrid Panel Configurations

4.2.2 Material Properties

In all cases, the material properties for Grade A 235 steel correspond to the stress-strain relationship illustrated in Figure 4.3, for which the modulus of elasticity is 206 000 MPa and the yield stress is 235 MPa. The density of steel is 7850 kg/m^3 and Poisson's ratio is taken as 0.287.

It is assumed that the composite material for the hybrid panel corresponds to a chopped-strand mat or premix having a density of 1500 kg/m^3. Since the analysis is limited to the examination of the load associated with the initial buckling of a stiffened panel, the composite is taken as a linear-elastic material only, effective over the full range of the stress-strain relationship for steel. Correspondingly, an ideal bond strength is assumed between the composite and the steel. Since the composite is considered in general terms for this evaluation, only generalized material properties (not associated with a specific composite product or application) are assumed. Thus, the behaviour of the hybrid panel has been evaluated using a modulus of elasticity for the composite layer of 10 GPa, which is consistent with a typical chopped-strand FRP. In addition, the analysis of the hybrid panels has included a range of values for the modulus of elasticity including 10 MPa, 100 MPa, 1000 MPa and 20 GPa.

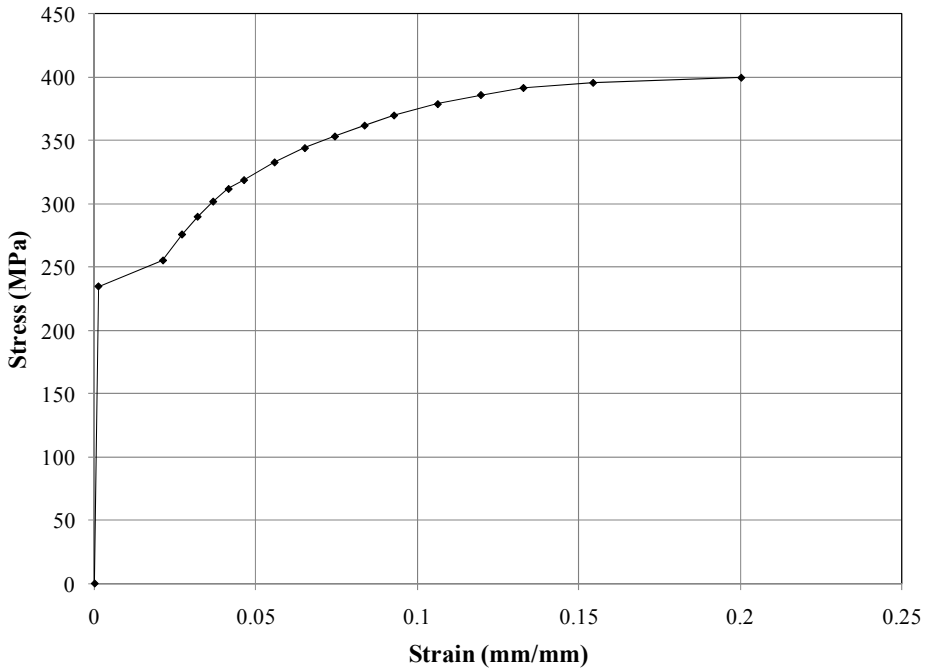

Figure 4.3: Multi-linear Stress-Strain Relationship for Grade A 235 Steel

4.2.3 Finite Elements

The topology of the finite element model is three-dimensional solids (volumes). However, due to the relatively thin volumes associated with both the shell plating and the longitudinal stiffeners, an element having a solid volume topology but shell element (surface) behaviour was required to mesh the FE geometry. The element overcomes issues associated with excessive aspect ratios resulting from meshing thin volumes with a refinement sufficient to capture the

required behaviour. In ANSYS (version 11.0), the SOLSH190 element was selected for this purpose. Since the volumes associated with the composite, when applied, are relatively thick, a more typical solid element (SOLID185) was used. These are each described subsequently.

4.2.3.1 SOLSH190

SOLSH190, shown in Figure 4.4(a), is used for simulating shell structures with a wide range of thickness (from thin to moderately thick). The element possesses the continuum solid element topology and features eight-node connectivity with three degrees of freedom at each node: translations in the nodal x, y, and z directions. Thus, connecting SOLSH190 with other continuum elements requires no additional effort. The element has plasticity, hyperelasticity, stress stiffening, creep, large deflection and large strain capabilities. The element formulation is based on logarithmic strain and true stress measures.

4.2.3.2 SOLID185

SOLID185, shown in Figure 4.4(b), is used for modeling general 3-D solid structures. It is defined by eight nodes having three degrees of freedom at each node: translations in the nodal x, y, and z directions. The element has plasticity, hyperelasticity, stress stiffening, creep, large deflection and large strain capabilities. It also has mixed formulation capability for simulating deformations of nearly incompressible elastoplastic materials and fully incompressible hyperelastic materials.

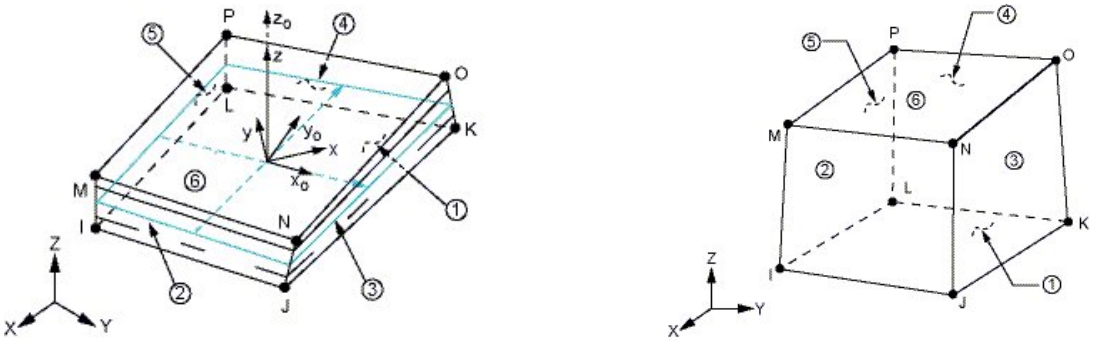

(a) SOLSH190 **(b) SOLID185**

Figure 4.4: Finite Element Types

4.2.4 Boundary Conditions

Figure 4.5 illustrates the meshed finite element model for the hybrid panel configuration and identifies the boundary conditions. Those for the conventional steel panel are equivalent. The boundary conditions for the plate represent the support provided by the centerline girder and the first longitudinal girder (at 9 feet 0 inches off centerline) along the longitudinal edges. Those across the aft and forward ends correspond to the support provided by the transverse frames at Frame 34 and Frame 33, respectively. Note the vertical translational constraints applied are valid for the local model analysis only. For analysis of global ship behaviour, the effects associated with hogging or sagging, as well as for hydrostatic pressures applied to the hull overall, would require this vertical constraint at the supporting transverse frames to be released.

4.2.5 Applied Loading

The applied loading on each panel for the analysis is considered as two components: (i) static hydrostatic pressure and (ii) end displacement. The hydrostatic pressure component is that associated with the normal operating draft of the vessel, which is taken as 4,900 mm, applied uniformly over the bottom face of either the shell plating for the conventional steel panel configuration or of the composite face for the hybrid panel configuration.

A compressive displacement is applied longitudinally (negative X-direction) at the forward end while the aft end remains fixed in position. The displacement is incremented just until the buckling load is achieved since an examination of the post-buckling behaviour of the panel is not considered for this study. Figure 4.6 illustrates the applied loading using the model for the hybrid panel configuration.

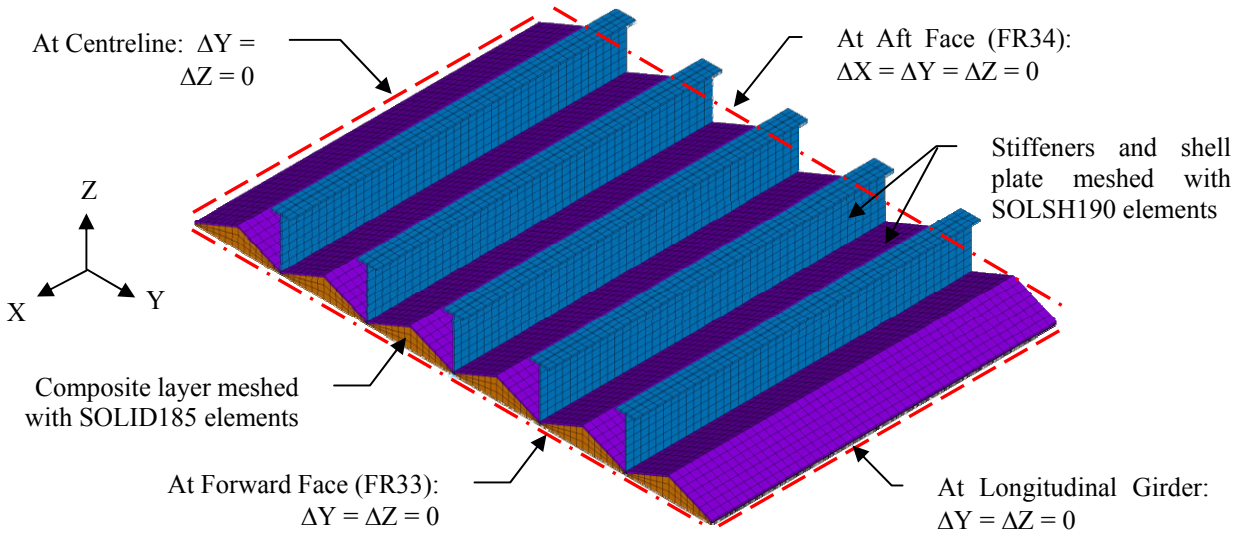

Figure 4.5: Finite Element Model Boundary Conditions

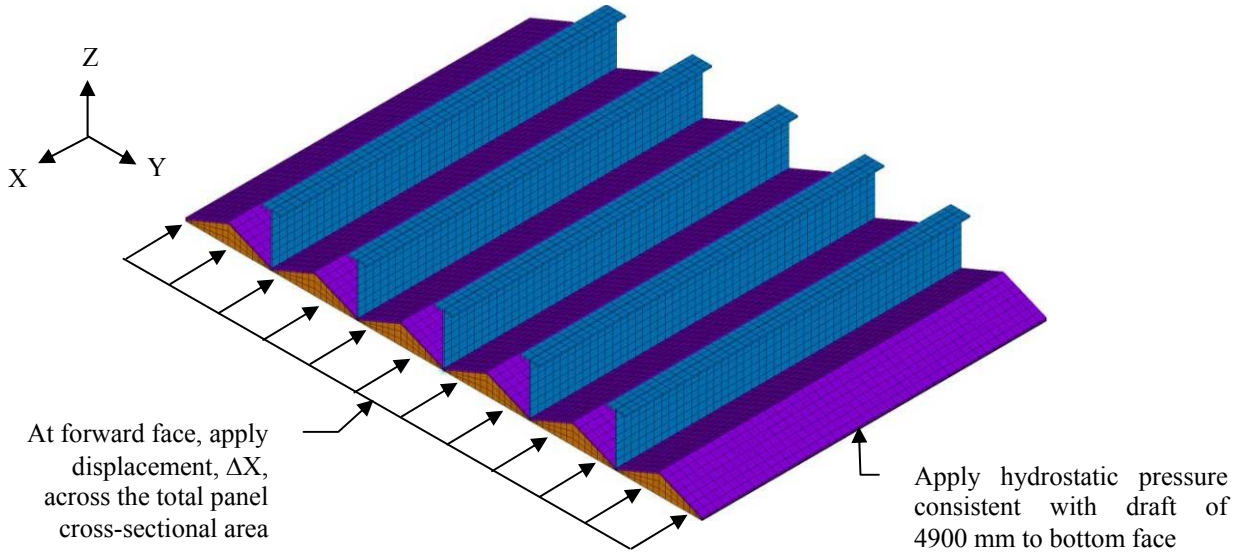

Figure 4.6: Finite Element Model Applied Loading

4.3 Analytical Calculations

4.3.1 Conventional Steel Panel Configurations

To establish a baseline for subsequent comparison the stiffened, flat conventional steel panel was analyzed in the existing condition with a bottom shell thickness of 7/16 inches (11.1 mm) and a panel length of 6 feet (1830 mm). This baseline configuration has an approximate moment of inertia (based on the cross-sectional area of steel), $I_x = 61.4 \times 10^6$ mm^4 and a minimum section modulus, $S_{top} = 351 \times 10^3$ mm^3.

Table 4.1 lists the calculated section properties for the panels with t_{shell} carried between 3/16 inches (4.8 mm) and 7/16 inches (11.1 mm) by a thickness of 1/16 inches and for the three values of f_{bend} considered for the analyses: 0, 0.5 and 0.10. Also included are the ratios of S_{top} to S_{bottom} for each configuration. (Note that the minimum section modulus corresponds to S_{top}, at the top face of the longitudinal stiffener.) For the baseline configuration the ratio of S_{top} to S_{bottom} is about 0.52, indicating that the steel section is unbalanced with the neutral axis at an elevation of 90.2 mm, passing close to, but below the mid-height of the stiffeners, 139.4 mm (using the bottom face of the shell plating as a datum). For the same shell plate thickness, the effect of f_{bend} is to increase the elevation of the neutral axis, which balances the section properties, though with some reduction relative to the baseline condition. For example, with $f_{bend} = 10.0$ and $t_{shell} = 0.4375$ inches the ratio of S_{top} / S_{bottom} is now increased to 0.65 but the respective values are reduced to 0.47 and 0.59 times their original values. Table 4.1 also provides the values for S_{bottom} and S_{top} for each configuration relative to the corresponding values for the baseline configuration with $f_{bend} = 0$ and $t_{shell} = 0.4375$ inches. Figure 4.7 illustrates the calculated section modulus versus the bend factor for each configuration.

Table 4.1: Calculated Steel Section Properties

Shell, t_{shell} (in)	Bend		Moment of Inertia, I_x	Section Modulus		S_{top} / S_{bottom}	S_{bot} / $(S_{bot})_{Baseline}$	S_{top} / $(S_{top})_{Baseline}$
	f_{bend}	Height (mm)	($\times 10^6$ mm^4)	S_{bot} ($\times 10^3$ mm^3)	S_{top} ($\times 10^3$ mm^3)			
0.1875	0	0.0	42.7	346	302	0.87	0.51	0.86
	5.0	23.8	41.0	332	290	0.87	0.49	0.82
	10.0	47.6	38.7	312	274	0.88	0.46	0.78
0.2500	0	0.0	48.3	428	317	0.74	0.63	0.90
	5	31.8	45.1	398	297	0.75	0.58	0.85
	10	63.5	40.6	353	271	0.77	0.52	0.77
0.3125	0	0.0	53.2	512	330	0.65	0.75	0.94
	5	39.7	48.0	455	301	0.66	0.67	0.86
	10	79.4	40.3	369	259	0.70	0.54	0.74
0.3750	0	0.0	57.5	596	341	0.57	0.88	0.97
	5	47.6	49.9	501	302	0.60	0.74	0.86
	10	95.3	38.0	359	238	0.66	0.53	0.68
0.4375	0	0.0	61.4	681	351	0.52	1.00	1.00
	5	55.6	50.9	534	300	0.56	0.79	0.85
	10	111.1	33.4	321	208	0.65	0.47	0.59

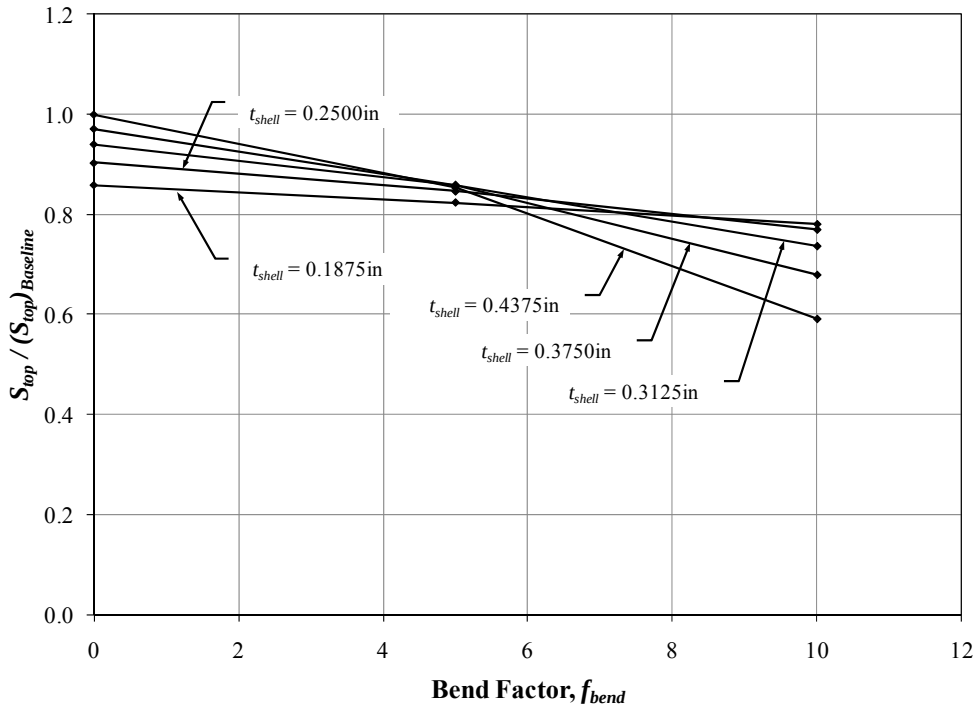

(a) Section Moduli at Top (Top of Stiffener Flange)

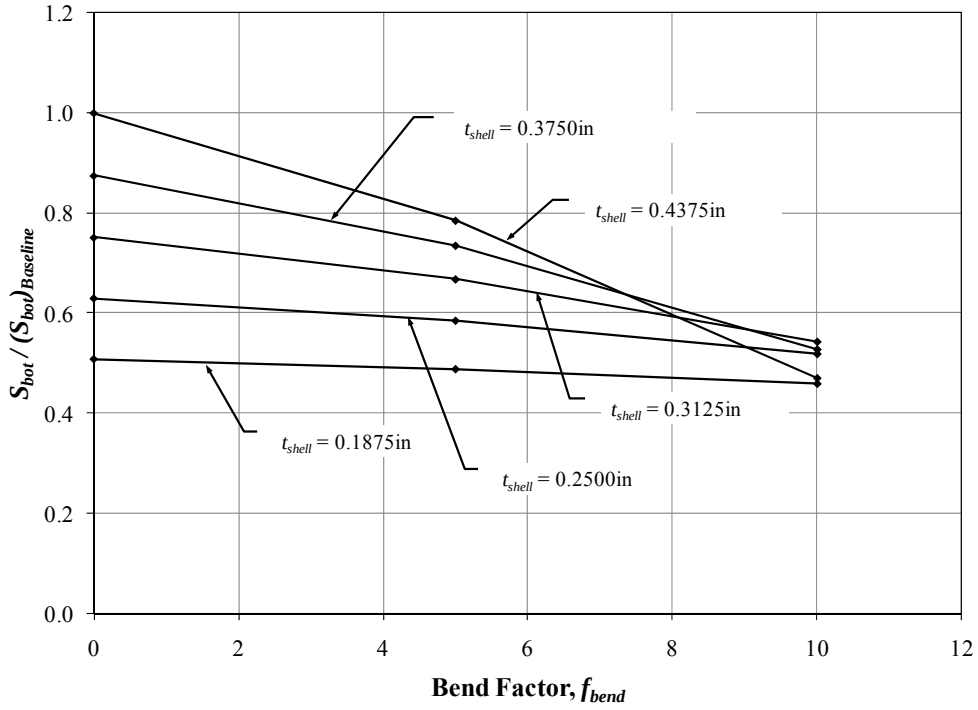

(b) Section Moduli at Bottom (Bottom of Shell Plate)

Figure 4.7: Steel Section Modulus vs. Bend Factor

The panel buckling load was calculated for each panel configuration having a bottom shell plating thickness varying between 3/16 inches (4.8 mm) and 7/16 inches (11.1 mm) and a panel span of 6 feet (1830 mm) or 9 feet (2743 mm). In addition, the panel buckling loads were calculated for the folded conventional steel panels using $f_{bend} = 5.0$ and $f_{bend} = 10.0$. Table 4.2 lists the matrix of analyzed conventional panel configurations with the estimated volume and mass quantities for the steel (based on the finite element model). For the bent conventional panels, the difference in the volume of the shell plating due to the bends (small increase in length between stiffening elements) is included. Table 4.2 also lists the mass of each panel design relative to the baseline condition, identified as panel A-5. The loading considered in this analysis would appear on a ship in hogging condition.

Figure 4.8(a) and Figure 4.8(b) illustrate the calculated load-deflection curves and the normalized stress-mass curves, respectively, for the 6 foot and 9 foot long, flat steel conventional panel models when the shell plate thickness varies from 3/16 inches to 7/16 inches. The maximum applied stress (σ_{max}) is based on the maximum calculated reaction (R_{max}) for the range of applied displacement relative to the cross-sectional area of steel (A_{steel}).

$$\delta_{max} = \frac{R_{max}}{A_{steel}}$$

The normalized maximum stresses (σ_{max}) are plotted relative to the nominal yield stress of the Grade A 235 steel ($\sigma_y = 235$ MPa) versus the mass of the panel relative to that for panel A-5 (the baseline configuration) in Figure 4.8(b).

The calculated out-of-plane deflections, longitudinal normal stresses and transverse normal stresses for the baseline panel A-5 are shown in Figure 4.9, Figure 4.10 and Figure 4.11, respectively. The buckled mode of the shell plating and longitudinal stiffeners is evident in the deflected shapes, which are shown scaled by a factor of 10 and at three points during the buckling analysis, including (a) following the application of the hydrostatic pressure load (b) at the displacement corresponding to σ_{max}; and, at the final applied end displacement (which is arbitrary and varies between analyses).

Similarly, Figure 4.12, Figure 4.13 and Figure 4.14 illustrate the calculated out-of-plane deflections, longitudinal normal stresses and transverse normal stresses for the 9-foot long panel D-5. Although the calculated results for the 9-foot panels will be tabulated, detailed finite element plots for the deflections and stresses for these panels will not be shown further.

Figure 4.15(a) and Figure 4.15(b) illustrate the load-deflection curves and the normalized peak stresses versus normalized mass, respectively, for panel sets B and E corresponding to the bent conventional steel panels with $f_{bend} = 5.0$ and a panel length of 6 feet and 9 feet. The finite element plots illustrating the calculated deflections and stresses are shown for panel B-5 (shell plating thickness of 7/16 inches) in Figure 4.16, Figure 4.17 and Figure 4.18. The finite element results corresponding to panel C-6 (again, shell plating thickness of 7/16 inches) are shown in Figure 4.19 to Figure 4.22.

Table 4.3 summarizes the calculated results for the conventional steel panel configurations.

Table 4.2: Quantities for the Conventional Steel Panel Configurations

Panel Designation			Shell Thickness (in)	Shell Thickness (mm)	Bend f_{bend}	Bend Height (mm)	Volume (m^3) Steel	Volume (m^3) Composite	Mass (kg) Steel	Mass (kg) Composite	Mass (kg) Total	Relative to Baseline at A-5
6 ft Long Panels	A	1	3/16	4.8	0	0	0.046	0	361	0	361	0.591
		2	1/4	6.4	0	0	0.054	0	424	0	424	0.693
		3	5/16	7.9	0	0	0.062	0	486	0	486	0.795
		4	3/8	9.5	0	0	0.070	0	549	0	549	0.898
		5	7/16	11.1	0	0	0.078	0	611	0	611	1.000
	B	1	3/16	4.8	5	23.8	0.046	0	362	0	362	0.592
		2	1/4	6.4	5	31.8	0.054	0	425	0	425	0.695
		3	5/16	7.9	5	39.7	0.062	0	489	0	489	0.799
		4	3/8	9.5	5	47.6	0.070	0	553	0	553	0.904
		5	7/16	11.1	5	55.6	0.079	0	618	0	618	1.011
	C	1	3/16	4.8	10	47.6	0.046	0	363	0	363	0.594
		2	1/4	6.4	10	63.5	0.055	0	428	0	428	0.701
		3	5/16	7.9	10	79.4	0.063	0	495	0	495	0.811
		4	3/8	9.5	10	95.3	0.072	0	565	0	565	0.924
		5	7/16	11.1	10	111.1	0.081	0	636	0	636	1.041
9 ft Long Panels	D	1	3/16	4.8	0	0	0.069	0	542	0	542	0.886
		2	1/4	6.4	0	0	0.081	0	635	0	635	1.040
		3	5/16	7.9	0	0	0.093	0	729	0	729	1.193
		4	3/8	9.5	0	0	0.105	0	823	0	823	1.347
		5	7/16	11.1	0	0	0.117	0	917	0	917	1.500
	E	1	3/16	4.8	5	23.8	0.069	0	542	0	542	0.887
		2	1/4	6.4	5	31.8	0.081	0	637	0	637	1.043
		3	5/16	7.9	5	39.7	0.093	0	733	0	733	1.199
		4	3/8	9.5	5	47.6	0.106	0	829	0	829	1.357
		5	7/16	11.1	5	55.6	0.118	0	926	0	926	1.516
	F	1	3/16	4.8	10	47.6	0.069	0	545	0	545	0.891
		2	1/4	6.4	10	63.5	0.082	0	643	0	643	1.051
		3	5/16	7.9	10	79.4	0.095	0	743	0	743	1.216
		4	3/8	9.5	10	95.3	0.108	0	847	0	847	1.385
		5	7/16	11.1	10	111.1	0.122	0	954	0	954	1.561

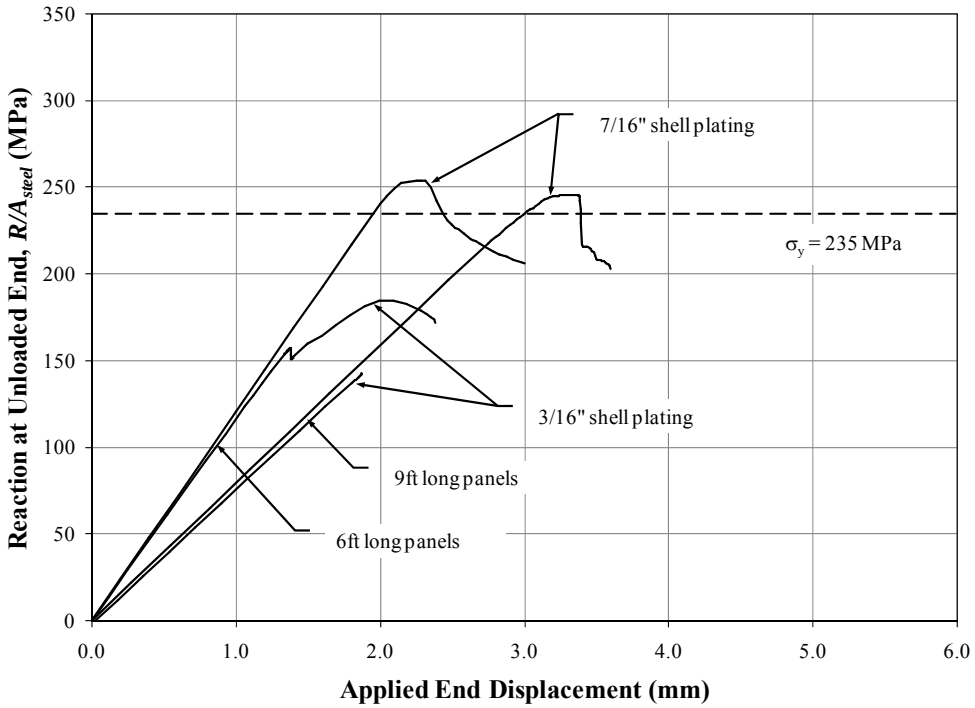

(a) Load-Deflection Curves for Panels A-1/A-5 and D-1/D-5

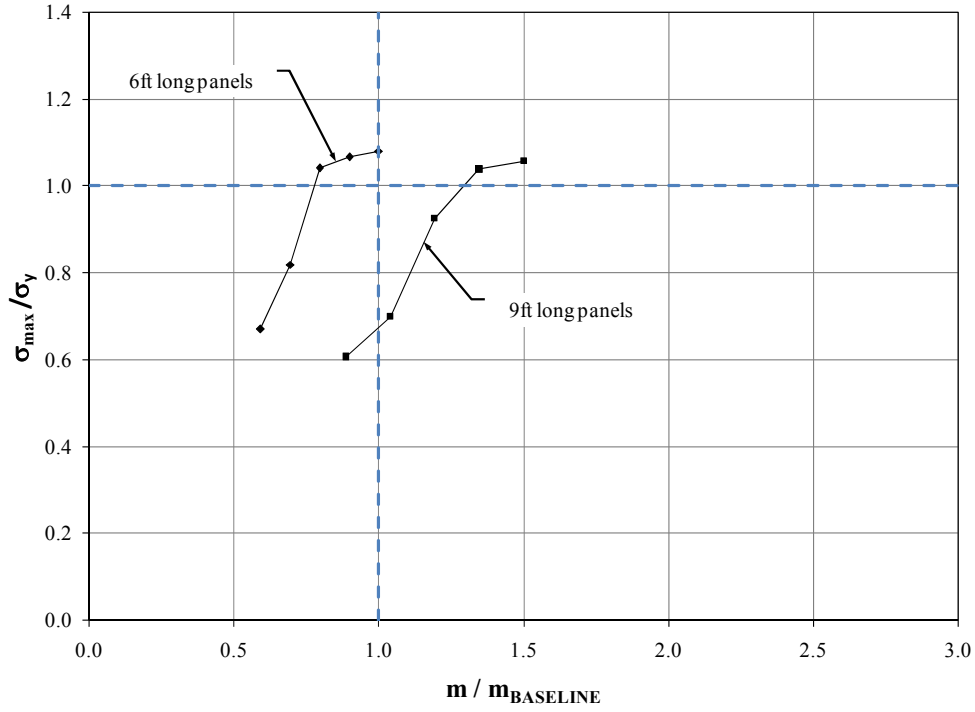

(b) Normalized Stress-Mass Curves for Panels A-[1:5] and D-[1:5]

Figure 4.8: Calculated Results for the Flat Conventional Panel Configurations

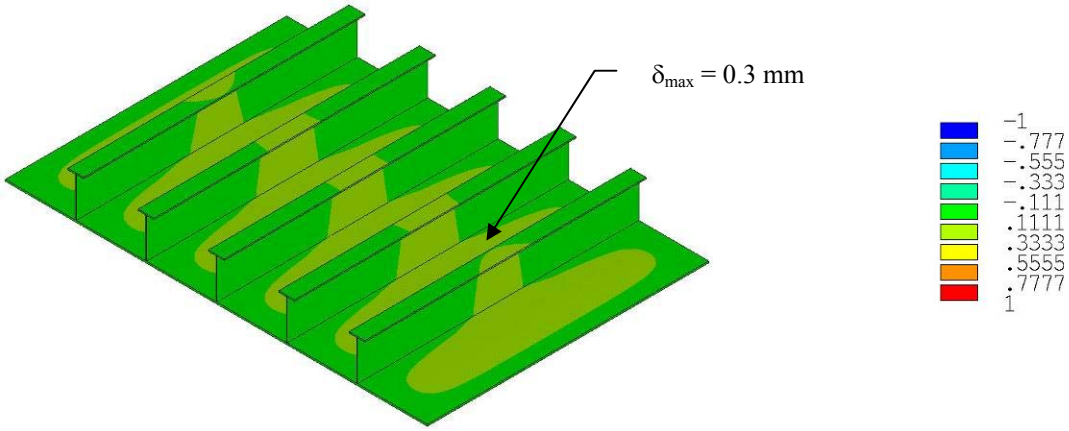

(a) Hydrostatic pressure load (no applied end displacement)

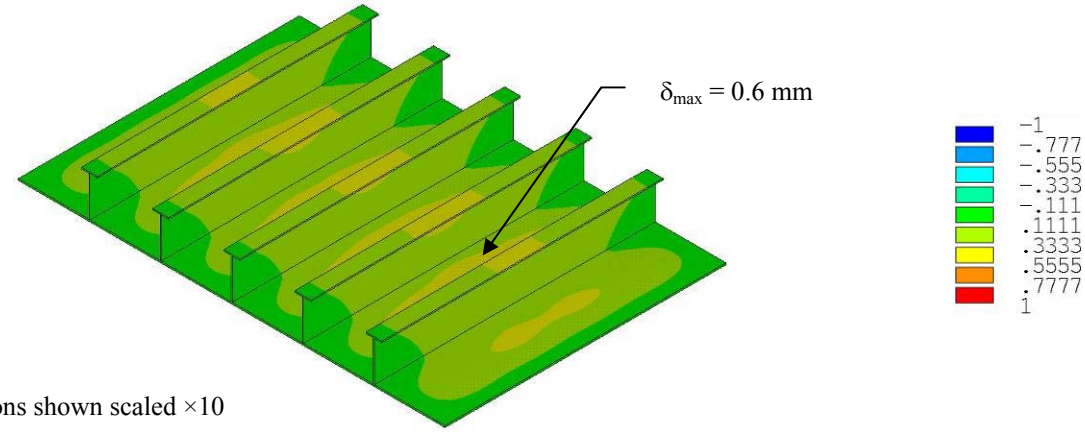

Note:

- Deflections shown scaled ×10

(b) At σ_{max} (or applied end displacement of 2.2 mm)

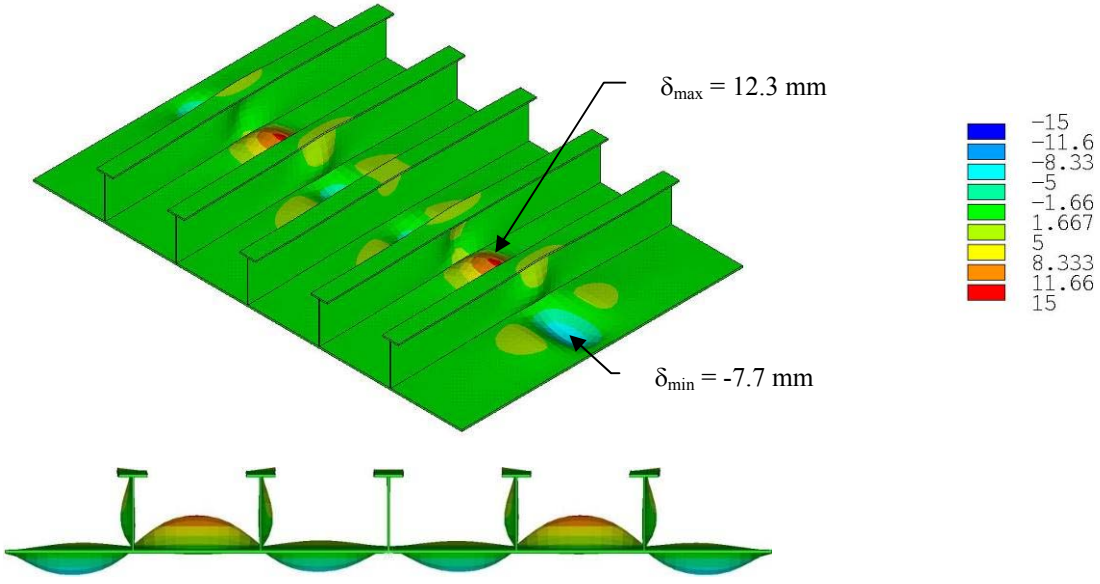

(c) At final applied end displacement of 3.0 mm

Figure 4.9: Calculated Out-of-Plane Deflections for Conventional Panel A-5 (mm)

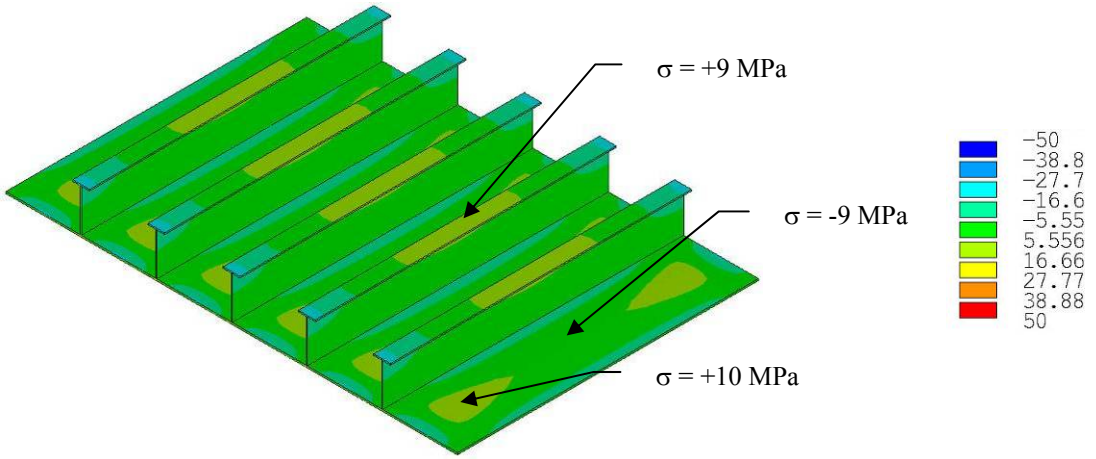

(a) Hydrostatic pressure load (no applied end displacement)

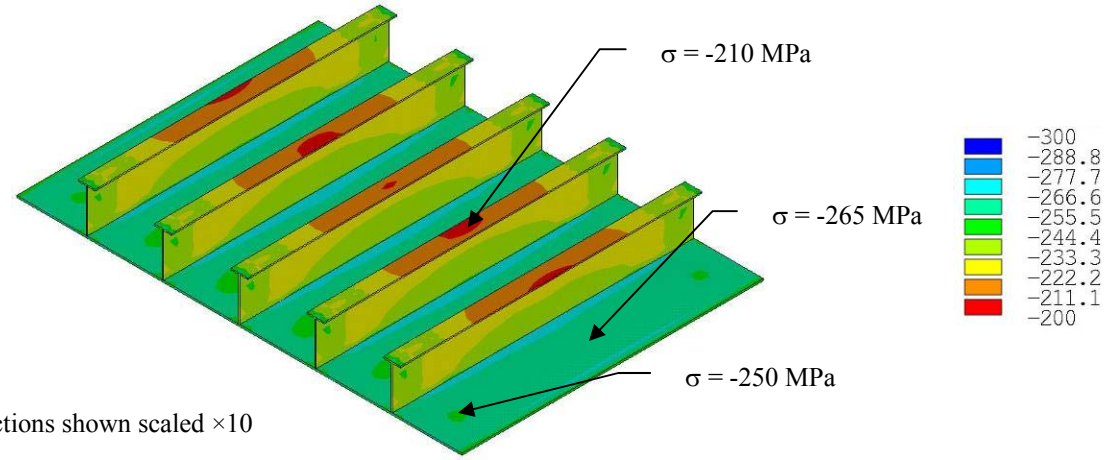

Note:
- Deflections shown scaled ×10

(b) At σ_{max} (or applied end displacement of 2.2 mm)

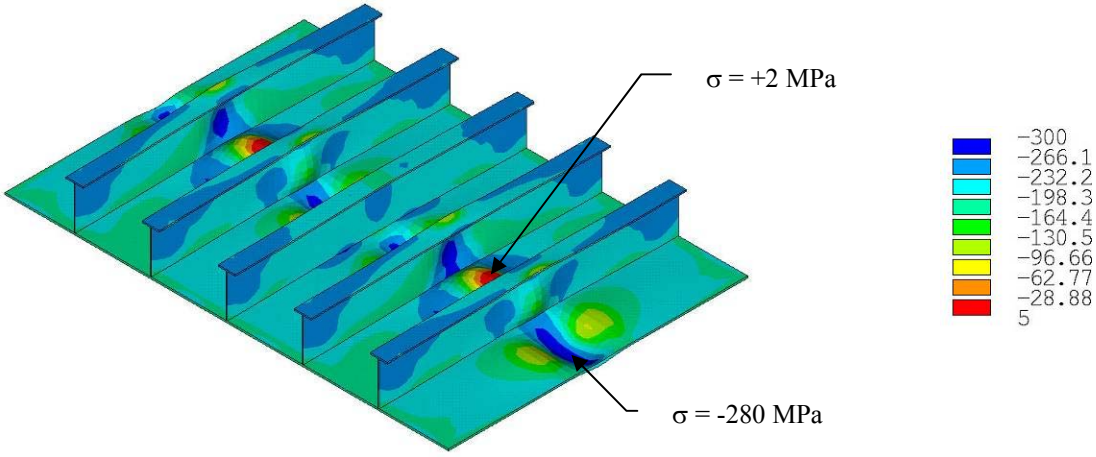

(c) At final applied end displacement of 3.0 mm

Figure 4.10: Calculated Longitudinal Normal Stresses for Conventional Panel A-5 (MPa)

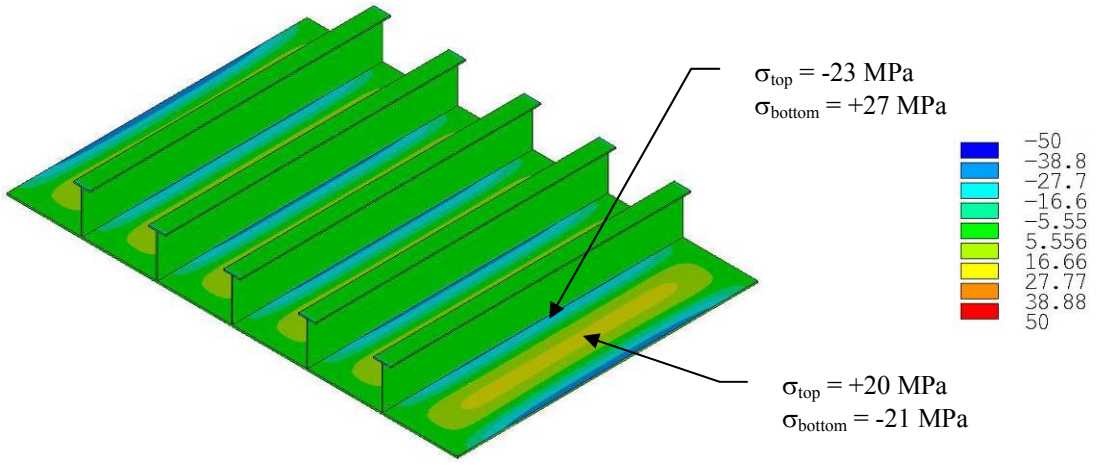

(a) Hydrostatic pressure load (no applied end displacement)

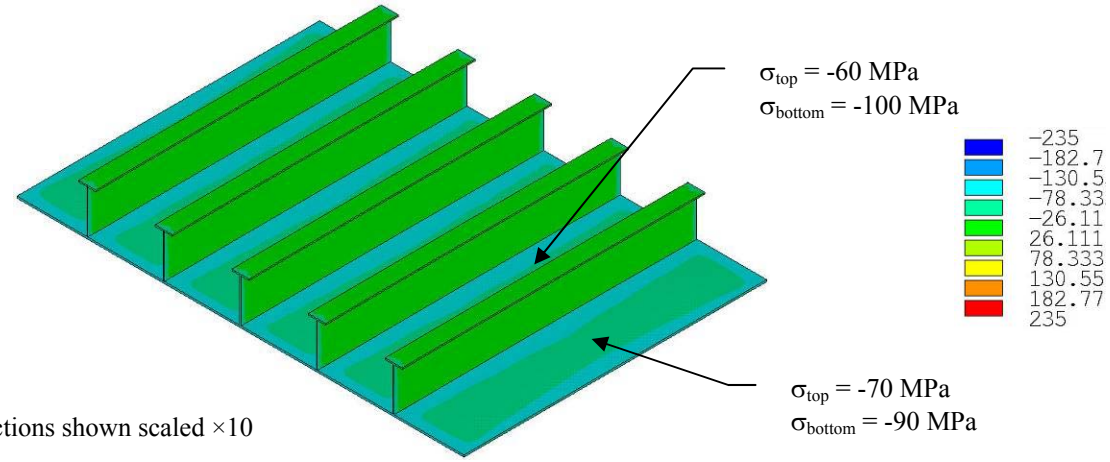

Note:
- Deflections shown scaled ×10

(b) At σ_{max} (or applied end displacement of 2.2 mm)

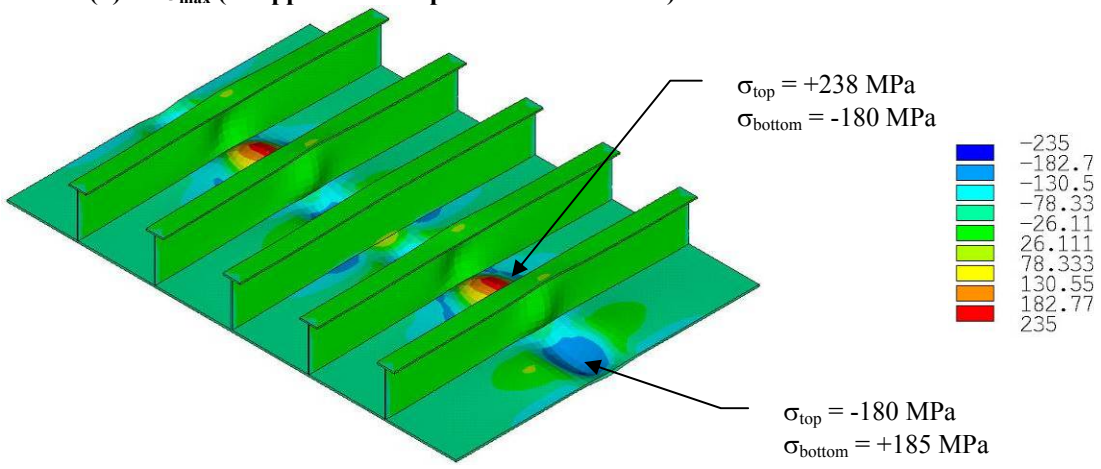

(c) At final applied end displacement of 3.0 mm

Figure 4.11: Calculated Transverse Normal Stresses for Conventional Panel A-5 (MPa)

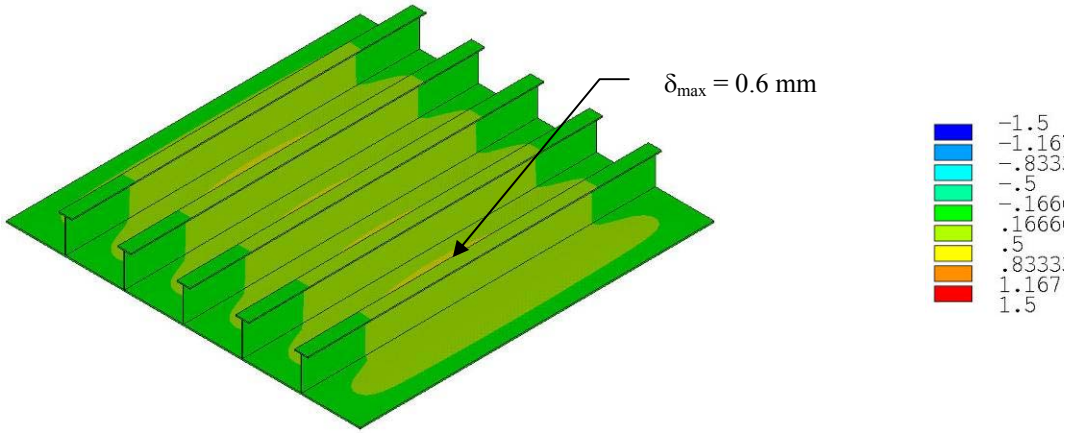

(a) Hydrostatic pressure load (no applied end displacement)

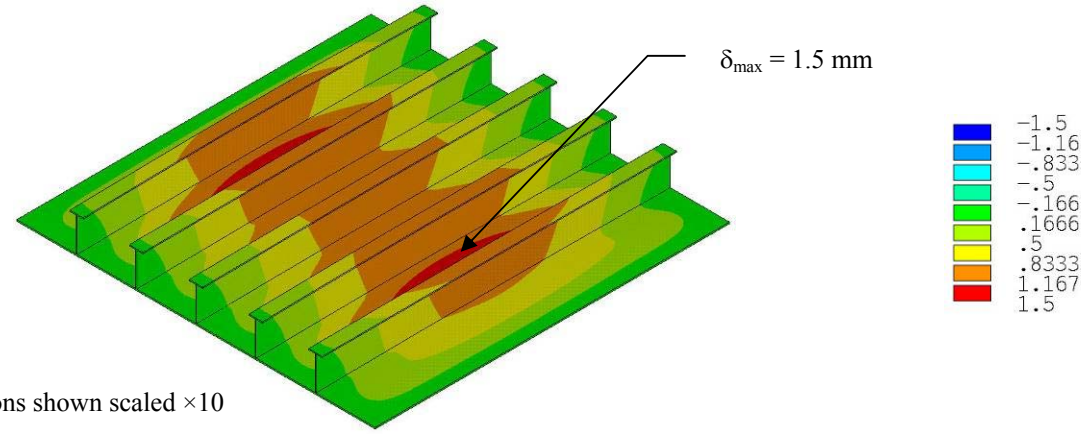

Note:
- Deflections shown scaled ×10

(b) At σ_{max} (or applied end displacement of 3.2 mm)

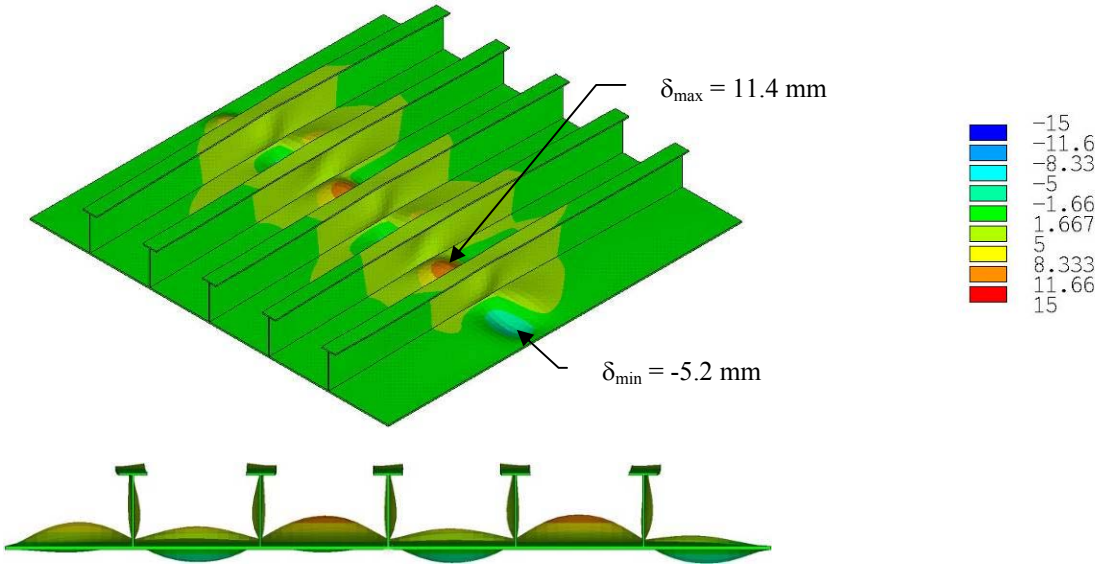

(c) At final applied end displacement of 3.6 mm

Figure 4.12: Calculated Out-of-Plane Deflections for Conventional Panel D-5 (mm)

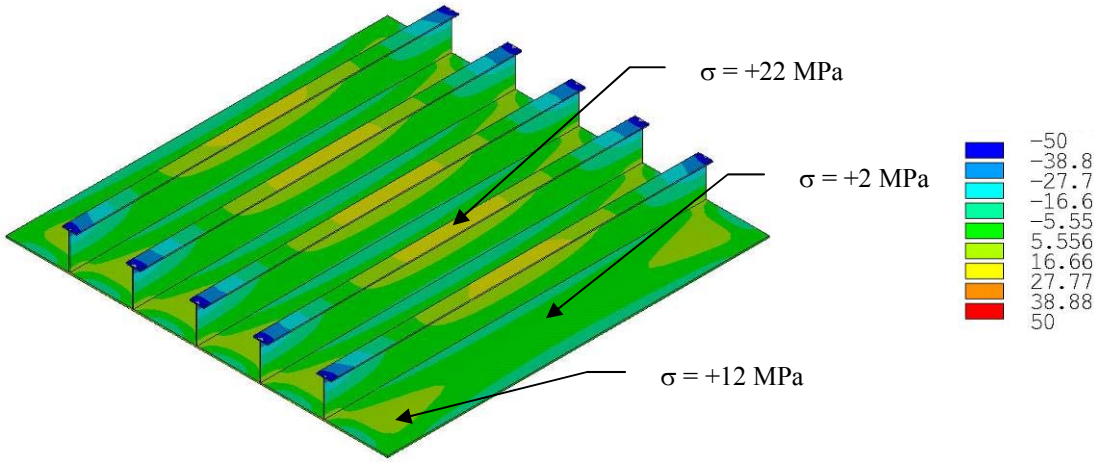

(a) Hydrostatic pressure load (no applied end displacement)

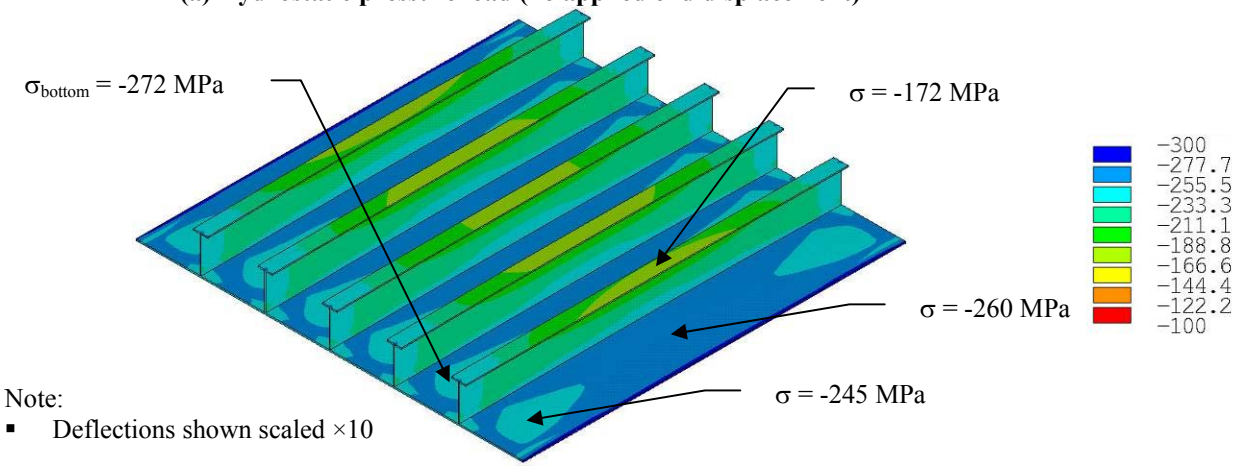

Note:
- Deflections shown scaled ×10

(b) At σ_{max} (or applied end displacement of 3.2 mm)

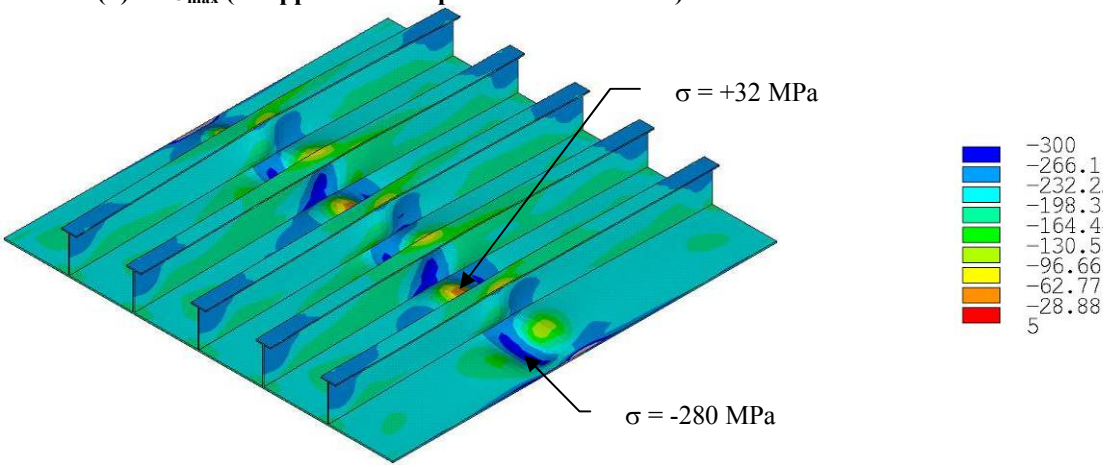

(c) At final applied end displacement of 3.6 mm

Figure 4.13: Calculated Longitudinal Normal Stresses for Conventional Panel D-5 (MPa)

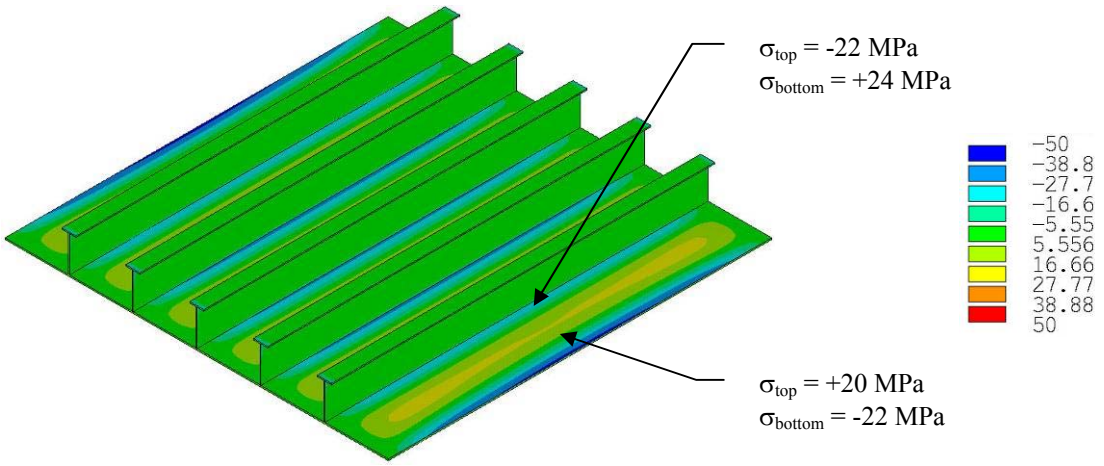

(a) Hydrostatic pressure load (no applied end displacement)

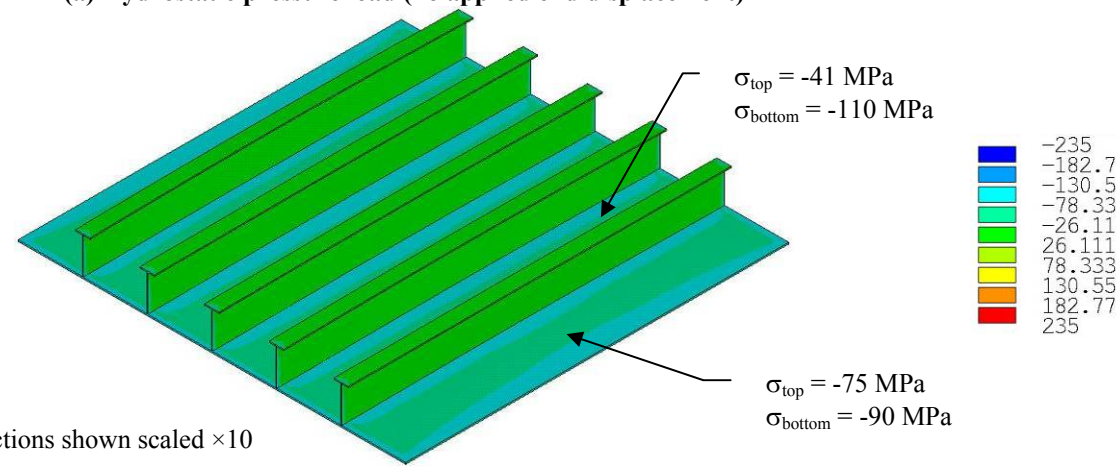

Note:
- Deflections shown scaled ×10

(b) At σ_{max} (or applied end displacement of 3.2 mm)

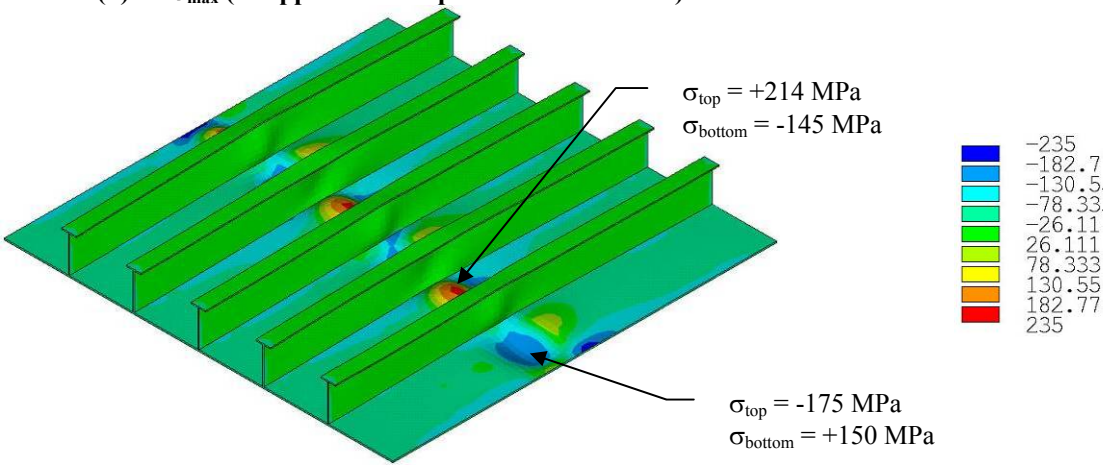

(c) At final applied end displacement of 3.6 mm

Figure 4.14: Calculated Transverse Normal Stresses for Conventional Panel D-5 (MPa)

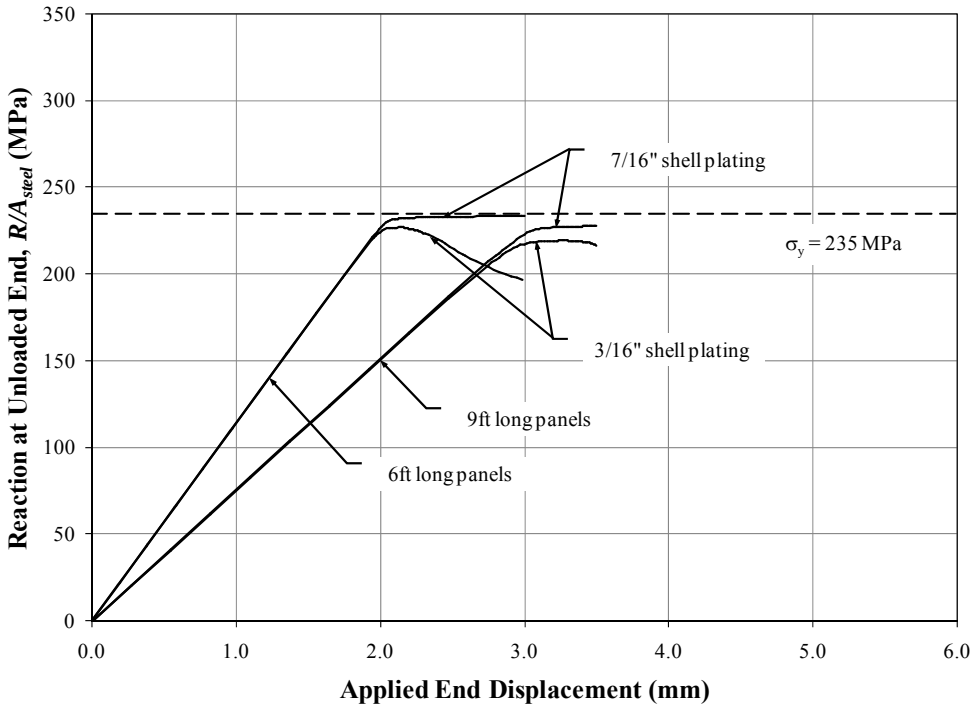

(a) Load-Deflection Curves for Panels B-1/B-5 and E-1/E-5

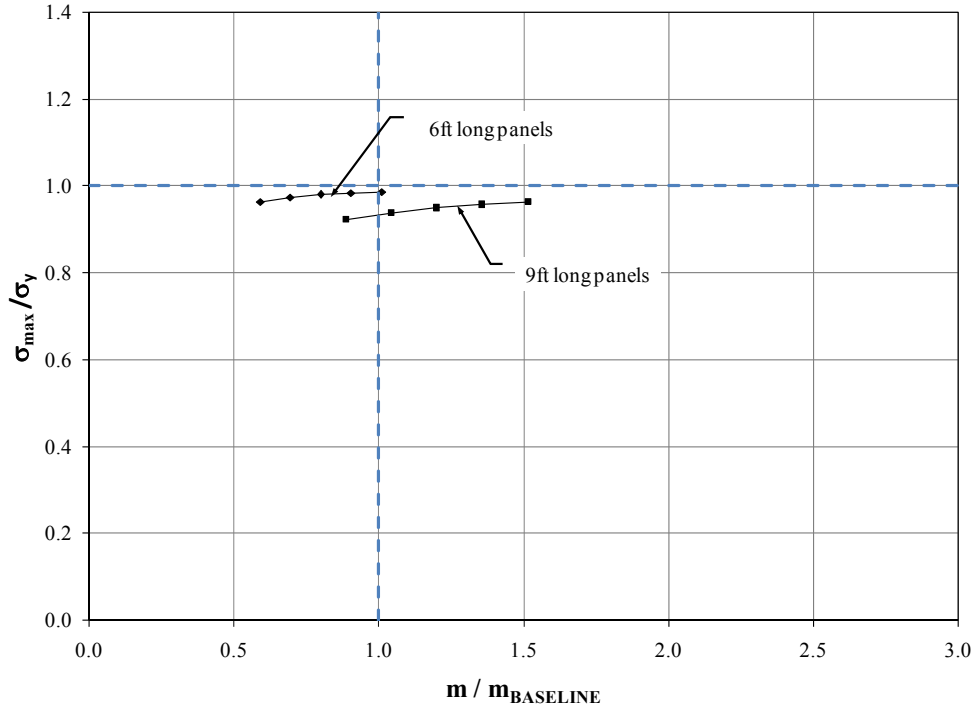

(b) Normalized Stress-Mass Curves for Panels B-[1:5] and E-[1:5]

Figure 4.15: Calculated Results for the Folded Conventional Panel Configurations

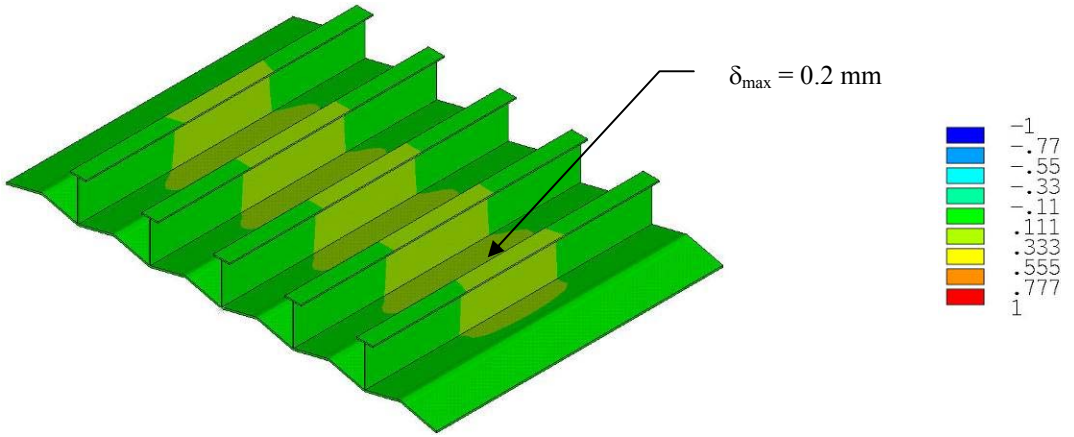

(a) Hydrostatic pressure load (no applied end displacement)

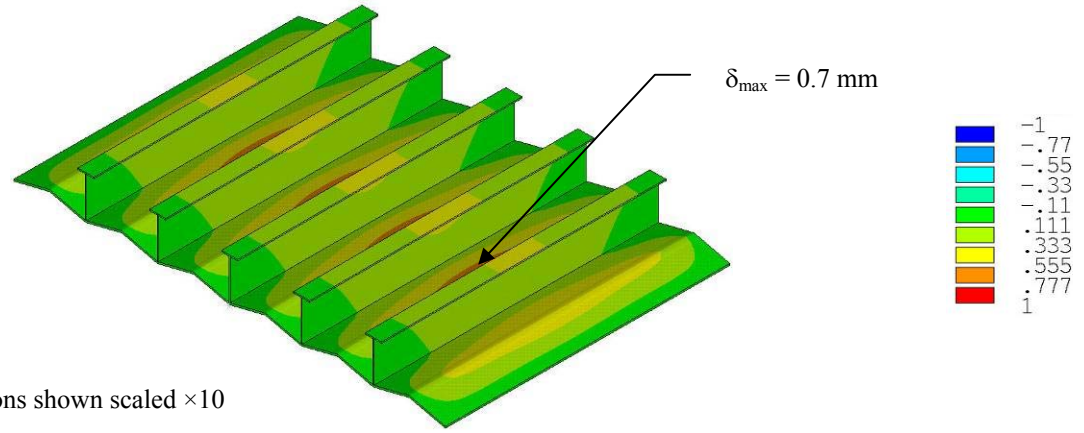

Note:

- Deflections shown scaled ×10

(b) At σ_{max} (or applied end displacement of 2.12 mm)

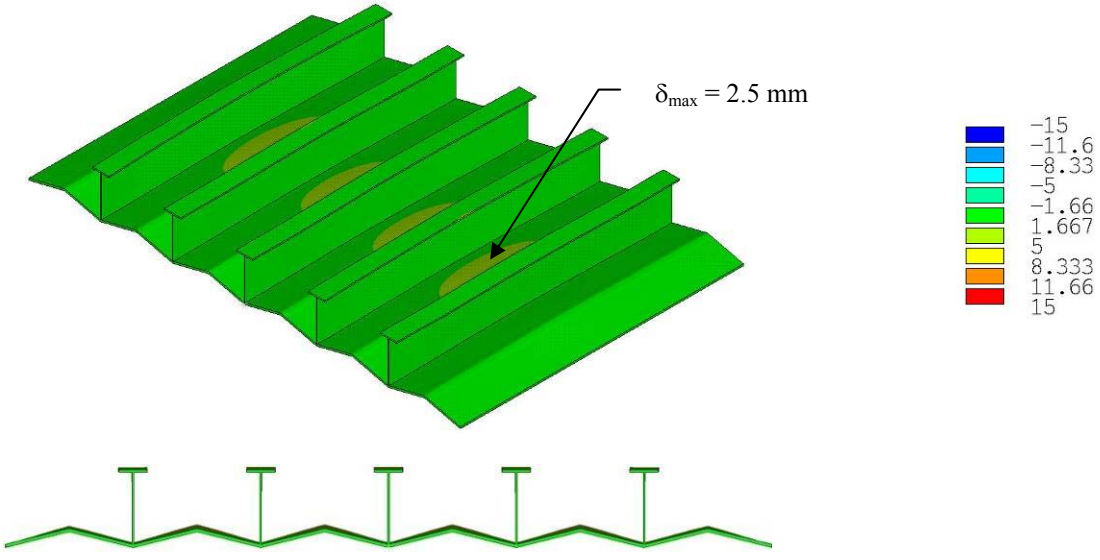

(c) At final applied end displacement of 3.0 mm

Figure 4.16: Calculated Out-of-Plane Deflections for Folded Conventional Panel B-5 (mm)

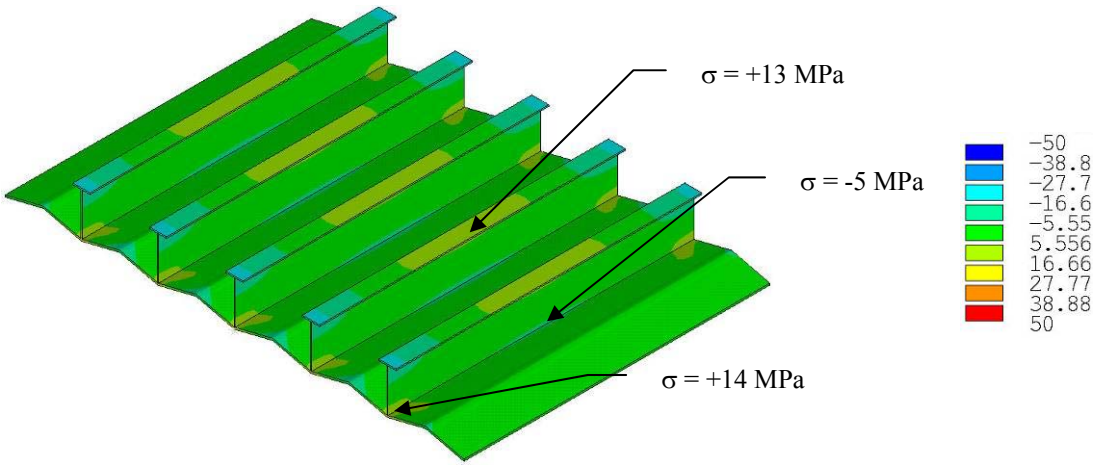

(a) Hydrostatic pressure load (no applied end displacement)

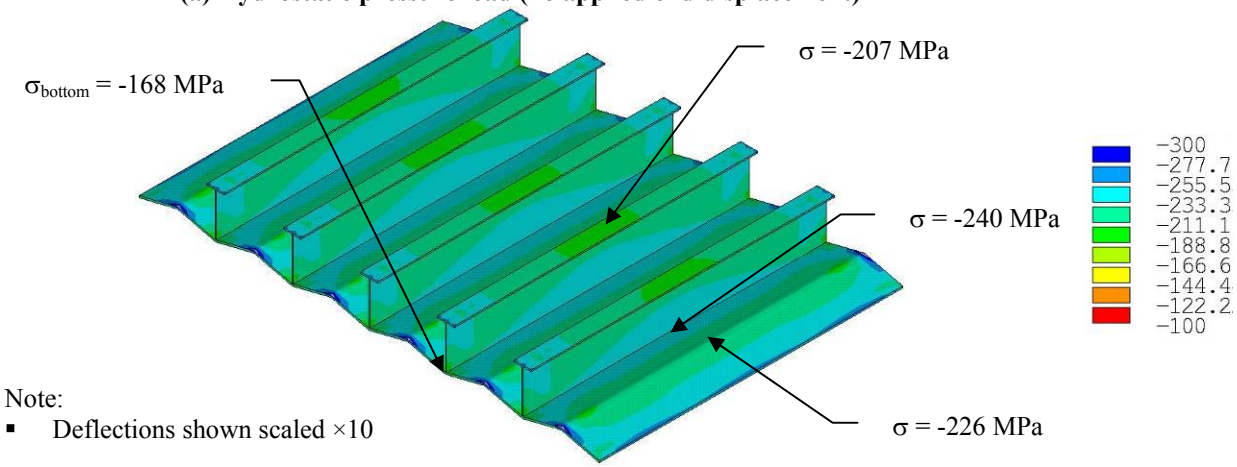

Note:
- Deflections shown scaled ×10

(b) At σ_{max} (or applied end displacement of 2.12 mm)

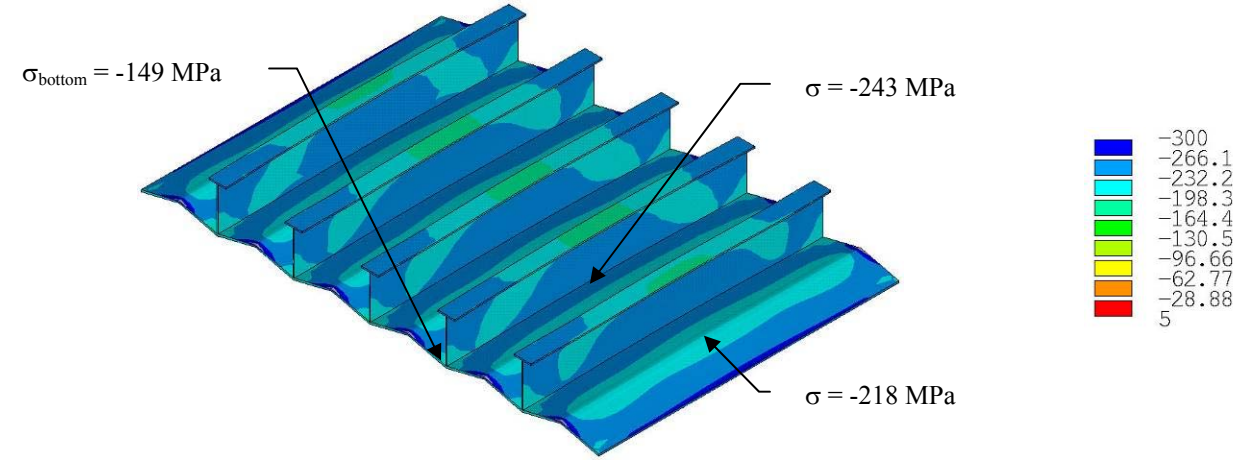

(c) At final applied end displacement of 3.0 mm

Figure 4.17: Calculated Longitudinal Normal Stresses for Conventional Panel B-5 (MPa)

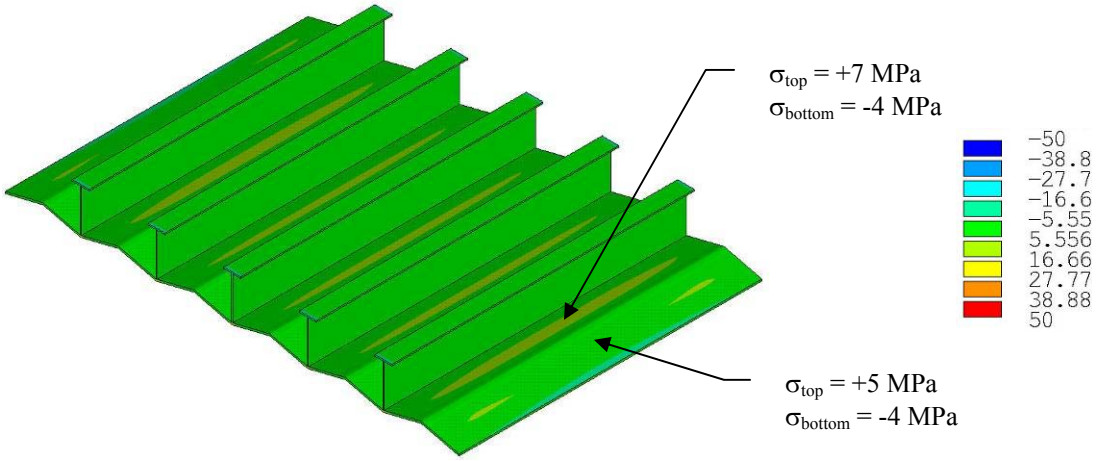

(a) Hydrostatic pressure load (no applied end displacement)

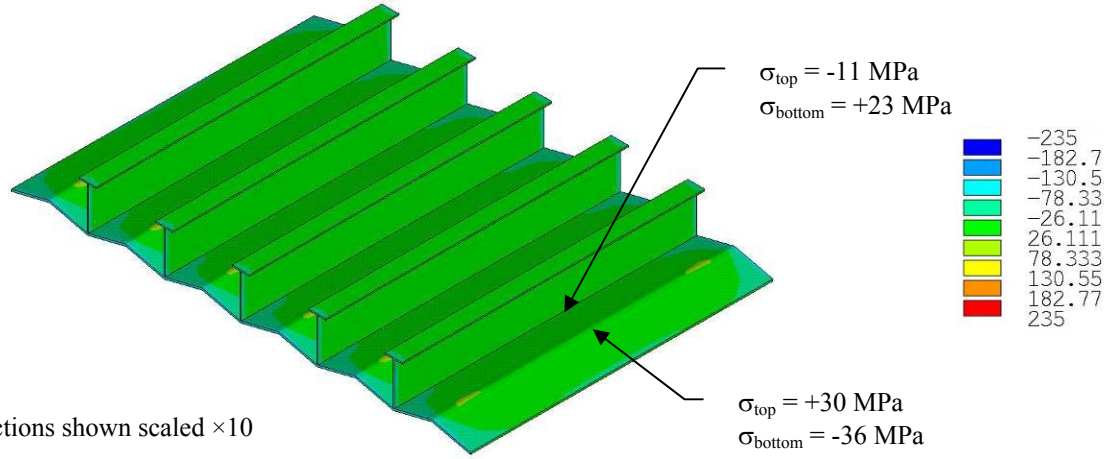

Note:
- Deflections shown scaled ×10

(b) At σ_{max} (or applied end displacement of 2.12 mm)

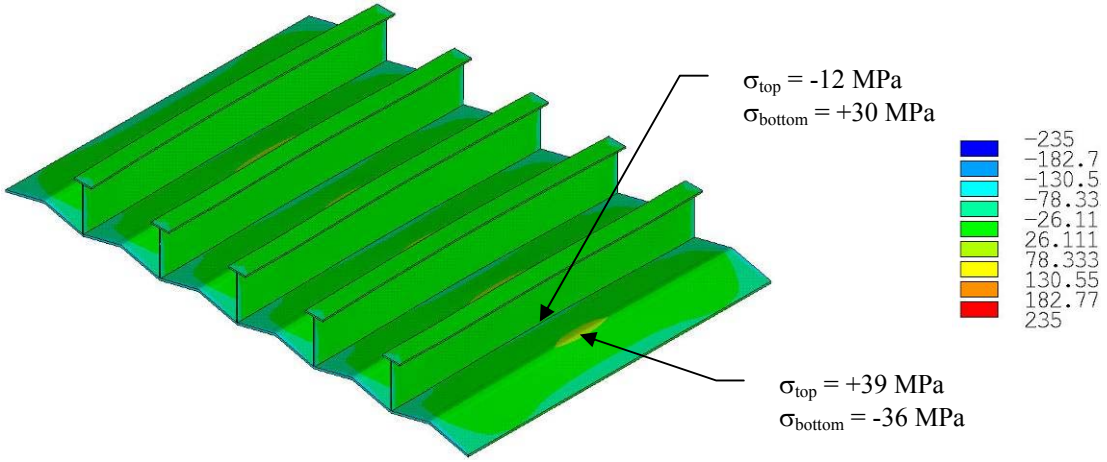

(c) At final applied end displacement of 3.0 mm

Figure 4.18: Calculated Transverse Normal Stresses for Conventional Panel B-5 (MPa)

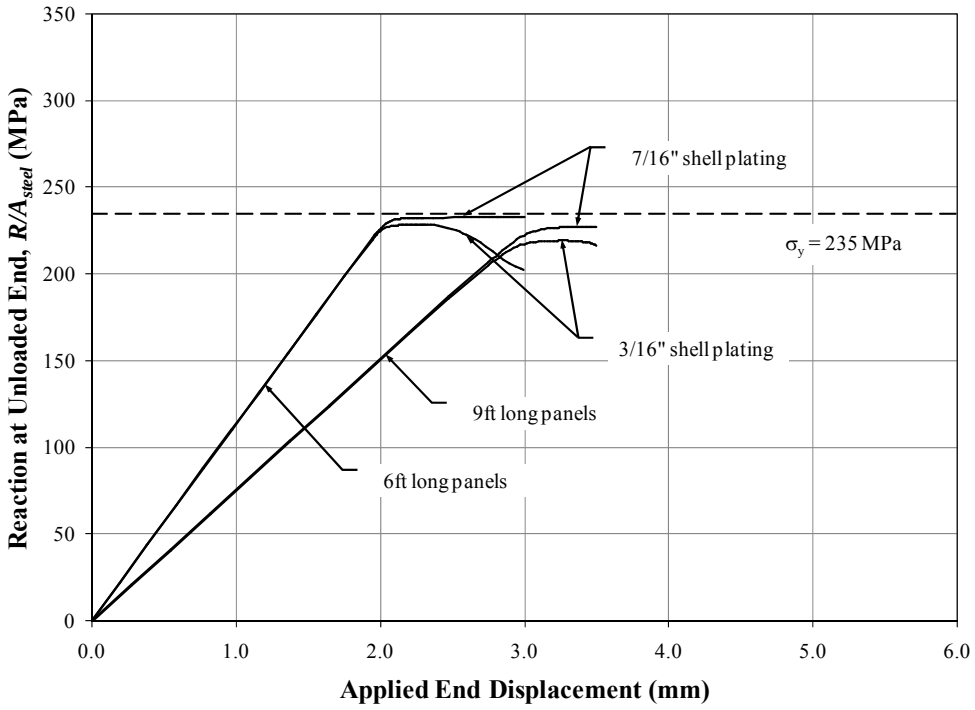

(a) Load-Deflection Curves for Panels C-1/C-5 and F-1/F-5

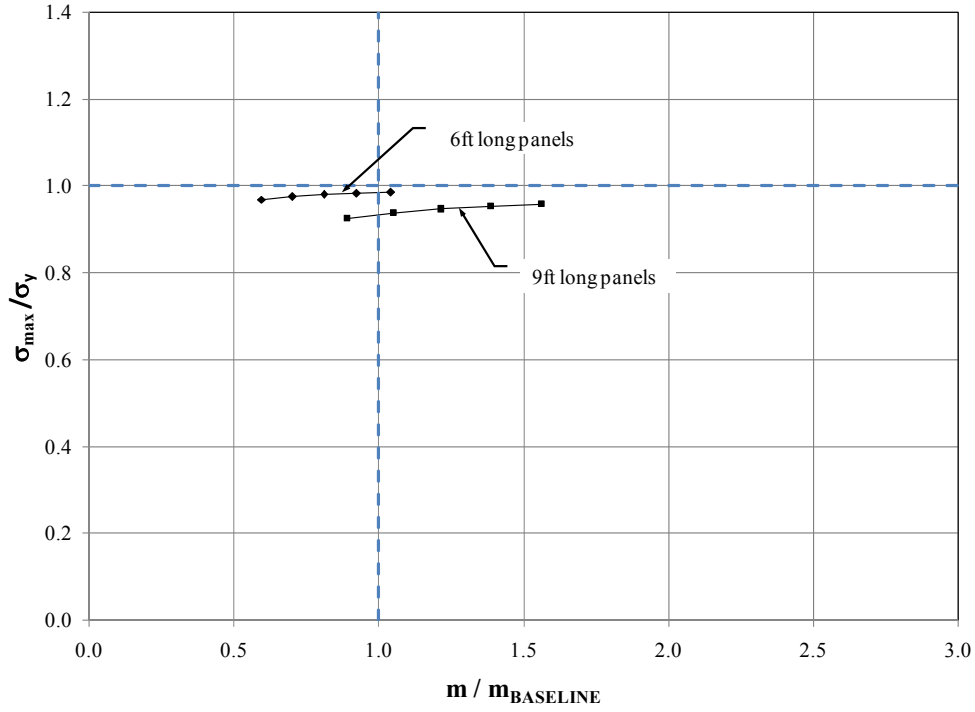

(b) Normalized Stress-Mass Curves for Panels C-[1:5] and F-[1:5]

Figure 4.19: Calculated Results for the Folded Conventional Panel Configurations

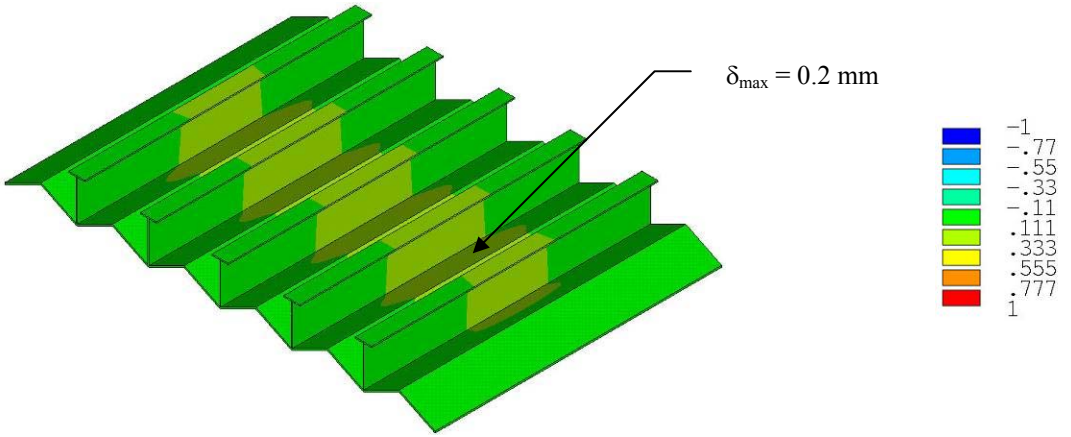

(a) Hydrostatic pressure load (no applied end displacement)

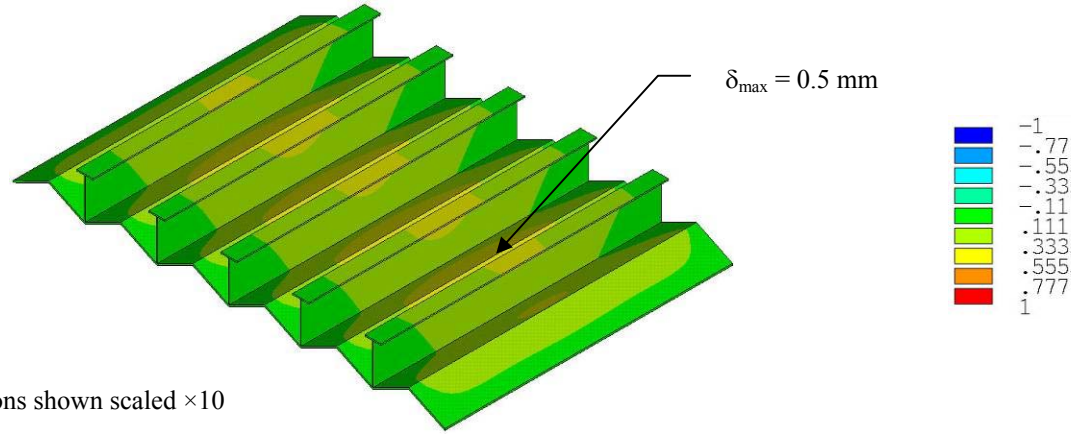

Note:
- Deflections shown scaled ×10

(b) At σ_{max} (or applied end displacement of 2.12 mm)

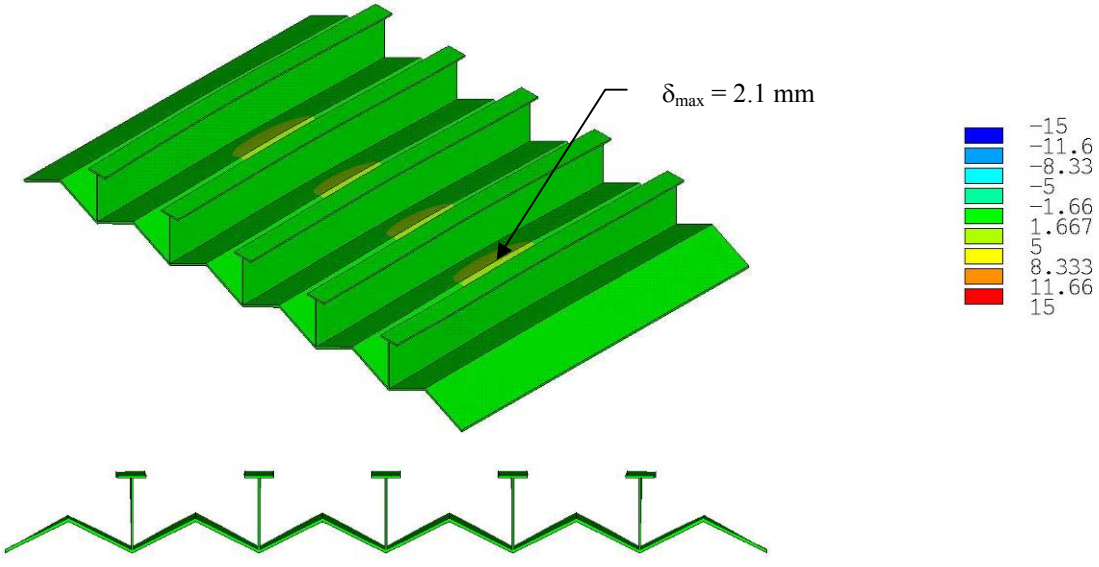

(c) At final applied end displacement of 3.0 mm

Figure 4.20: Calculated Out-of-Plane Deflections for Folded Conventional Panel C-5 (mm)

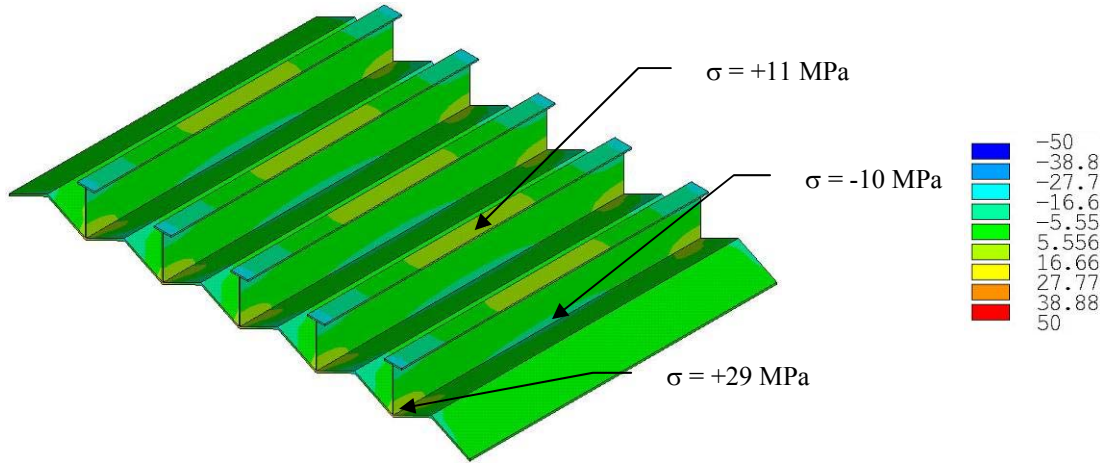

(a) Hydrostatic pressure load (no applied end displacement)

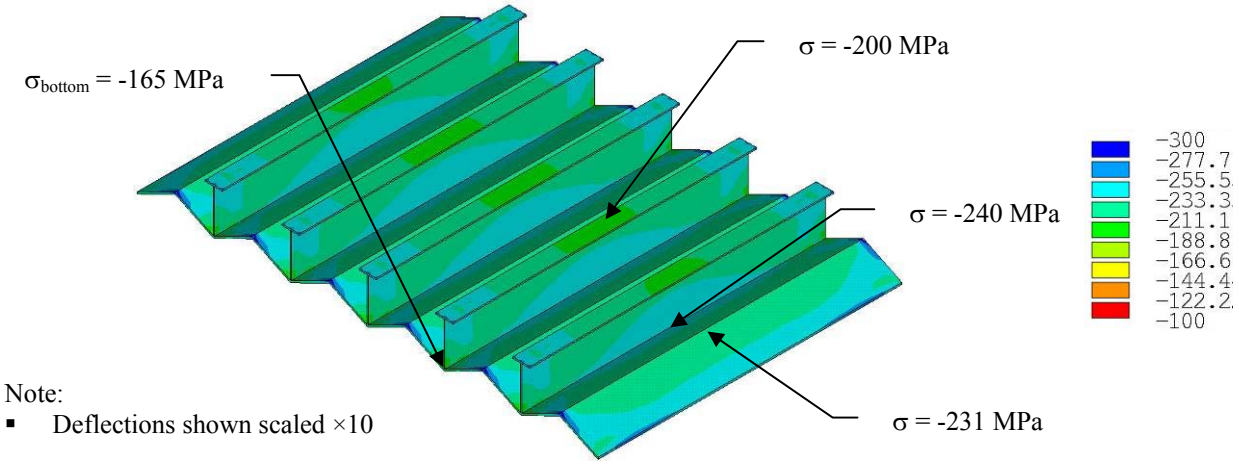

Note:
- Deflections shown scaled ×10

(b) At σ_{max} (or applied end displacement of 2.12 mm)

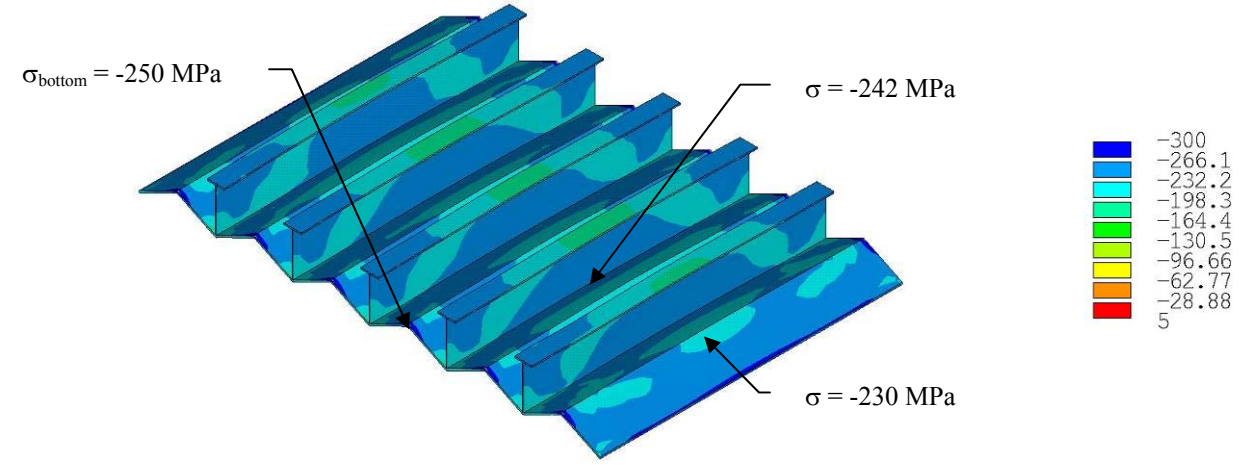

(c) At final applied end displacement of 3.0 mm

Figure 4.21: Calculated Longitudinal Normal Stresses for Conventional Panel C-5 (MPa)

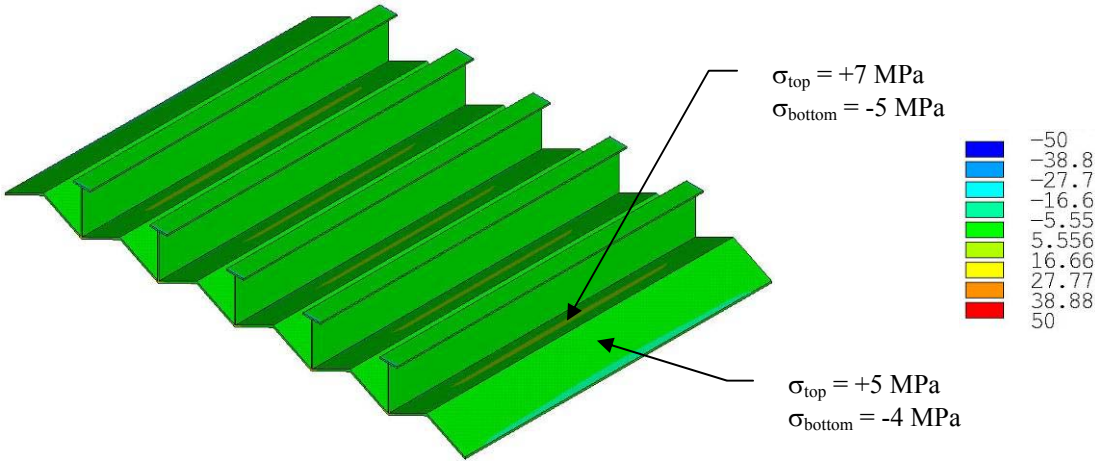

(a) Hydrostatic pressure load (no applied end displacement)

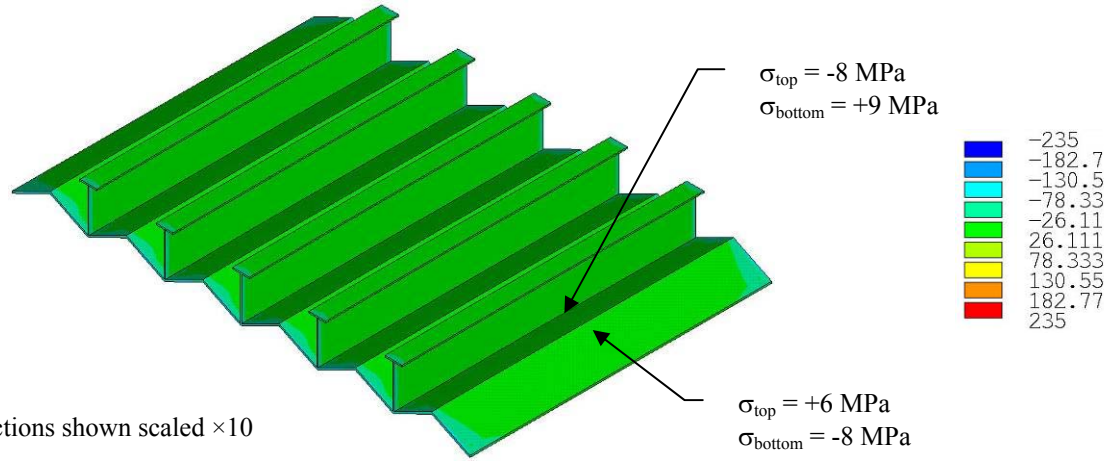

Note:
- Deflections shown scaled ×10

(b) At σ_{max} (or applied end displacement of 2.12 mm)

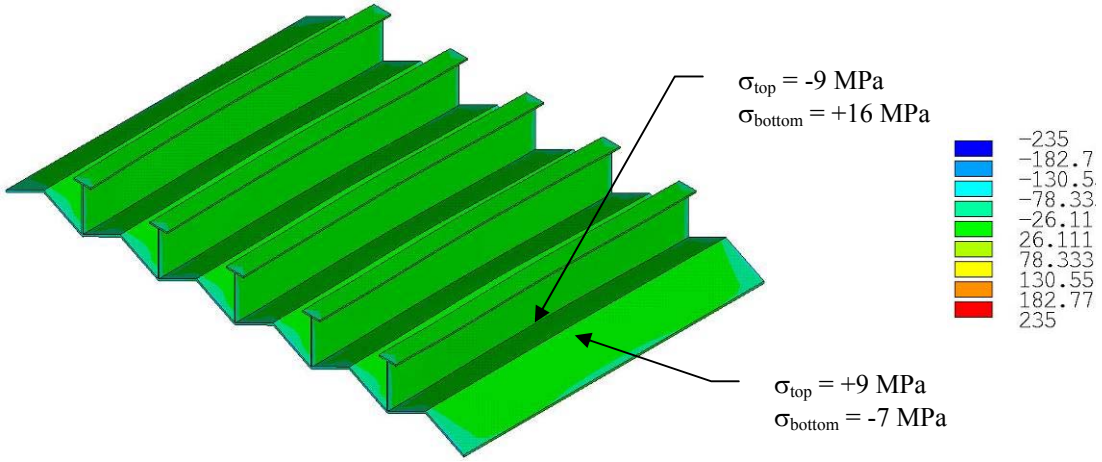

(c) At final applied end displacement of 3.0 mm

Figure 4.22: Calculated Transverse Normal Stresses for Conventional Panel C-5 (MPa)

Table 4.3: Summary of Calculated Results for the Conventional Panel Configurations

Panel Designation			Shell Thickness (in)	Shell Thickness (mm)	f_{bend}	A_{steel} (mm)	m / $m_{Baseline}$	σ_{max} (MPa)	σ_{max} / σ_y	Applied End Displacement at σ_{max} (mm)
6 ft Long Panels	A	1	3/16	4.8	0	25153	0.591	157	0.67	1.38
		2	1/4	6.4	0	29507	0.693	193	0.82	1.68
		3	5/16	7.9	0	33862	0.795	245	1.04	2.09
		4	3/8	9.5	0	38217	0.898	251	1.07	2.17
		5	7/16	11.1	0	42572	1.000	254	1.08	2.20
	B	1	3/16	4.8	5	25188	0.592	227	0.96	2.07
		2	1/4	6.4	5	29592	0.695	229	0.97	2.10
		3	5/16	7.9	5	34028	0.799	230	0.98	2.11
		4	3/8	9.5	5	38502	0.904	231	0.98	2.12
		5	7/16	11.1	5	43022	1.011	232	0.99	2.12
	C	1	3/16	4.8	10	25295	0.594	228	0.97	2.09
		2	1/4	6.4	10	29842	0.701	229	0.98	2.11
		3	5/16	7.9	10	34509	0.811	230	0.98	2.11
		4	3/8	9.5	10	39322	0.924	231	0.98	2.12
		5	7/16	11.1	10	44302	1.041	232	0.99	2.12
9 ft Long Panels	D	1	3/16	4.8	0	25153	0.886	143	0.61	1.87
		2	1/4	6.4	0	29507	1.040	165	0.70	2.09
		3	5/16	7.9	0	33862	1.193	218	0.93	2.82
		4	3/8	9.5	0	38217	1.347	244	1.04	3.14
		5	7/16	11.1	0	42572	1.500	248	1.06	3.20
	E	1	3/16	4.8	5	25188	0.887	217	0.92	3.01
		2	1/4	6.4	5	29592	1.043	220	0.94	3.04
		3	5/16	7.9	5	34028	1.199	223	0.95	3.08
		4	3/8	9.5	5	38502	1.357	225	0.96	3.10
		5	7/16	11.1	5	43022	1.516	226	0.96	3.12
	F	1	3/16	4.8	10	25295	0.891	217	0.92	3.00
		2	1/4	6.4	10	29842	1.051	220	0.94	3.04
		3	5/16	7.9	10	34509	1.216	222	0.95	3.06
		4	3/8	9.5	10	39322	1.385	224	0.95	3.08
		5	7/16	11.1	10	44302	1.561	225	0.96	3.10

4.3.2 Hybrid Panel Configurations (10 GPa Composite)

Table 4.4 lists the matrix of hybrid panel configurations with the estimated volume and mass quantities for the steel and for the composite. Table 4.5 also lists the mass of each panel design relative to the baseline condition (conventional steel panel with 7/16 inches shell plating), or panel A-5, provided in Table 4.3.

Figure 4.23(a) and Figure 4.23(b) illustrate the calculated load-deflection curves and the normalized maximum stresses respectively for the set of hybrid panels with a value for $E_{composite}$ = 10 GPa and f_{bend} = 5.0. Again, the maximum stress is based on the maximum calculated reaction (R_{max}) for the range of applied displacement relative to the cross-sectional area of steel (A_{steel}) and the nominal yield stress of the Grade A 235 steel (σ_y = 235 MPa).

Figure 4.24, Figure 4.25 and Figure 4.26 illustrate the calculated out-of-plane deflections and longitudinal and transverse normal stresses for the hybrid panel G-1 with f_{bend} = 5.0 and a shell plating thickness of 3/16 inches. Similarly, the calculated results for panel H-1 are shown in Figure 4.27 to Figure 4.30 with f_{bend} = 10.0. In both cases, the value of $E_{composite}$ is taken as 10 GPa.

Table 4.5 summarizes the calculated results for the hybrid panel configurations G, H, I and J.

4.3.3 Hybrid Panel Configurations (Various Composite Properties)

Figure 4.31 and Figure 4.32 illustrate the load-deflection curves for the set of hybrid panels corresponding to G1/G5 and H1/H5 spanning 6 feet and 9 feet respectively versus the value of $E_{composite}$, which has been taken as 10 MPa, 100 MPa, 1 GPa, 10 GPa and 20 GPa. The corresponding normalized stress-mass curves for the 6 foot long and the 9 foot long panels are shown in Figure 4.33(a) and Figure 4.33(b) respectively.

Table 4.4: Quantities for the Hybrid Panel Configurations

Panel Designation			Shell Thickness (in)	Shell Thickness (mm)	Fold f_{bend}	Fold Height (mm)	Volume (m^3) Steel	Volume (m^3) Composite	Mass (kg) Steel	Mass (kg) Composite	Mass (kg) Total	Relative to Baseline at A-5
6 ft Long Panels	G	1	3/16	4.8	5	23.8	0.046	0.084	362	126	488	0.798
		2	1/4	6.4	5	31.8	0.054	0.104	425	156	581	0.950
		3	5/16	7.9	5	39.7	0.062	0.124	489	185	674	1.102
		4	3/8	9.5	5	47.6	0.070	0.143	553	215	768	1.256
		5	7/16	11.1	5	55.6	0.079	0.163	618	244	862	1.410
	H	1	3/16	4.8	10	47.6	0.046	0.143	363	215	578	0.946
		2	1/4	6.4	10	63.5	0.055	0.183	428	274	702	1.149
		3	5/16	7.9	10	79.4	0.063	0.222	495	333	828	1.355
		4	3/8	9.5	10	95.3	0.072	0.261	565	392	957	1.565
		5	7/16	11.1	10	111.1	0.081	0.301	636	451	1087	1.779
9 ft Long Panels	I	1	3/16	4.8	5	23.8	0.069	0.126	542	189	732	1.197
		2	1/4	6.4	5	31.8	0.081	0.156	637	234	871	1.425
		3	5/16	7.9	5	39.7	0.093	0.185	733	278	1011	1.654
		4	3/8	9.5	5	47.6	0.106	0.215	829	322	1151	1.884
		5	7/16	11.1	5	55.6	0.118	0.244	926	367	1293	2.116
	J	1	3/16	4.8	10	47.6	0.069	0.215	545	322	867	1.419
		2	1/4	6.4	10	63.5	0.082	0.274	643	411	1053	1.724
		3	5/16	7.9	10	79.4	0.095	0.333	743	499	1243	2.033
		4	3/8	9.5	10	95.3	0.108	0.392	847	588	1435	2.348
		5	7/16	11.1	10	111.1	0.122	0.451	954	677	1631	2.668

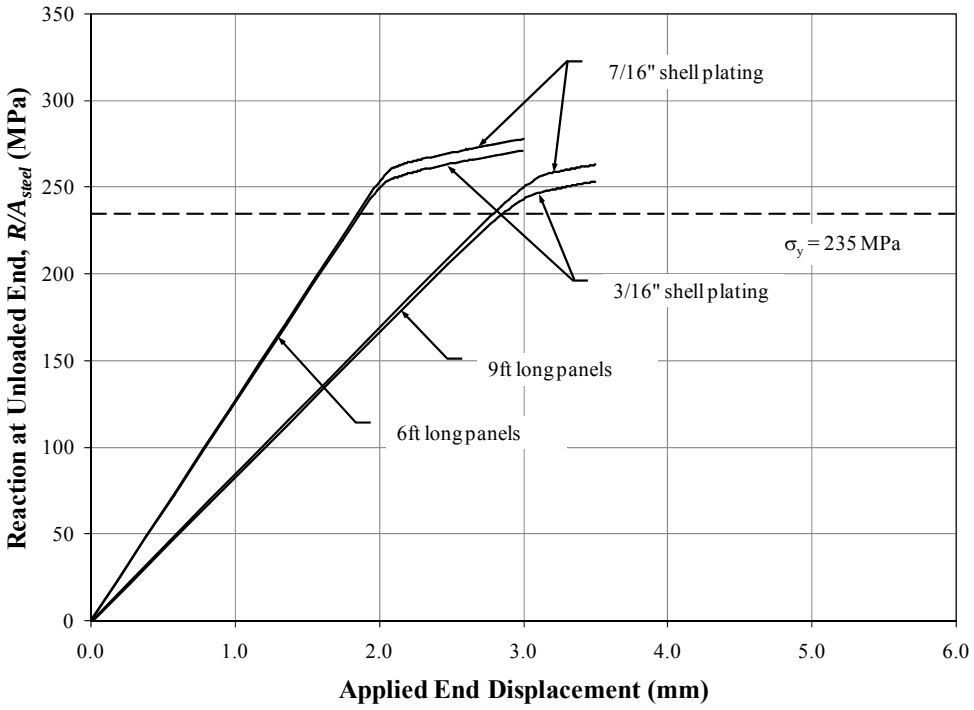

(a) Load-Deflection Curves for Panels G-1/G-5 and I-1/I-5

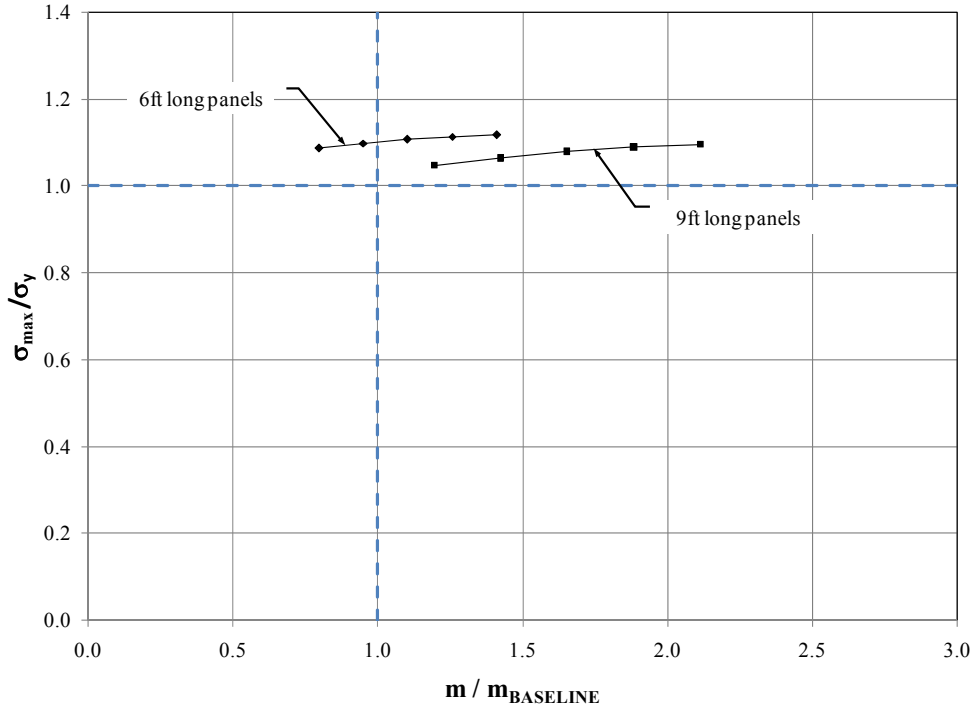

(b) Normalized Stress-Mass Curves for Panels G-[1:5] and I-[1:5]

Figure 4.23: Calculated Results for the Hybrid Panel Configurations

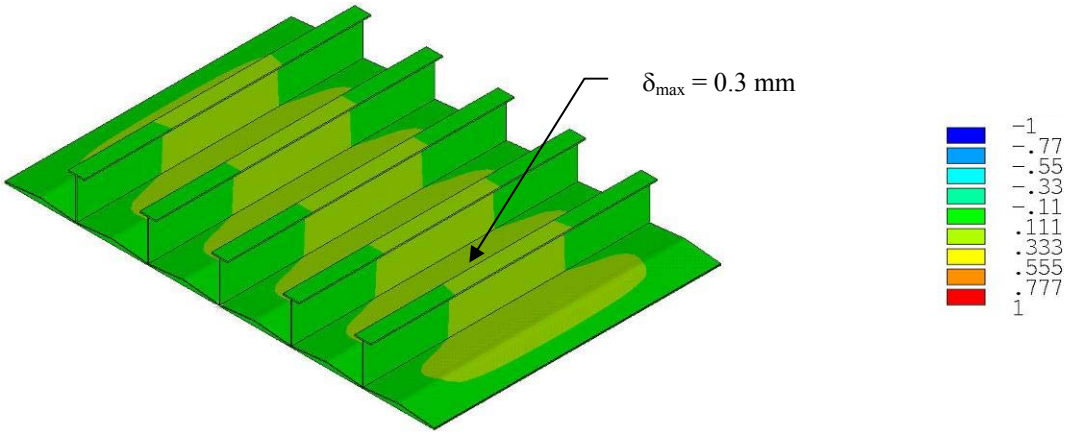

(a) Hydrostatic pressure load (no applied end displacement)

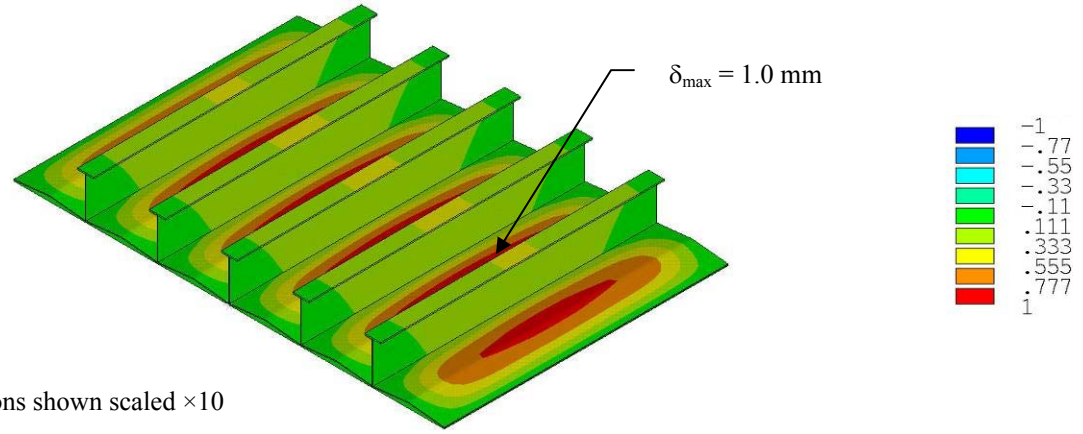

Note:

- Deflections shown scaled ×10

(b) At σ_{max} (or applied end displacement of 2.11 mm)

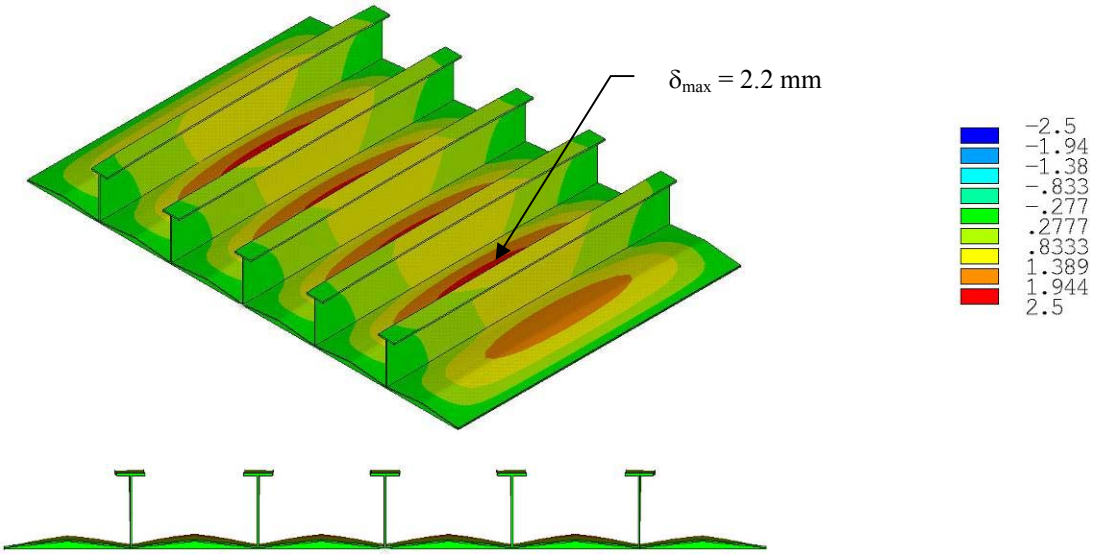

(c) At final applied end displacement of 2.99 mm

Figure 4.24: Calculated Out-of-Plane Deflections for Hybrid Panel G-1 (mm)

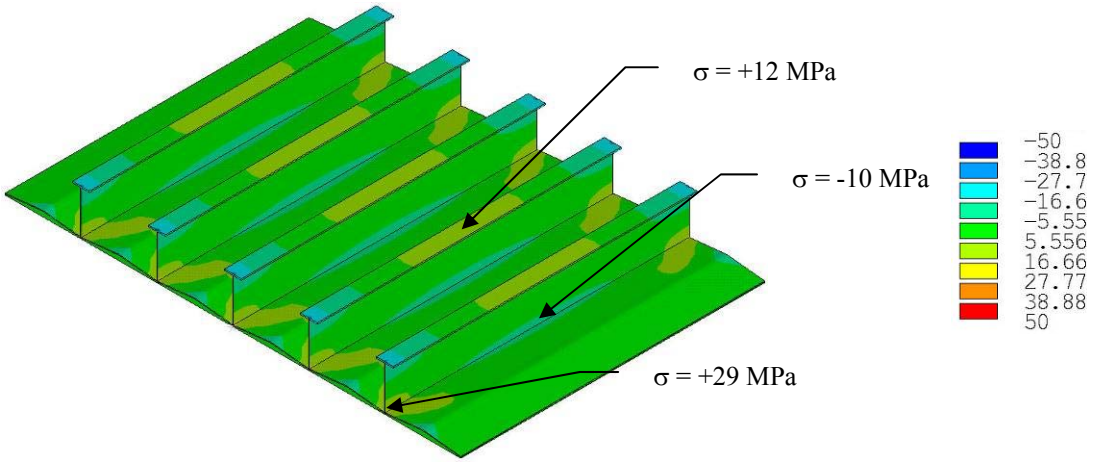

(a) Hydrostatic pressure load (no applied end displacement)

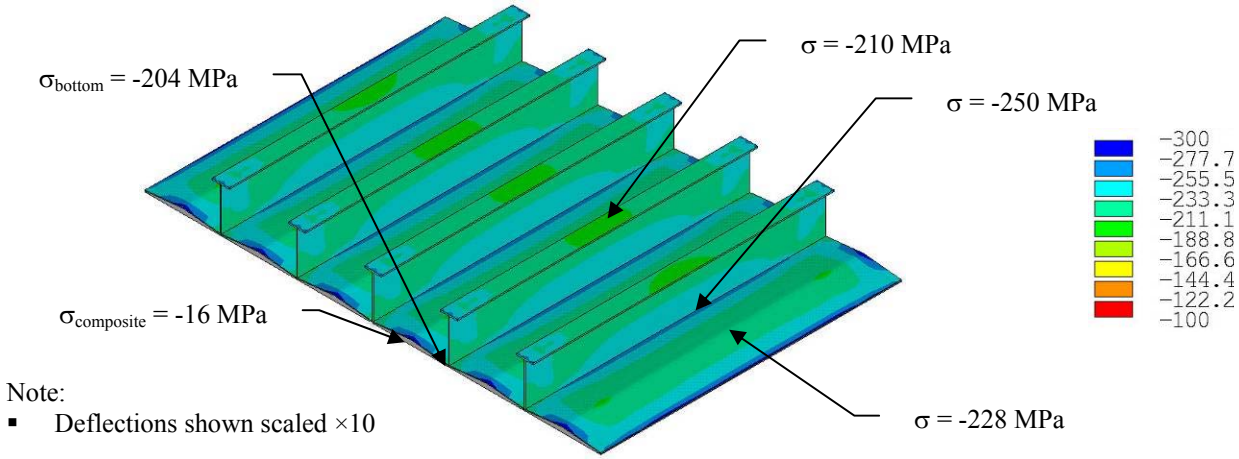

(b) At σ_{max} (or applied end displacement of 2.12 mm)

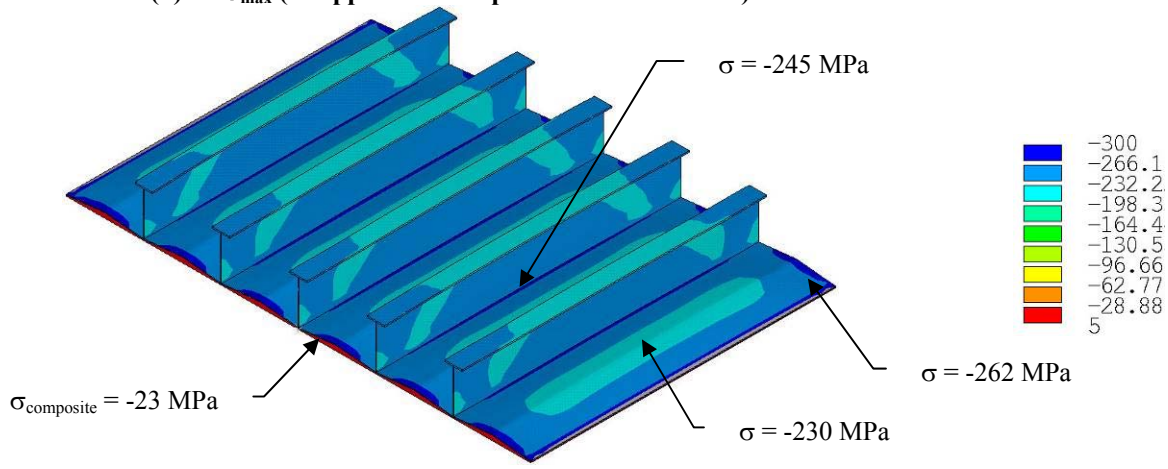

(c) At final applied end displacement of 3.0 mm

Figure 4.25: Calculated Longitudinal Normal Stresses for Hybrid Panel G-1 (MPa)

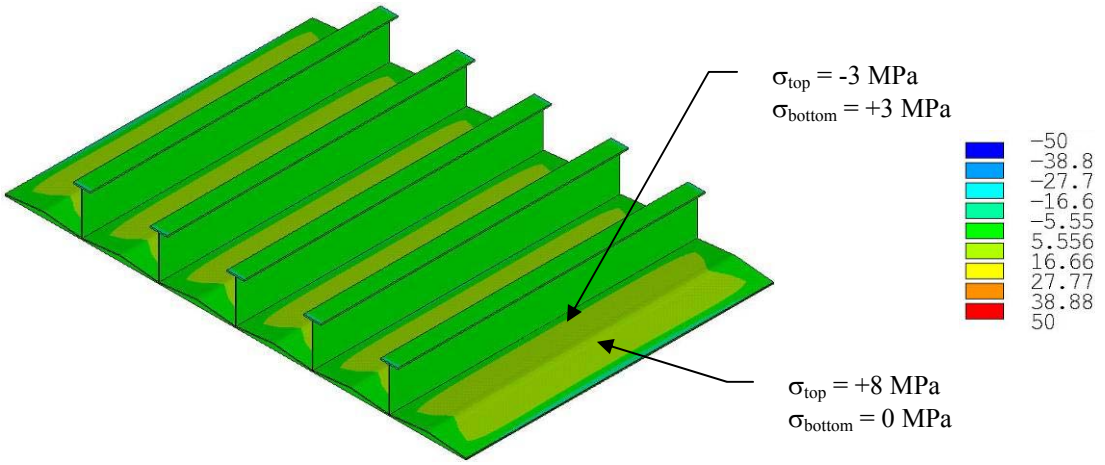

(a) Hydrostatic pressure load (no applied end displacement)

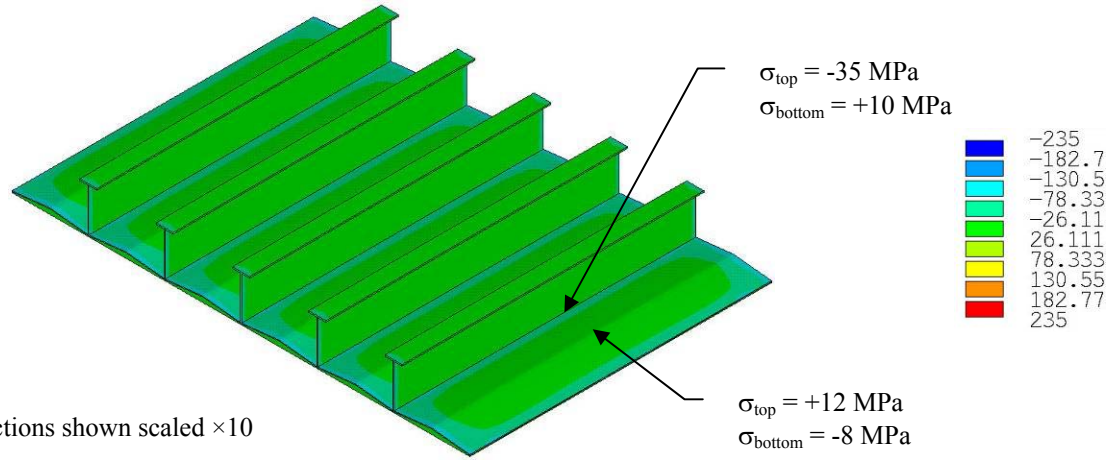

Note:
- Deflections shown scaled ×10

(b) At σ_{max} (or applied end displacement of 2.12 mm)

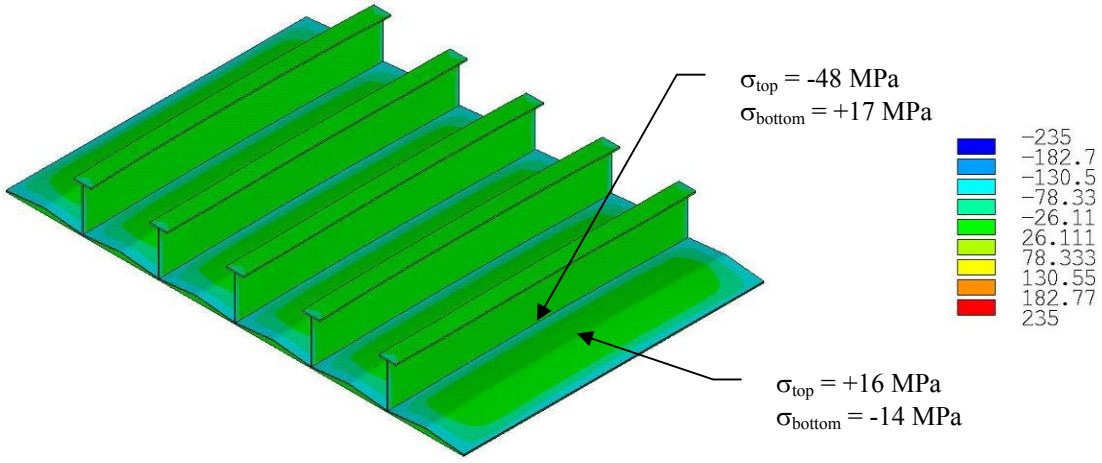

(c) At final applied end displacement of 3.0 mm

Figure 4.26: Calculated Transverse Normal Stresses for Hybrid Panel G-1 (MPa)

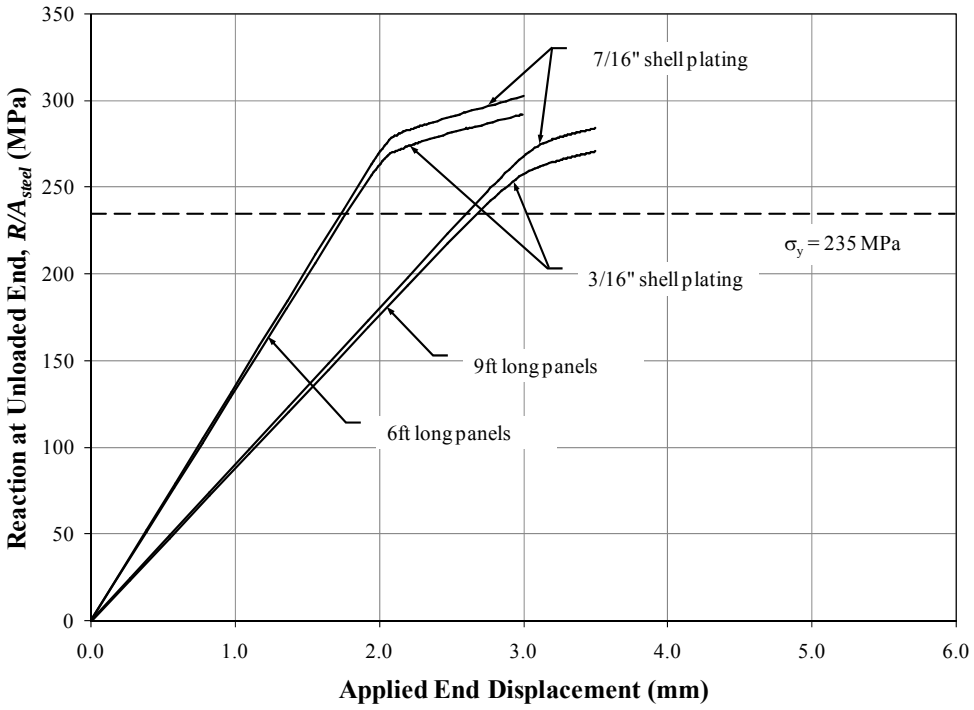

(a) Load-Deflection Curves for Panels H-1/H-5 and J-1/J-5

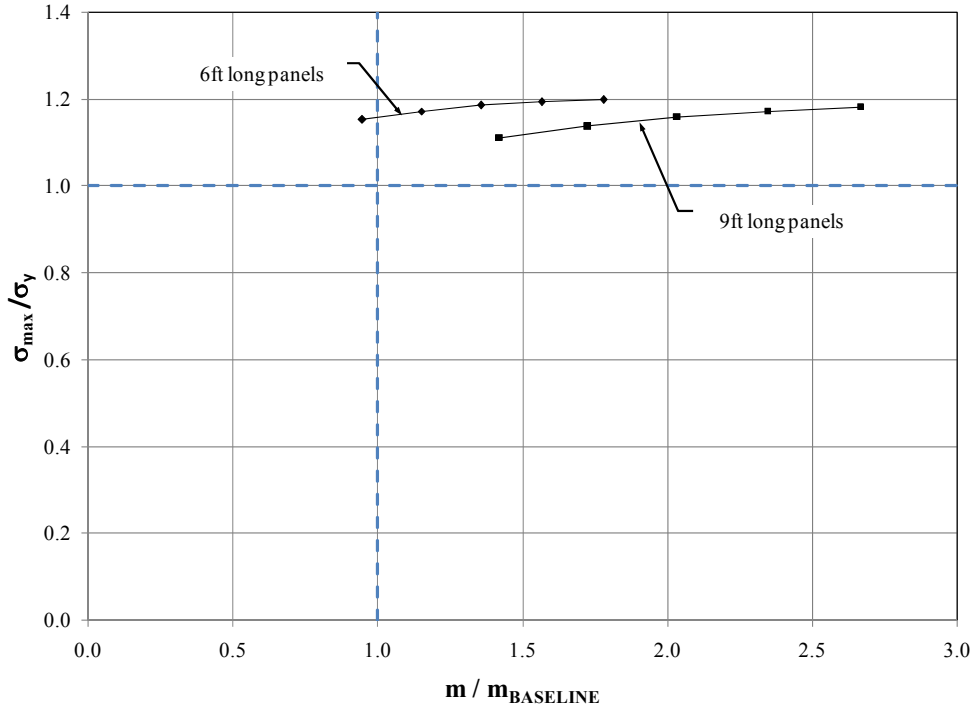

(b) Normalized Stress-Mass Curves for Panels H-[1:5] and J-[1:5]

Figure 4.27: Calculated Results for the Hybrid Panel Configurations

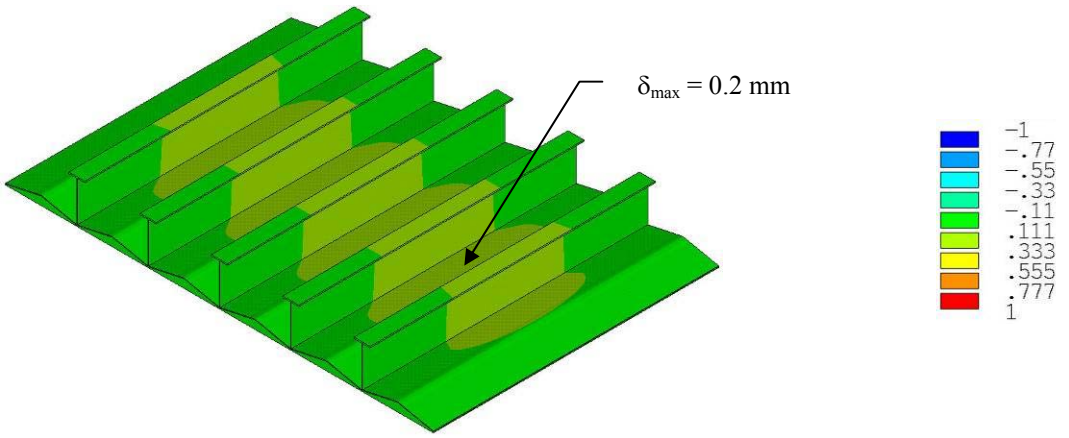

(a) Hydrostatic pressure load (no applied end displacement)

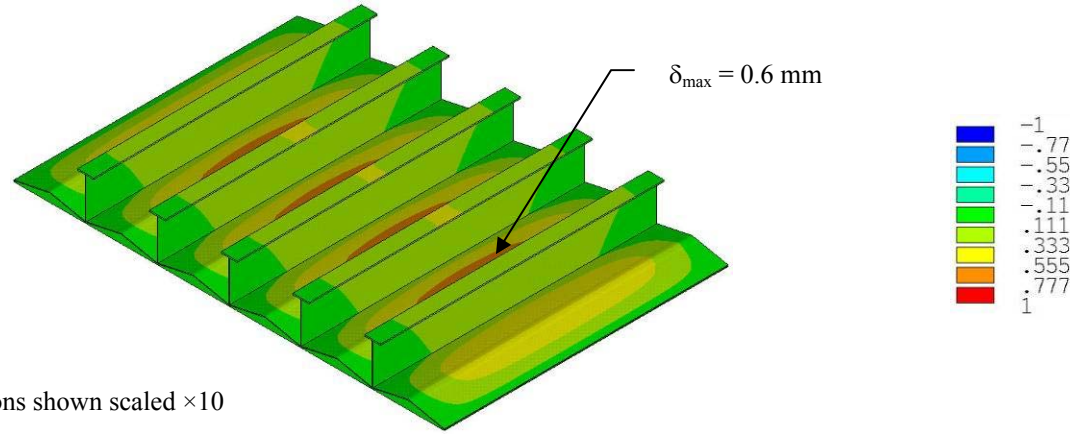

Note:

- Deflections shown scaled ×10

(b) At σ_{max} (or applied end displacement of 2.13 mm)

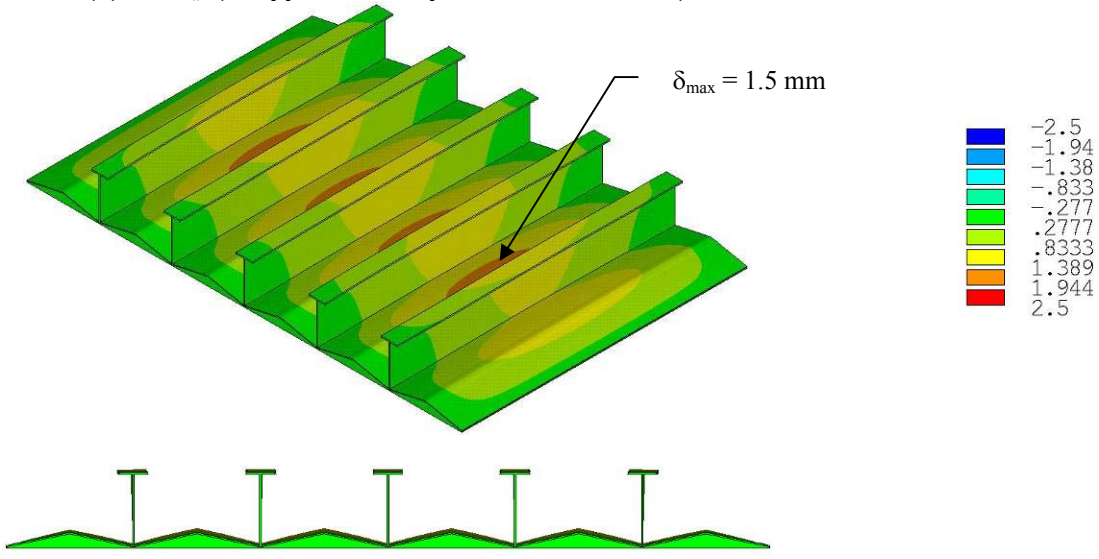

(c) At final applied end displacement of 3.0 mm

Figure 4.28: Calculated Out-of-Plane Deflections for Hybrid Panel H-1 (mm)

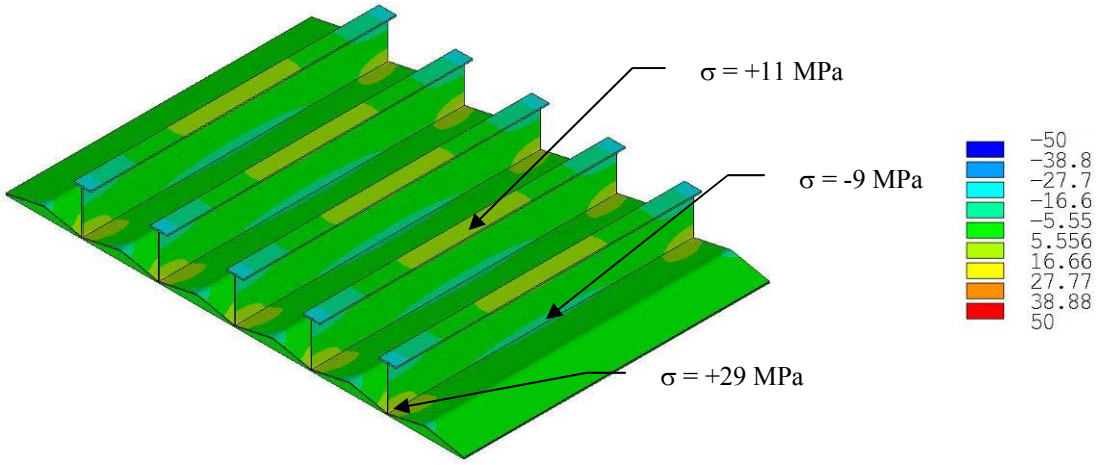

(a) Hydrostatic pressure load (no applied end displacement)

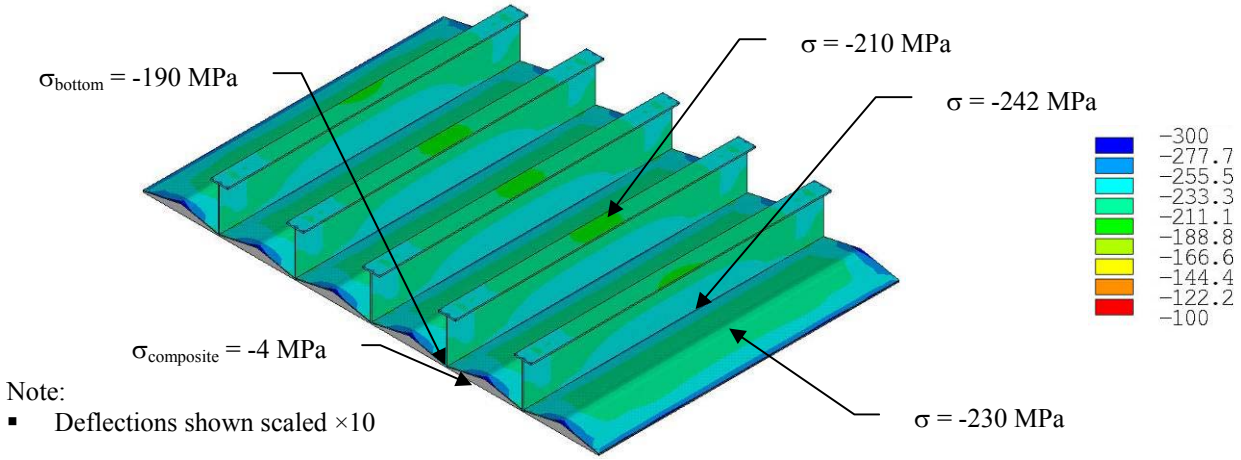

Note:
- Deflections shown scaled ×10

(b) At σ_{max} (or applied end displacement of 2.12 mm)

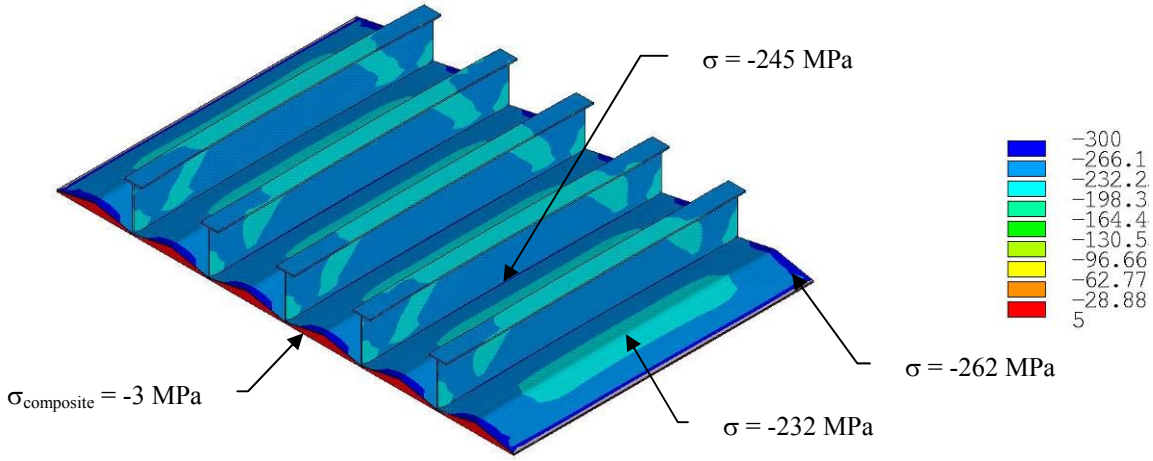

(c) At final applied end displacement of 3.0 mm

Figure 4.29: Calculated Longitudinal Normal Stresses for Hybrid Panel H-1 (MPa)

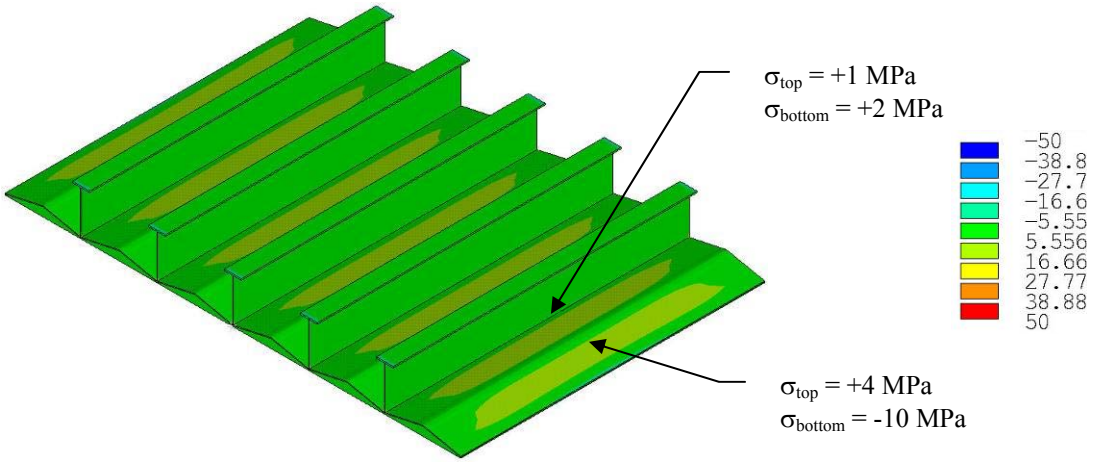

(a) Hydrostatic pressure load (no applied end displacement)

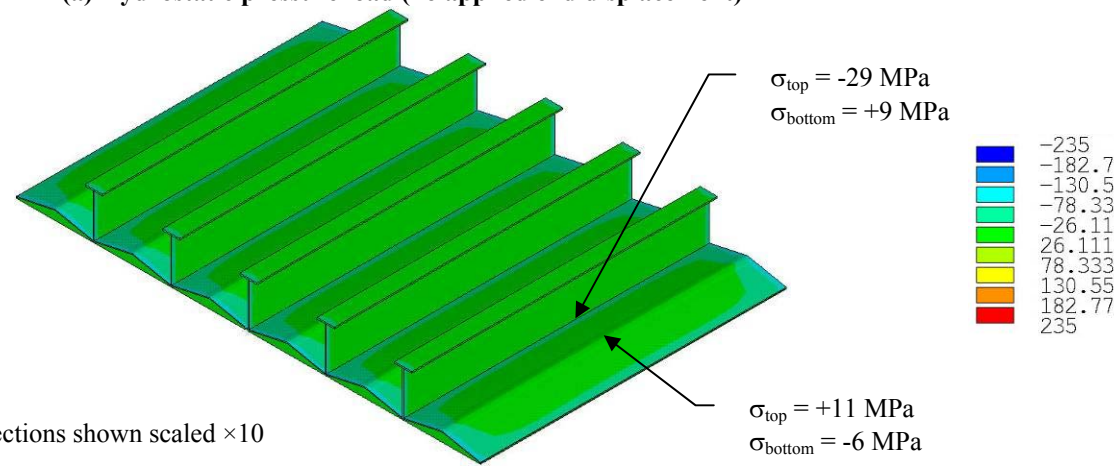

Note:
- Deflections shown scaled ×10

(b) At σ_{max} (or applied end displacement of 2.12 mm)

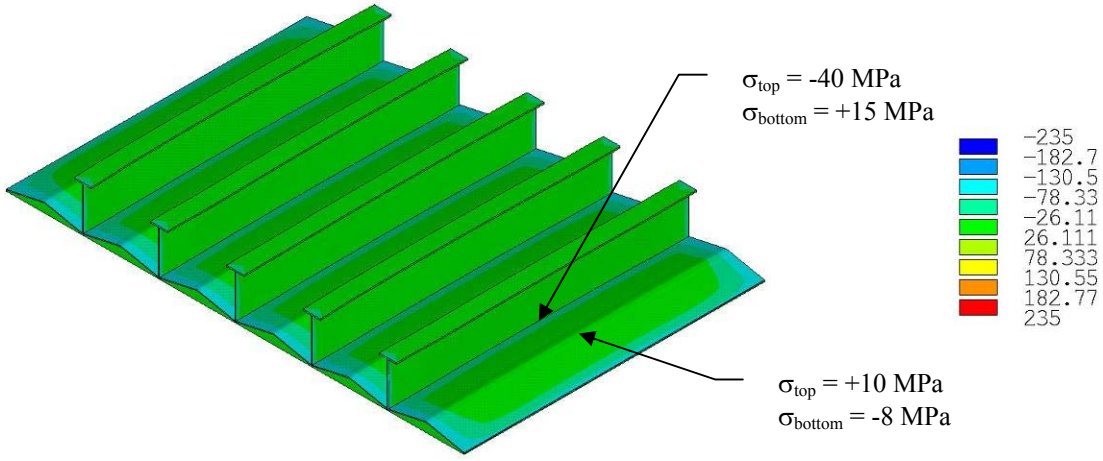

(c) At final applied end displacement of 3.0 mm

Figure 4.30: Calculated Transverse Normal Stresses for Hybrid Panel H-1 (MPa)

Table 4.5: Summary of Calculated Results for the Hybrid Panel Configurations

Panel Designation			Shell Thickness (in)	Shell Thickness (mm)	f_{bend}	A_{steel} (mm)	m / $m_{Baseline}$	σ_{max} (MPa)	σ_{max} / σ_y	Applied End Displacement at σ_{max} (mm)
6 ft Long Panels	G	1	3/16	4.8	5	25188	0.798	255	1.09	2.11
		2	1/4	6.4	5	29592	0.950	258	1.10	2.13
		3	5/16	7.9	5	34028	1.102	260	1.11	2.14
		4	3/8	9.5	5	38502	1.256	262	1.11	2.15
		5	7/16	11.1	5	43022	1.410	263	1.12	2.15
	H	1	3/16	4.8	10	25295	0.946	271	1.15	2.13
		2	1/4	6.4	10	29842	1.149	275	1.17	2.14
		3	5/16	7.9	10	34509	1.355	279	1.19	2.15
		4	3/8	9.5	10	39322	1.565	281	1.19	2.16
		5	7/16	11.1	10	44302	1.779	282	1.20	2.16
9 ft Long Panels	I	1	3/16	4.8	5	25188	1.197	246	1.05	3.08
		2	1/4	6.4	5	29592	1.425	250	1.06	3.10
		3	5/16	7.9	5	34028	1.654	254	1.08	3.14
		4	3/8	9.5	5	38502	1.884	256	1.09	3.16
		5	7/16	11.1	5	43022	2.116	257	1.10	3.16
	J	1	3/16	4.8	10	25295	1.419	261	1.11	3.08
		2	1/4	6.4	10	29842	1.724	267	1.14	3.12
		3	5/16	7.9	10	34509	2.033	272	1.16	3.16
		4	3/8	9.5	10	39322	2.348	275	1.17	3.18
		5	7/16	11.1	10	44302	2.668	278	1.18	3.20

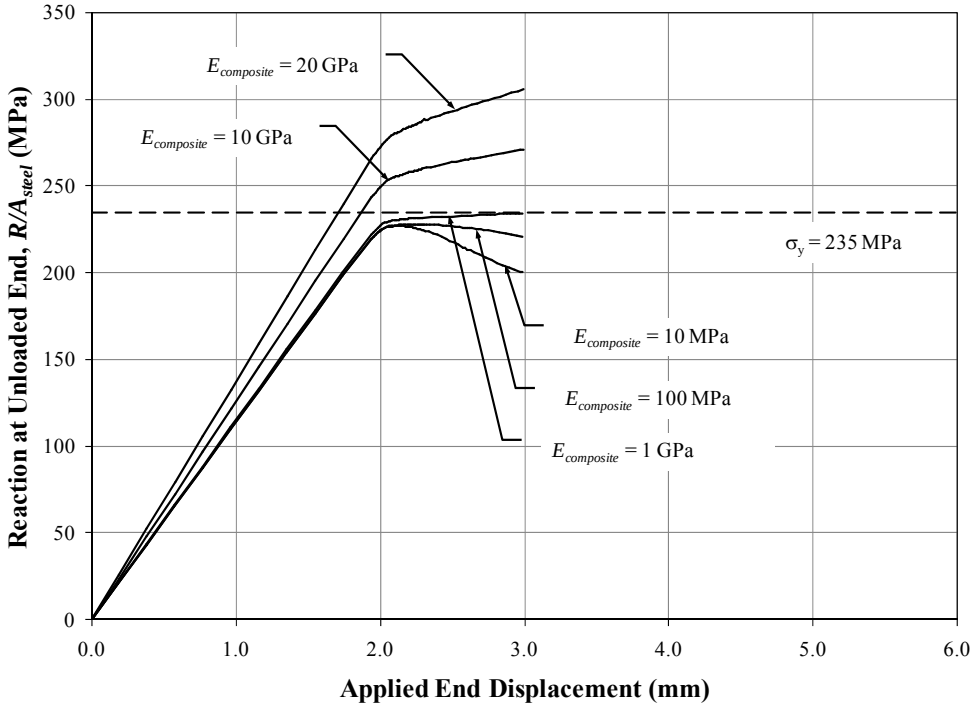

(a) Load-Deflection Curves (t_{shell} = 3/16″)

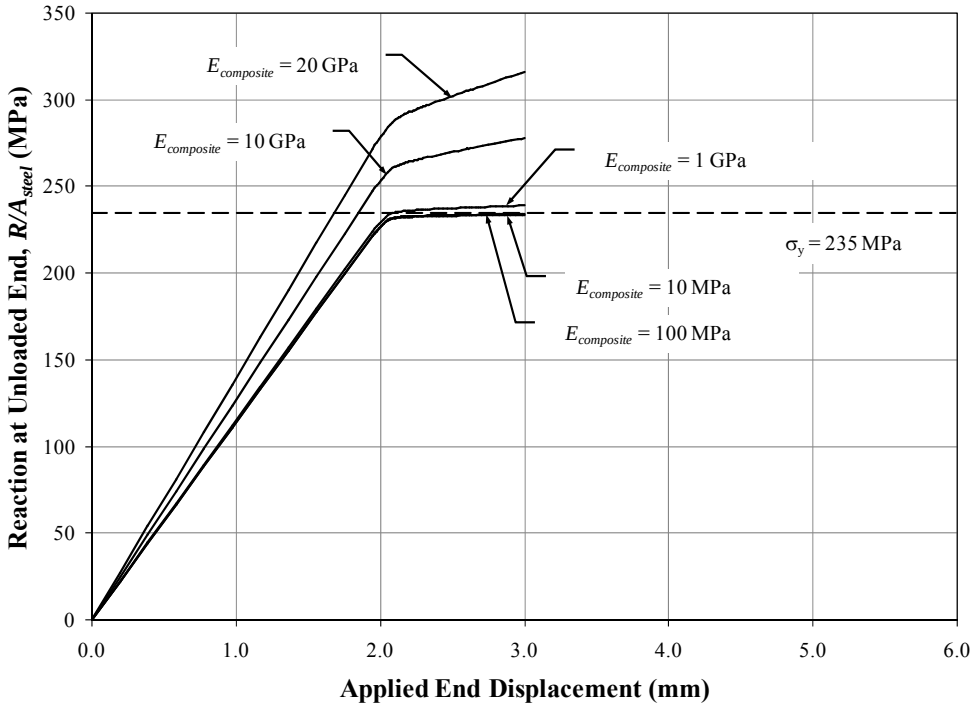

(b) Load-Deflection Curves (t_{shell} = 7/16″)

Figure 4.31: Calculated Load-Deflection Curves for the Hybrid Panel Configurations

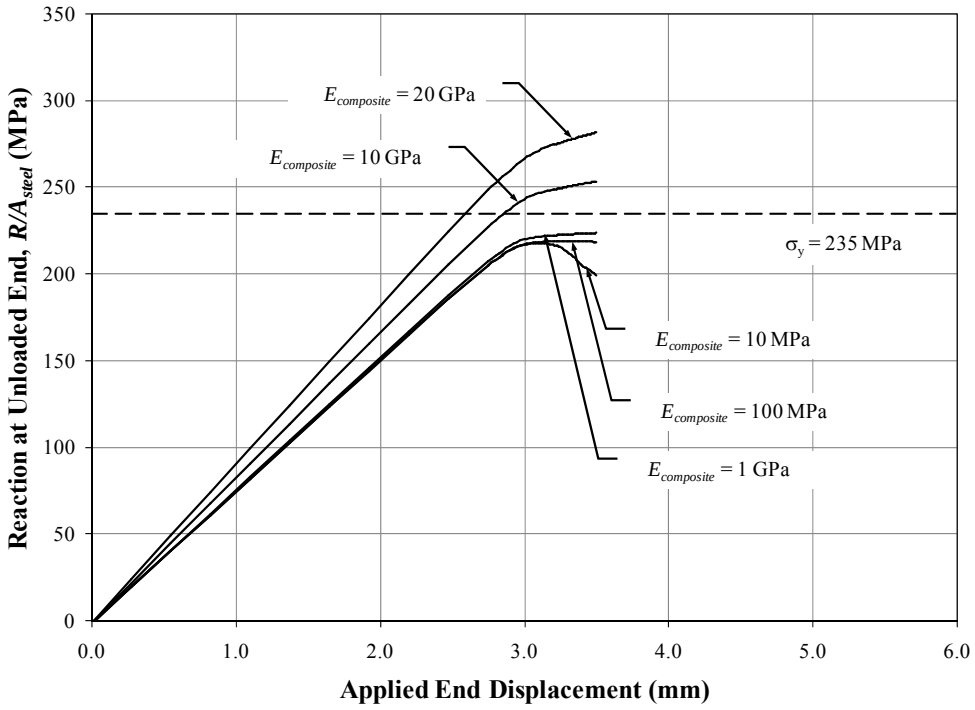

(a) Load-Deflection Curves (t_{shell} = 3/16″)

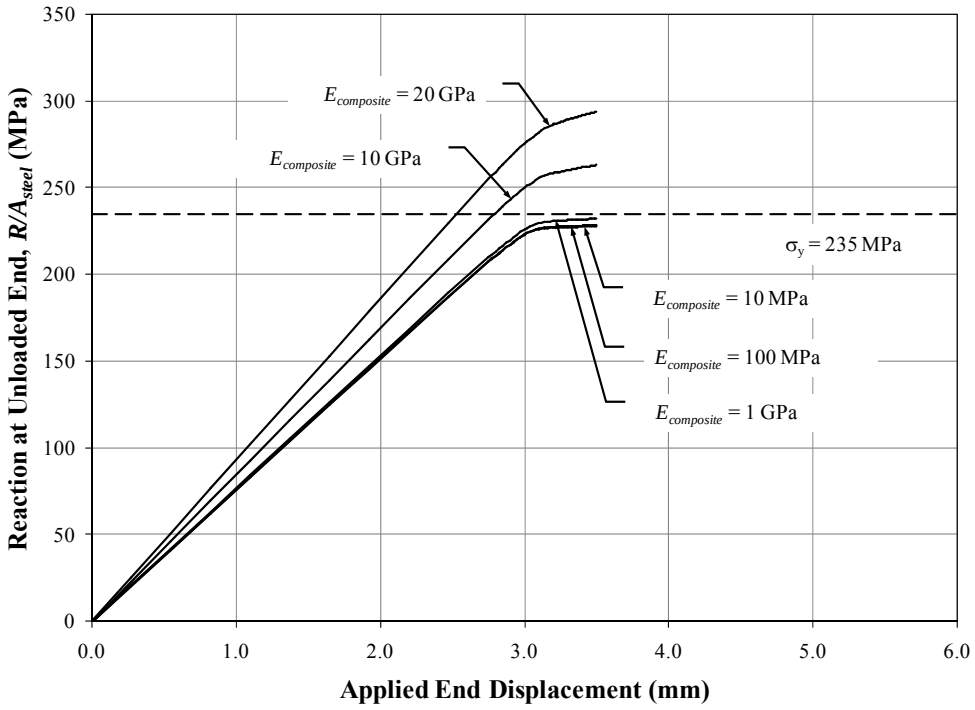

(b) Load-Deflection Curves (t_{shell} = 7/16″)

Figure 4.32: Calculated Load-Deflection Curves for the Hybrid Panel Configurations vs. Ecomposite (f_{bend} = 5.0 and 9 foot long panel)

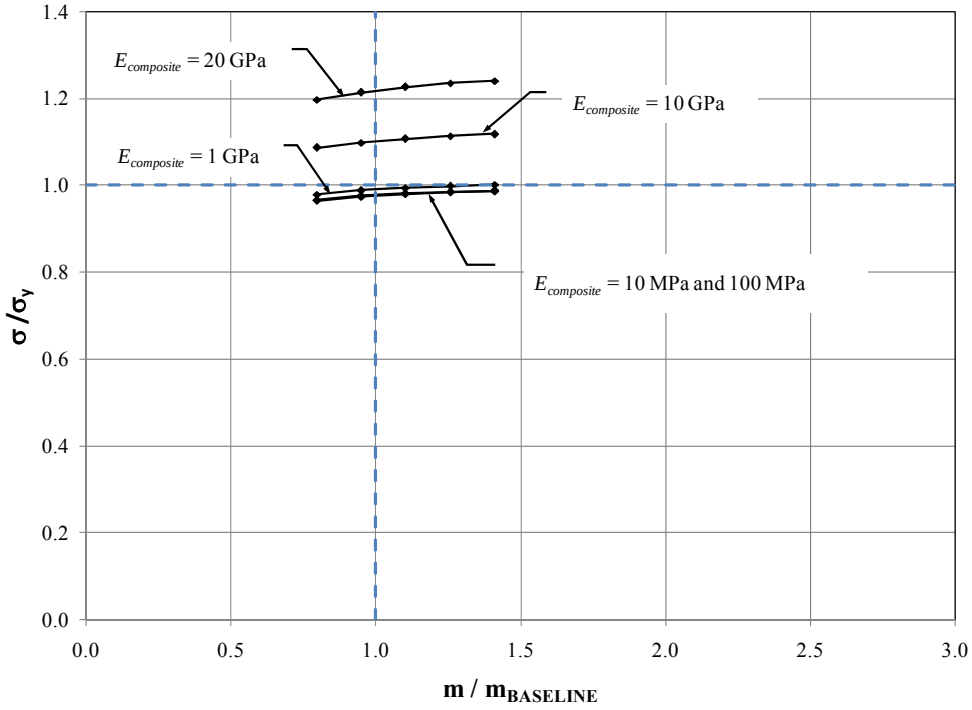

(a) 6 foot panel length

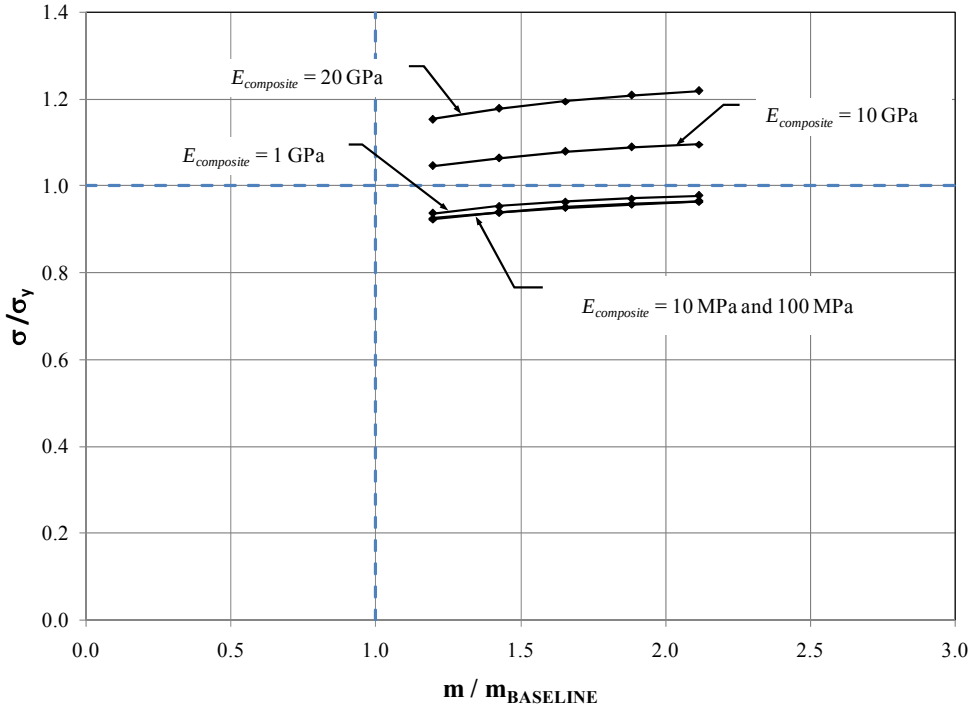

(b) 9 foot panel length

Figure 4.33: Normalized Stress-Mass Curves for the Hybrid Panel Configurations

4.4 Summary of FE Analysis Results

4.4.1 Conventional Steel Panel Configurations

The section properties based on the cross-sectional area of steel for the stiffened panel, whether flat or bent, are provided. The effect of bending the shell plate is to increase the elevation of the neutral axis, which balances the section (S_{bottom} approaches S_{top}). However, this results in a corresponding reduction in the value of S_{bottom}. For thicker shell plating, this reduction is more significant as f_{bend} increases. For thinner shell plate, the effect of f_{bend} is effectively negligible, in particular given the total reduction in section properties relative to the baseline configuration (reduced total area of effective steel due to the thin plate).

The existing conventional panel reached a buckling load of $\sigma_{max} = 1.08\sigma_y$. At the applied displacement corresponding to σ_{max} (just at the onset of buckling) the maximum out-of-plane deflection is 0.6 mm and the panel is uniformly in compression with the peak longitudinal normal stress equal to -265 MPa at midspan. Between the longitudinal stiffening, the transverse normal stresses in the shell plate are compressive but with the top (inner bottom) face less compressive due (in part) to the initial application of the hydrostatic pressure. The flexural distribution of stresses through the thickness provides an indication of the mode of local buckling, which becomes clearly evident as the applied end displacement progresses.

Similar behaviour is observed from the analysis of panel D-5 for the 9-foot span. However, this panel reaches $\sigma_{max} = 1.08\sigma_y$ with an applied end displacement of 3.2/2.2 = 1.45 times that for panel A-5. Although all other parameters remained constant, the increased slenderness of the panel reduced the buckling capacity, as expected. For practical applications, in order to increase the span between transverse frames, the arrangement of longitudinal stiffening would be modified to account for the increased flexibility of the panel.

With reducing shell plate thickness, the buckling capacity of the flat conventional steel panel decreases substantially. When reducing the plate thickness from 7/16 inches (11.1 mm) to 3/16 inches (4.76 mm), the maximum stress decreases from $1.08\sigma_y$ to $0.67\sigma_y$, or approximately 1.6 times. This is intuitive due to the instability introduced by increasing the slenderness of the shell plate while maintaining the unsupported span (the distance between longitudinal stiffeners).

The calculated out-of-plane deflection at σ_{max} for the conventional steel panel B-5 with $f_{bend} = 5.0$ is 0.7 mm and, like for panel A-5, the shell plate is uniformly in compression longitudinally. In the transverse direction, the plate (being in a deformed configuration initially) has a flexural distribution of stress through the thickness, though to a lesser magnitude as compared to that for panel A-5. The behaviour of panel C-5, with $f_{bend} = 10.0$, is equivalent to that of panel B-5.

From the analysis of the conventional steel panel with a bent shell plate, the effect of the bends (whether by a factor, f_{bend}, of 5.0 or of 10.0) is to reduce the initial buckling capacity of the panel. Considering the baseline 6-foot long panel with 7/16 inches (11.1 mm) shell plate, σ_{max} is reduced from $1.08\sigma_y$ for the flat plate to $0.99\sigma_y$, or 1.09 times, for the bent plate (whether f_{bend} equals 5.0 or 10.0). However, a reduction in shell plate thickness from 7/16 inches (11.1 mm) to 3/16 inches (4.76 mm) only results in a decrease from $0.99\sigma_y$ to $0.97\sigma_y$, or 1.02 times as compared to 1.6 times for the set of flat panels.

The differences in the calculated deflections and stresses between the bent steel panels with f_{bend} equal to either 5.0 or 10.0 is shown to be negligible.

4.4.2 Hybrid Panel Configurations (10 GPa Composite)

The analysis of the hybrid panels with $E_{composite}$ = 10 GPa, shows that regardless of the panel length (6 foot or 9 foot) and of the value for f_{bend} (5.0 or 10.), the panels achieved a buckling load greater than $1.0\sigma_y$. For example, the 6-foot long panel G-1, which has f_{bend} = 5.0, reached a buckling load of 1.09, which is equivalent to that for the baseline panel A-5.

Application of the composite to the bent shell plate provides additional capacity beyond the initial buckling, as indicated by the positive slope of the load-deflection curve beyond σ_{max}. (Note: again, the post-buckling behaviour was not included within the scope of this investigation.) The composite provides uniform support to the thinner plates, which precludes or defers localized buckling. It is anticipated that as the in-plane load continues to be applied, more of the panel becomes engaged in diaphragm action and the full moment capacity of the entire steel section is approached.

Assuming a density for the composite material of 1500 kg/m^3, the additional mass of the hybrid panel (relative to the baseline conventional panel A-5) is offset only for shell plate thickness less than or equal to about 0.25″ (6.35 mm) and based on a panel length of 6-feet with f_{bend} = 5.0. When f_{bend} = 10.0, the volume of composite added to the overall mass becomes more limiting.

4.4.3 Hybrid Panel Configurations (Various Composite Properties)

The effect of the value for $E_{composite}$ is investigated for the hybrid panel configurations with f_{bend} = 5.0. From the calculated load-deflection relationships with $E_{composite}$ taken as 10 MPa, 100 MPa, 1 GPa, 10 GPa and 20 GPa suggest a minimum modulus of elasticity of 1 GPa is required to preclude local buckling and to provide some additional capacity into the post-buckling range. Values of $E_{composite}$ of 100 MPa and 10 MPa show a negative slope on the load-deflection curves after σ_{max} is achieved for the 6 foot long panels. The curves also show a significant increase in the capacity of the stiffened hybrid panel for values of $E_{composite}$ above 1 GPa, in particular for decreasing shell plate thickness. This is also reflected in the plots showing σ_{max}/σ_y versus the normalized mass, $m/m_{baseline}$ for each panel.

5. RELIABILITY-BASED DESIGN

5.1 Methodology

The main goal of the reliability analysis in the context of this project was to compare the indices for the parent hull and the new hybrid hull. Since the absolute accuracy of the calculated reliability indices was not deemed extremely important, simpler methods for calculation of the indices were selected whenever possible. The lack of some important inputs, such as accurate longitudinal weight distribution or likely transit routes, has also influenced the choice of analysis methods.

Of many methods available for reliability assessment of ship structures, the Mean Value First Order Second Moment Analysis was selected for the project. The safety indices were calculated using the short-term procedure. This analysis was deemed more suitable for the case in hand because the long-term analysis is applicable only if the ship's route is more or less permanent, which is not the case with naval vessels. The probabilities or reliability indices coming out of short-term analysis are conditional only. They are conditioned on encountering the design storm.

The loads on the hull were estimated using the ship motions prediction software, ShipmoPC. Hogging loads were greater than sagging and the reliability analysis was therefore performed only for this condition.

5.2 Loads

The dynamic wave bending moment acting on the hybrid hull was calculated using the software tool, ShipmoPC. ShipmoPC is a seakeeping predictions program which uses strip theory, and is based on DRDC's computational engine SHIPMO7. The program is capable of computing the Root-Mean Square (RMS) vertical bending moments acting on the vessel. It includes effects due to wave forcing as well as ship motions. As the program is based on linear wave theory, its accuracy declines at large wave amplitudes. This inaccuracy becomes particularly prominent when the wave is so large that keel emergence occurs.

To evaluate the extreme wave bending moment, a series of wave environments that could be expected in the North Atlantic were considered. These were drawn from East Coast Area 12 in the Canadian Wind-Wave Atlas, which lies to the east of Newfoundland. The ten-year return significant wave height for this area is 13 m. However, the wavelength required for such a high wave is over twice the length of the vessel and may, therefore, be expected to cause lesser bending moments than a wave of the same length as the vessel. Using data from the Canadian Wind-Wave Atlas, a series of wave environments having the highest possible significant wave height for a given wavelength were identified.

Constant weight distribution was assumed as the weight distribution of the vessel was unknown. The calculations were carried out at zero speed, using a Bretschneider wave spectrum and short-crested seas.

For the baseline vessel, the results show that the largest RMS vertical bending moment occurs in head seas, very close to midship section, at Station 11 (with 0 at the forward perpendicular and 20 at the aft perpendicular) and in a wave environment smaller than the 10-year return storm. This environment was chosen to be the design storm for the reliability analysis. In this wave environment, the significant wave height is 11.85 m, the modal wave period is 13.5 s, and the corresponding modal wavelength is 284 m (2.34 times the ship length).

In a storm with 10,000 cycles, the corresponding mean value of the extreme wave bending moment is 319 MN-m. The return period for the design wave environment (Hs = 11.85 m) is 3.7 years. When the vessel operates in this storm, the extreme bending moment is a statistical parameter that does not follow a Gaussian distribution. When a Gaussian distribution is fit to the probability distribution for the extreme bending moment (with special attention paid to fitting the upper portion of the distribution), the mean is 328 MN-m, and the standard deviation is 23.5 MN-m. The calculated and the fitted cumulative distributions are shown in Figure 5.1.

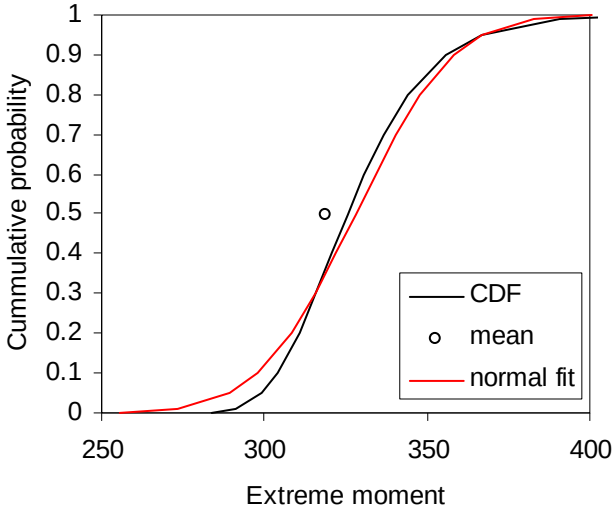

Figure 5.1: Extreme Bending Moment Cumulative Distribution

The still water hogging moment of 286 MN-m corresponds to fully loaded DDH-280, at level keel. Most ships, including naval vessels, operate at varying loading conditions and only infrequently are fully loaded to their design conditions. It is reasonable to assume that the loading condition and the corresponding still water bending moment are statistical variables that follow normal distribution. Since the still water bending moment was calculated for the fully loaded condition, the mean value had to be reduced from the calculated largest value. For the naval vessel, the mean value is assumed to be 80 percent of the full load calculated value (SSC 398, SSC 373). In accordance with the recommendations from the same references, it was assumed that the moment would have a normal distribution with a coefficient of variation of 15 percent.

The hybrid hull was calculated to be somewhat lighter (90 tonnes) due to reduced plating thickness. Using the same environmental condition for the hybrid hull, the RMS dynamic bending moment at Station 11 was found to be effectively identical to the values found for the baseline hull (within 0.03 percent). The still water hogging moment for the fully loaded hybrid hull vessel is slightly less: 282 MN-m.

5.3 Ultimate Strength (Hull Capacity)

Three types of behaviour are usually considered in the analysis of ship structures: primary, secondary and tertiary. The primary behaviour is associated with the ship as a whole. The ship's hull is considered a beam subject to its own weight, (including machinery, provisions and cargo) and supported by buoyancy distributed along its length. Dynamic loads due to acceleration of the ship in the seaway and varying wave loads are also included in the loading analysis. Only primary behaviour was investigated in the course of the project.

As applied loads increase, structural members of the hull will buckle in compression and yield in tension. The hull can normally carry further loading beyond the onset of member buckling or yielding, but the structural effectiveness of the failed members decreases or can even become negative. The stresses carried by the failing members get redistributed to the adjacent intact members. The most highly compressed member will collapse first and the stiffness of the overall hull will decrease gradually. Buckling and collapse of the structural members will occur progressively until the ultimate limit state is reached. This ultimate overall hull strength is used as a basis for structural safety and reliability analysis of ship hulls.

Classification societies provide design criteria for structural scantlings, which are usually based on first yielding and elastic buckling with a simple correction for plasticity. These expressions may not represent the true ultimate limit state. Hull girder inertia is one of the criteria used in Class Rules. DDH-280 was not designed to class standards and likely has lower inertia than that required by Rules. The hybrid concept would certainly have even lower inertia. To obtain a reasonably accurate assessment of safety against overall hull collapse, the ultimate hull strength provides a better criterion than the conventional elastic buckling or first yield criteria.

The ultimate strengths of the parent and the hybrid hulls were calculated using a simplified method proposed in SSC-398 report (Assessment of Reliability of Ship Structures). The method considers only the vertical bending moment but takes into account the ultimate strength of the compression flange and the sides in the vicinity of the compression flange of the hull girder. The method is fully explained in Section 2.2.3 of the reference [2].

5.4 Reliability Indices

Reliability indices were calculated for three different structural concepts: baseline hull, a hull made with creased steel panels and a hybrid hull. The methodology proposed in Section 2.3.4.3.B of the reference [2] was used (Mean Value First Order Second Moment Analysis).

The FE analysis revealed that creasing the panel without adding composite material reduces the buckling capacity compared to the flat panel. However, the thickness of the creased panel can be substantially reduced without significantly eroding its buckling strength. This could potentially be utilized to reduce the weight of the vessel which, in turn, will reduce the draught and the loads on the hull. With this in mind, all 7/16-inch panels in the parent hull model were replaced with 5/16-inch creased panels thickness in to test the assumption that the reduction in loads will outweigh the reduction in strength. Panels thicker or thinner than 7/16-inch (keel, bilge, sheer strake) were kept unchanged in the model. The results are shown in Table 5.1.

Panel G2 (1/4-inch) was used in the hybrid composite concept reliability analysis. As with the creased panel analysis, only 7/16-inch panels in the parent hull were replaced with the G2 panels. The thickness of 1/4 inch was selected because the weight of such structure would be comparable to that of the parent hull. The results are shown in Table 5.1.

The simplified method used for the ultimate strength estimation is pushed over the limits with the addition of the composite material and the results should be treated with great caution. It is likely that the short-term reliability of the hybrid hull is going to be higher than that of a conventional steel hull, but the simplified approach used in the project can not accurately predict by how much. Rigorous treatment would require an FE model of the whole hull and many runs, both of which go beyond the scope of the project.

Table 5.1: Reliability Indices Comparison

Parameter	Units	Parent Hull	Creased 5/16"	Hybrid Panel 5/16 in.
Ultimate strength (Mu)	MNm	1,420	1,153	1,995
σ_{Mu}	MNm	213	173	299
Stillwater Bending Moment (Ms)	MNm	229	226	226
σ_{Ms}	MNm	34	34	34
Wave Bending Moment (Mw)	MNm	328	328	328
σ_{Mw}	MNm	24	24	24
Limit State Function Mean (g)		863	599	1,442
σ_g		217	178	302
Reliability Index (β)		3.98	3.37	4.77

It is shown in Table 5.1 that creasing the panel without adding composite material decreases the reliability significantly. With the addition of composite material with 10GPa ultimate strength the reliability of the hybrid structure exceeds that of the parent hull by a significant margin.

6. CONCLUSIONS

A new hybrid hull concept was proposed and analyzed in this report. The concept involves the creased plating between the longitudinal stiffeners. This change in geometry was expected to increase the in-plane load carrying capacity of the panel, thus improving its buckling resistance. Creasing the panels changes the behaviour of the panel in a significant way. For the same plating thickness, the buckling strength is lower than with the flat plating. However, it remains relatively constant if the thickness of the skin is reduced by significant amounts, unlike with conventional flat panels where the strength declines sharply with the reduction in plating thickness. This behaviour alone cannot be simply exploited to reduce the structural scantlings while maintaining the original strength. If all other scantlings are maintained as they were in this project, there are no benefits in doing this. However, there may be potential in this approach and more research is recommended.

The addition of composite material to the creased panels improves the buckling capacity; but in order to get a noticeable improvement, high performance composite materials are required. Using standard, widely available shipbuilding composites such as glass fibres in polyester matrix does not even help the creased panel reach the strength of the flat panel. To improve the buckling strength beyond that of a flat steel panel, composite material as strong as steel would be required. In the reliability analysis in this report, 10GPa modulus of elasticity was assumed for the composite material. The addition of composite material also increases the weight of the panel substantially.

This project was regarded as exploratory. The analysis performed in the course of the project did not include some very important aspects of structural design that could only be addressed in a more advanced phase of ship hull design. This includes fatigue considerations, inclusion of interlaminar stresses in the analysis, etc.

It should be noted that the parent hull design is already highly optimized and it is difficult to improve its reliability without significant design efforts; and even then, the improvements would likely be small.

It can be concluded that the hybrid hull analyzed in this report is technically feasible if most advanced composite materials with strength many times exceeding that of steel are used. However, the cost of such ship would be prohibitive for many applications. In addition to high cost, there would be a number of technical challenges that could not have been addressed within the scope of the project: ensuring proper and uniform bonding over the very large contact area between steel and composite, issues with de-lamination, in-service inspections, repair welding of steel plating, docking, etc.

7. REFERENCES

[1] DDH-280 Structural Drawings
[2] SSC-398 Assessment of Reliability of Ship Structures
[3] SSC 373 Probability Based Ship Design; Loads and Load Combination

APPENDIX A - HYBRID SHIP MATERIAL SELECTION

1. INTRODUCTION

The physical behavior of composites is rather different from materials more commonly used in shipbuilding like steel or aluminum. Steel or aluminum will have similar composition regardless where material sample is taken. Composite materials are anisotropic meaning that physical properties of the composite will vary with location and orientation of the principal axes. This necessitates an in-depth knowledge of material micromechanics, consequently making the design with composites more complex. Furthermore quality control and simplicity of manufacture have important role when selecting the adequate composites material configuration. As opposed to steel and aluminum which are fabricated as raw materials with numerous quality control systems in-place before coming to shipyard, composites itself are actually blended and compound on site by semi-skilled or skilled workers. During the fabrication of composite hulls or in our case hybrid steel-composite hull, composite materials will have to be brought together, metered, thoroughly mixed and de-aerated by the hull manufacturer.

All composite materials can be broadly classified in following three groups:

- Resins;
- Reinforcements, and
- Core Materials.

In the context of this project, core materials were not considered.

2. RESINS

Resins are acting as a matrix holding the reinforcement fibers in alignment. To fulfill this requirement cured resin must have good bonding and shear properties. In general any resin system for use in a composite material must meet the following requirements:

- Good mechanical properties;
- Good adhesive properties;
- Good toughness properties; and
- Good resistance to environmental degradation.

All resins that are used in fiber-reinforced composites are polymers. The main molecular characteristics of the polymers are that they consist from long chain like molecules with many simple repeating units. They can be classified in two groups: thermoplastic and thermosetting polymers.

Thermoplastic polymers lose their mechanical properties with heat and eventually melt, and they can harden again with cooling. The process of softening and hardening can be repeated as often as required without any effect on polymer material properties in either state. Typical thermoplastic include nylon and polypropylene, and typical reinforcement used with thermoplastic is chopped glass.

Thermosetting polymers are formed by chemical reaction in situ. Resin or hardener or resin and catalyst are mixed to form hard-infusible product. Once cured, the thermosetting polymers cannot become liquid again, although above the certain temperature their mechanical properties will change significantly. This temperature is known as glass transition temperature and depends largely on the type of resin used, degree of cure and if resin-hardener (resin-catalyst) are mixed correctly. Thermosetting polymers are almost exclusively used as structural resins. Typical thermosetting polymers include polyester, vinyl ester and epoxy.

The frequency of application of various resin systems in the marine industry is given in Figure A2.1.

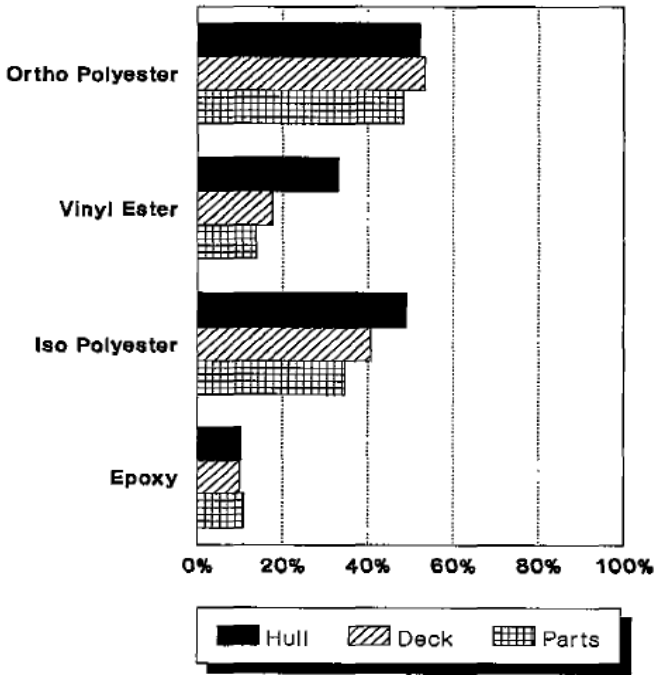

Figure A2.1: Resins Used in Marine Industry (from SSC-360)

Polyester resins are the simplest and most economical resin systems. They are easy to use and show good chemical resistance. They are suitable for hand lay-up or spray application. Two types of polyester resins are used as standard in composite industry: orthophthalic and isophthalic. Both of them are unsaturated type, capable of being cured from liquid or solid state when subject to right conditions. The isophthalic resins generally have better mechanical properties, chemical and resistance to water permeation. For use in molding polyester resins require the addition of:

- A catalyst;
- An accelerator; and
- Additives.

Catalyst and accelerators are used to accomplish the curing of the resin without heat input. Additives are used to modify viscosity of resin if vertical or overhead surface is being laminated.

Vinylester resins have a similar handling procedure as polyesters. They have the advantage in better toughness, water resistance, corrosion resistance and better fatigue performance. The disadvantage is the cost of vinylester; it is about twice the cost of polyester resins.

Epoxy resins are generally made by mixing two ingredients: epoxide or resin and hardener. These ingredients must be mixed immediately prior to processing. Epoxies have superior abrasion resistance, less water absorption, greater bonding strength and much lower shrinkage after curing then polyesters or vinylesters. Their disadvantage is high cost, longer curing time and complicated handling. Another disadvantage is that uncured epoxy resins can cause allergic problems.

For the hybrid composite – steel ship, the preferred resin is considered to be the vinylester. Vinylester resins reassemble polyesters in simplicity of processing and have better overall mechanical and chemical properties. The most important mechanical property of vinylester for steel-composite hybrid is elongation. Selected resin must be able to deform at least same as selected reinforcement and hull steel plating to achieve maximum hybrid tensile properties. Vinylesters can deform approx. 1.5 time more than polyesters.

Compared with epoxy resins, vinylesters have lower cost, shorter curing time and simpler processing. Additionally, as illustrated in Figure A2.1, the experience with vinylesters in the marine industry exceeds that of epoxy resins. Hence manufacturing quality is expected to be better.

3. REINFORCEMENT MATERIALS

3.1 Reinforcement Material Selection

The role of the reinforcement in a composite material is to increase mechanical properties of resins. Mechanical properties of most reinforcing fibers are considerably higher than those of unreinforced resins; and therefore, the mechanical properties of fiber/resin system are dominated by fiber selection.

The four main factors define the fibers' contribution to the fiber/resin system:

- The basic mechanical properties of the fiber itself;
- The surface interaction of fiber and resin;
- The amount of fiber in the composite; and
- The orientation of fiber in the composite.

The mechanical properties of the most common fibers are given in Table A3.1.

Table A3.1: Mechanical Properties of Most Common Fibers

	Density 10^3-kg/m^3	Modulus (Gpa)	Tensile strength Mpa	Specific stiffness (GPa)*	Specific strength (MPa)*
E-glass	2.5	70	1700	28	680
carbon	1.8	230 to 820	2000 to 820	128 to	1111 to
			7000	455	3900
Ararnid	1.4	130	3000	98	2140
Polyethylene	0.97	170	3000	175	3090
HT steel	7.8	210	750	27	96
Aluminium	2.7	75	260	28	96

*Stiffness or strength divided by Specific Gravity

The quality of bonding between the fiber and the resin depends on the surface interaction between two, and it is heavily influenced by the treatment given to the fiber surface.

The amount of fiber controls the stiffness and the strength of the composite. In general the stiffness and the strength of the composite will increase in proportion to the amount of fiber present. The measure of the fiber amount in the composite is called Fiber Volume Fraction (FVF). At over about 60 to 70 percent FVF (depending on how fibers are packed together), although tensile strength may continue to increase, the composite strength will reach its peak and then begin to decrease due to the lack of sufficient resin to hold the fibers together. In addition to the amount of fiber, the fiber diameter is an important factor in the stiffness and the strength of composites. Fibers with smaller diameters are providing more fiber surface area, consequently spreading the fiber/matrix interfacial loads making the composite stronger.

The orientation of fibers in composite creates direction specific properties; fibers are designed to be loaded along their length.

The most common types of reinforcement used in marine industry are glass fibers. They have low cost and relatively good strength and workability characteristics. The usage percentage of different kinds of reinforcements in marine industry is given in Figure A3.1.

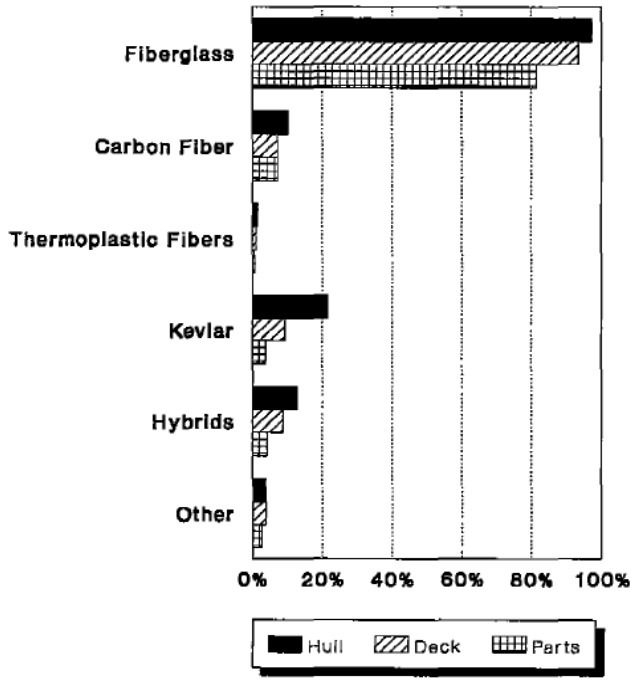

Figure A3.1: Reinforcement Materials Used in Marine Industry (From SSC-360)

In the hybrid composite–steel ship, the primary load carrying structure is high strength steel plating and framing. Composites are used mostly to postpone plate buckling. Hence, use of reinforcement with high stiffness and strength, such as Kevlar (Aramid) or carbon fibers, for a steel–composite hull is believed to be unnecessary. There are two additional reasons why the Kevlar (Aramid) or carbon fibers were not considered suitable. First, as illustrated in Figure A3.1, the experience with reinforcement materials other then glass is limited and manufacturing quality can be jeopardized. Secondly, the cost of the Kevlar or HM carbon (high modulus carbon) greatly exceeds that of glass fibers.

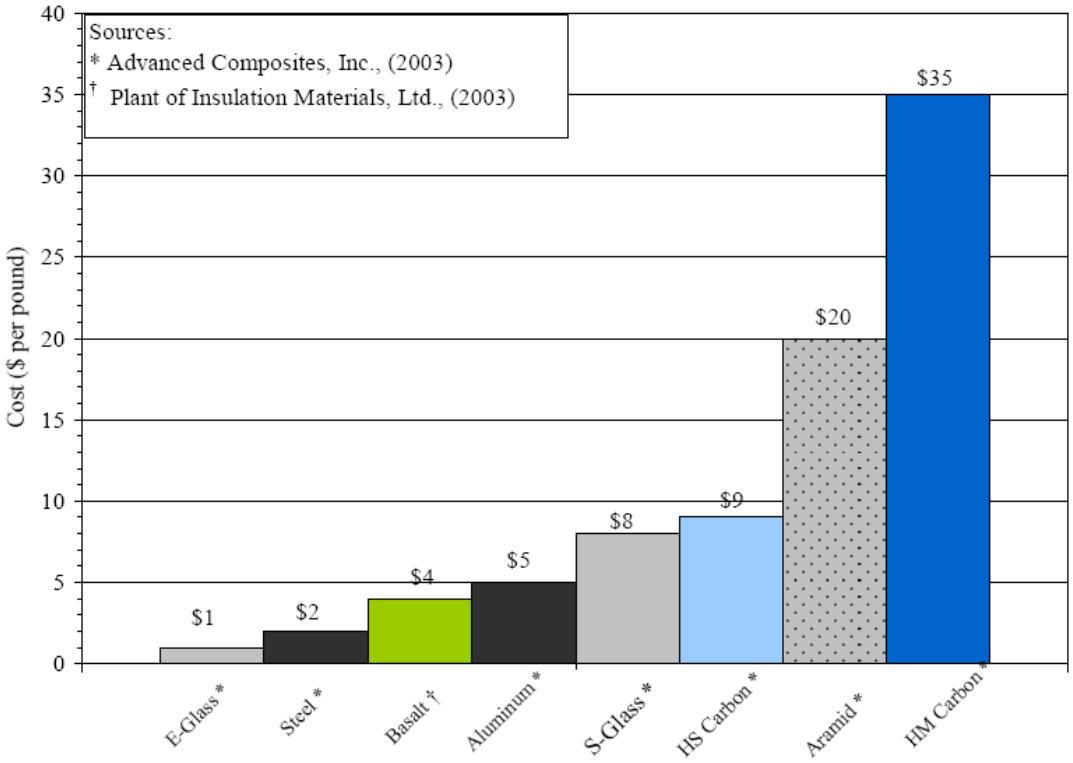

Figure A3.2: Raw Material Cost for Typical Reinforcement Fibers

The most appropriate reinforcement material for the steel-composite hybrid hull concept is likely the E-glass fibers.

Two types of glass fibers are commonly used in marine industry: E-glass and S-glass. E-glass (lime aluminum borosilicate) has good strength properties and good resistance to water degradation. S-glass (silicon dioxide, aluminum and magnesium oxides) exhibits about one third better tensile strength then E-glass. The downside is that the cost of S-glass is eight times that of E-glass (see Figure A3.2).

In the hybrid steel–composite concept, the tensile strength of steel will always be the governing factor. Hence the benefits of using the S-glass with better tensile properties are limited. Furthermore, because of the quantities involved, the higher cost of S-glass is unjustifiable.

3.2. Matrix selection

Reinforcement materials are combined with resins to produce structural composites. Based on reinforcement fiber matrix orientation composites can be categorized as:

- Unidirectional;
- Multi-axial;
- $0/90^{o}$; and
- Omni-directional.

The unidirectional composite is one in which the majority of reinforcement fibers are running in one direction. A small portion of fibers or other material can run in other directions with the primary function of holding main fibers together. In marine applications, unidirectional materials are usually used for stem and centerline stiffeners construction.

Multi-axial materials consist of one or more layers of long fabrics hold in place by secondary non structural stitching material. The stitching material is usually polyester regardless of main fibers material.

The most common forms of multi-axial composites are illustrated in Figure A3.3.

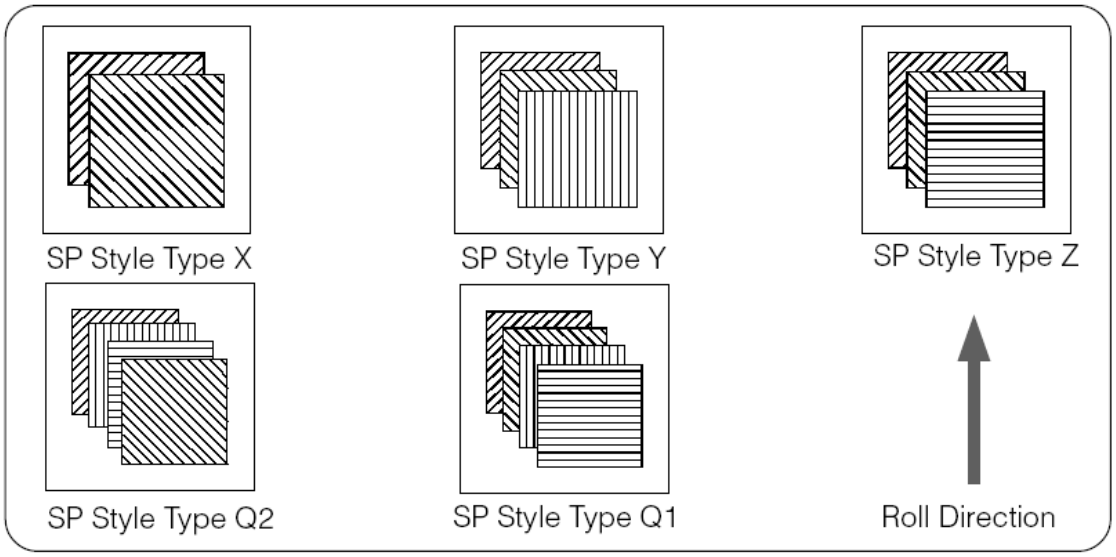

Figure A3.3: Most Common Forms of Multi-Axial Reinforcement

The majority of 0/90^{o} reinforcements are woven fiber materials. Woven reinforcements are produced by interlacing of warp 0^{o} fibers and weft 90^{o} fibers in regular pattern of weave style. The most common woven construction variations are shown in Figure A3.4.

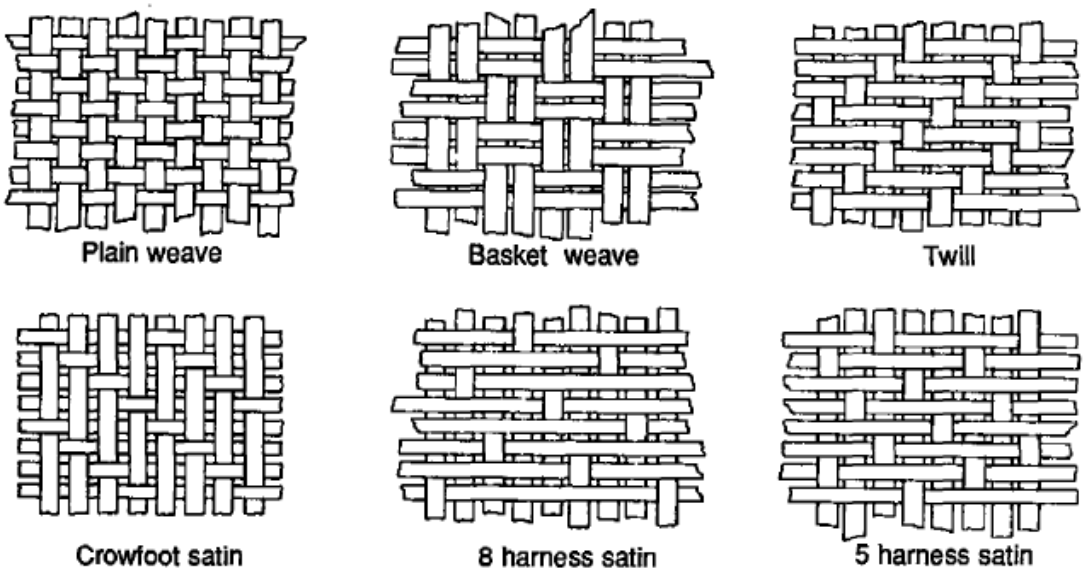

Figure A3.4: Most Common Woven Reinforcement Configurations

Woven roving reinforcements are often used in large marine structures because they are available in fairly heavy weights, which enable rapid build-up of thickness. All of the above mentioned reinforcements have a common disadvantage in that they have to be applied layer by layer, usually by hand and they have poor interlaminate properties.

Omni-directional reinforcements can be applied using the hand or machine lay-up technique as prefabricated mat or via spray process as a chopped strand mat. Both of those processes produce reinforcement with isotropic properties and good inter-laminar shear strength (Z axes –through composite thickness). The ultimate mechanical properties of omni-directional reinforcements are less than those of unidirectional reinforcements. The frequency of application of different kinds of reinforcement materials in the marine industry is presented in Figure A3.5.

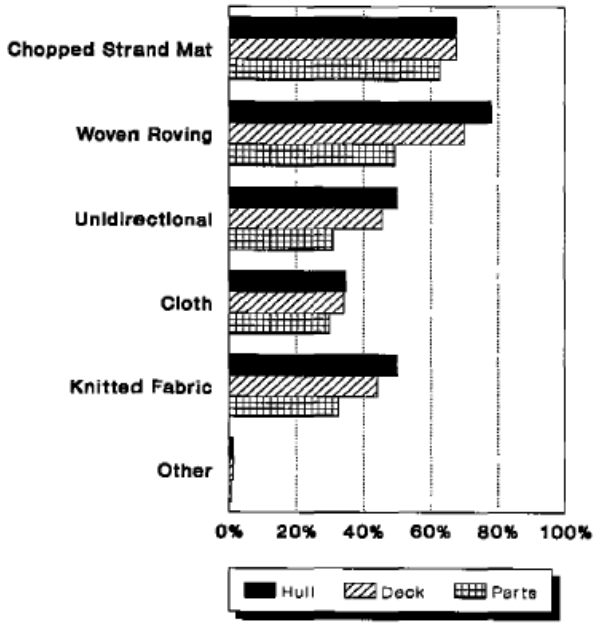

Figure A3.5: Reinforcement Matrixes Used in Marine Industry (From SSC-360)

For the application at hand, that is, the steel–composite hybrid concept, both omni-directional and uni-directional reinforcements can be used in the same project.

PROJECT TECHNICAL COMMITTEE MEMBERS

The following persons were members of the committee that represented the Ship Structure Committee to the Contractor as resident subject matter experts. As such they performed technical review of the initial proposals to select the contractor, advised the contractor in cognizant matters pertaining to the contract of which the agencies were aware, performed technical review of the work in progress and edited the final report.

Chairman

Loc	Nguyen	NSWCCD

Members:

Raymond	Kramer	Raytheon
Gangadhara	Prusty	University of New South Wales
Pradeep	Sensharma	Design and Planners
Matthew	Collette	SAIC
Yoo Sang	Choo	National University of Singapore
Harold	Reemsnyder	
Paul	Hess	Office of Naval Research
Robert	Curry	American Bureau of Shipping
Roger	Ghanem	Univ. of Southern California
Pramod	Dash	BIT Mesra
William	Caliendo	US Merchant Marine Academy
Jeom	Paik	Pusan National University
Roshdy	Barsoum	Office of Naval Research
Richard	Fonda	Naval Research Lab
Robert	Sielski	US Navy (retired)
Dhiren	Marjadi	Altair
Debu	Ghosh	U.S. Coast Guard Electronic Logistic Center (ELC)
Lothar	Birk	University of New Orleans
Chris	Barry	US Coast Guard ELC / SNAME
Daniel	Woods	Germanischer Lloyd
Rong	Huang	Chevron (retired)

SHIP STRUCTURE COMMITTEE LIAISON MEMBERS

LIAISON MEMBERS

American Iron and Steel Institute	Mr. Alexander Wilson
American Society for Testing & Materials	Captain Charles Piersall (Ret.)
American Society of Naval Engineers	Captain Dennis K. Kruse (USN Ret.)
American Welding Society	Mr. Richard Frank
Bath Iron Works	Mr. Steve Tarpy
Canada Ctr for Minerals & Energy Technology	Dr. William R. Tyson
Colorado School of Mines	Dr. Stephen Liu
Edison Welding Institute	Mr. Rich Green
International Maritime Organization	Mr. Igor M. Ponomarev
Int'l Ship and Offshore Structure Congress	Dr. Jack Spencer
INTERTANKO	Mr. Dragos Rauta
Massachusetts Institute of Technology	
Memorial University of Newfoundland	Dr. M. R. Haddara
National Cargo Bureau	Captain Jim McNamara
Office of Naval Research	Dr. Yapa Rajapaksie
Oil Companies International Maritime Forum	Mr. Phillip Murphy
Tanker Structure Cooperative Forum	
Technical University of Nova Scotia	Dr. C. Hsiung
United States Coast Guard Academy	Commander Kurt Colella
United States Merchant Marine Academy	Dr. C. B. Kim
United States Naval Academy	Dr. Ramswar Bhattacharyya
University of British Columbia	Dr. S. Calisal
University of California Berkeley	Dr. Robert Bea
University of Houston - Composites Eng & Appl.	Dr. Jerry Williams
University of Maryland	Dr. Bilal Ayyub
University of Michigan	Dr. Michael Bernitsas
University of Waterloo	Dr. J. Roorda
Virginia Polytechnic and State Institute	Dr. Alan Brown
Webb Institute	Prof. Roger Compton
Welding Research Council	Dr. Martin Prager
Worchester Polytechnic Institute	Dr. Nick Dembsey
Samsung Heavy Industries, Inc.	Dr. Satish Kumar

RECENT SHIP STRUCTURE COMMITTEE PUBLICATIONS

Ship Structure Committee Publications on the Web - All reports from SSC 1 to current are available to be downloaded from the Ship Structure Committee Web Site at URL: http://www.shipstructure.org

SSC 445 – SSC 393 are available on the SSC CD-ROM Library. Visit the National Technical Information Service (NTIS) Web Site for ordering hard copies of all SSC research reports at URL: http://www.ntis.gov

SSC Report Number	Report Bibliography
SSC 455	Feasibility, Conceptual Design and Optimization of a Large Composite Hybrid Hull, Braun D., Pejcic M. 2008
SSC 454	Ultimate Strength and Optimization of Aluminum Extrusions, Collette M., Wang C. 2008
SSC 453	Welding Distortion Analysis Of Hull Blocks Using Equivalent Load Method Based On Inherent Strain, Jang C.D. 2008
SSC 452	Aluminum Structure Design and Fabrication Guide, Sielski R.A. 2007
SSC 451	Mechanical Collapse Testing on Aluminum Stiffened Panels for Marine Applications, Paik J.K. 2007
SSC 450	Ship Structure Committee: Effectiveness Survey, Phillips M.L., Buck R., Jones L.M. 2007
SSC 449	Hydrodynamic Pressures and Impact Loads for High Speed Catamaran / SES, Vorus W. 2007
SSC 448	Fracture Mechanics Characterization of Aluminum Alloys for Marine Structural Applications, Donald J.K., Blair A. 2007
SSC 447	Fatigue and Fracture Behavior of Fusion and Friction Stir Welded Aluminum Components, Kramer R. 2007
SSC 446	Comparative Study of Naval and Commercial Ship Structure Design Standards, Kendrick A., Daley C. 2007
SSC 445	Structural Survivability of Modern Liners, Iversen R. 2005
SSC 444	In-Service Non-Destructive Estimation of the Remaining Fatigue Life of Welded Joints, Dexter R.J., Swanson K.M., Shield C.K. 2005
SSC 443	Design Guidelines for Doubler Plate Repairs on Ship Structures Sensharma P.K., Dinovitzer A., Traynham Y. 2005